



# Contribution of three rivers to floodplain and coastal productivity in the Gulf of Carpentaria: Finfish catch and growth

Component final report

JB Robins, SM Leahy, MJ Sellin, J Woodhead and R Maas

© Department of Agriculture and Fisheries (Queensland), 2021



*Contribution of three rivers to floodplain and coastal productivity in the Gulf of Carpentaria: Finfish catch and growth* is licensed by the Department of Agriculture and Fisheries (Queensland) for use under a Creative Commons Attribution 4.0 Australia licence. For licence conditions see [creativecommons.org/licenses/by/4.0](https://creativecommons.org/licenses/by/4.0)

This report should be cited as:

Robins JB,<sup>1</sup> Leahy SM,<sup>1</sup> Sellin MJ,<sup>1</sup> Woodhead J<sup>2</sup> and Maas R.<sup>2</sup> (2021). *Contribution of three rivers to floodplain and coastal productivity in the Gulf of Carpentaria: Finfish catch and growth*. Department of Agriculture and Fisheries (Queensland), Brisbane.

1. Department of Agriculture and Fisheries (Queensland)
2. University of Melbourne

Cover photographs

Front cover: Glenn Halliday with a southern Gulf of Carpentaria barramundi (photo courtesy of Carpentaria Barra and Sport Fishing Charters).

Back cover: Satellite image illustrating the distribution of floodwaters to the estuaries and near coastal waters of southern Gulf of Carpentaria (source: Zoom Earth, NASA, GSFC/EOSDID, Aqua/MODIS; [zoom.earth/#view=-16.9885,140.739,8z/date=2009-02-15,pm](https://zoom.earth/#view=-16.9885,140.739,8z/date=2009-02-15,pm)).

This report is available for download from the Northern Australia Environmental Resources (NAER) Hub website at [nespnorthern.edu.au](https://nespnorthern.edu.au)

The Hub is supported through funding from the Australian Government's National Environmental Science Program (NESP). The NESP NAER Hub is hosted by Charles Darwin University.

ISBN 978-1-922684-35-6

October, 2021

Printed by UniPrint

# Contents

Acronyms.....	vi
Acknowledgements .....	vii
Executive summary.....	1
1. Introduction.....	3
1.1 Rivers of interest .....	3
1.1.1 Mitchell River.....	4
1.1.2 Gilbert River .....	4
1.1.3 Flinders River .....	5
2. Methodology.....	7
2.1 Catch and age .....	7
2.1.1 Catch and age data.....	7
2.1.2 Year-class strength .....	9
2.1.3 Catch-at-age .....	10
2.1.4 Flow data.....	10
2.1.5 Analysis with flow .....	11
2.2 Growth.....	12
2.2.1 Otolith data.....	12
2.2.2 Environmental data .....	15
2.2.3 Growth rate modelling.....	17
2.2.4 Scenario testing .....	19
2.3 Otolith microchemistry .....	19
2.3.1 Otolith sample selection.....	19
2.3.2 Otolith sample preparation.....	21
2.3.3 Laser ablation – strontium isotopes.....	21
2.3.4 Water chemistry .....	21
2.3.5 <sup>87</sup> Sr/ <sup>86</sup> Sr profile classification .....	23
2.3.6 Total length as related to habitat class.....	23
3. Results.....	24
3.1 Catch and age.....	24
3.1.1 Mid sub-stock (Mitchell River).....	24
3.1.2 South sub-stock (including Flinders and Gilbert rivers) .....	30
3.2 Growth.....	37
3.2.1 Timing of increment formation .....	37
3.2.2 River and atmospheric index patterns.....	38
3.2.3 Drivers of otolith increment width .....	41
3.2.4 Scenario testing .....	45

3.3	Otolith microchemistry .....	45
3.3.1	Water chemistry .....	45
3.3.2	Habitat use inferred from $^{87}\text{Sr}/^{86}\text{Sr}$ profile.....	46
3.3.3	Total length as related to habitat class.....	53
4.	Discussion .....	56
4.1	Catch, age-frequency and catch-at-age .....	56
4.2	Growth.....	56
4.3	Otolith microchemistry .....	58
4.4	Summary .....	59
5.	Recommendations and conclusions.....	61
	References .....	62
	Appendix 1. Year-class strength visualisations .....	71
	Appendix 2. Site details and chemistry of additional water samples .....	78

## List of tables

Table 1. Summary rainfall/flow information (1930–2007).....	4
Table 2. Major rivers and creeks in the Mid and South regions of the southern Gulf of Carpentaria barramundi genetic stock area.....	11
Table 3. Data availability for key data types used in this study.....	18
Table 4. Summary information of samples selected for $^{87}\text{Sr}/^{86}\text{Sr}$ analysis from the DAF barramundi otolith collection. ....	20
Table 5. Site details and chemistry of water samples used to develop conservative mixing curves of $^{87}\text{Sr}/^{86}\text{Sr}$ to infer salinity and likely habitat residency of barramundi in south- eastern Gulf of Carpentaria rivers.....	22
Table 6. Results of the all-subsets generalised linear models predicting the abundance of barramundi age-classes (3 to 9 years) for the Mid sub-stock (13°S to 16°S) of the southern Gulf of Carpentaria with Mitchell River flow ( $F_M$ ). ....	29
Table 7. Results of the all-subsets generalised linear models predicting the abundance of barramundi age-classes (3 to 9 years) for the South sub-stock (16°S to Queensland/Northern Territory border) of the southern Gulf of Carpentaria with Flinders River flow. ....	35
Table 8. Results of the all-subsets generalised linear models predicting the abundance of barramundi age-classes (3 to 9 years) for the South sub-stock (16°S to Queensland/Northern Territory border) of the southern Gulf of Carpentaria with Gilbert River discharge.....	36
Table 9. Results of the all-subsets generalised linear models predicting the abundance of barramundi age-classes (3 to 9 years) for the South sub-stock (16°S to Queensland/Northern Territory border) of the southern Gulf of Carpentaria with Flinders ( $F_F$ ) and Gilbert ( $F_G$ ) rivers flow .....	37
Table 10. Pearson correlation coefficients between river flow variables and atmospheric indices for each study region. ....	39
Table 11. Linear mixed model design, parameter coefficients and statistical significance of fixed effects included in the top ( $\leq 2\text{AICc}$ ) models for river flow variables and atmospheric indices for the Mitchell, Gilbert and Flinders rivers.....	43
Table 12. Predicted changes in juvenile barramundi growth rates (otolith increment widths) in the Mitchell region for water development Scenario X, relative to current river discharge volumes.....	45
Table 13. Habitat residency of barramundi harvested from estuaries of the Mitchell, Gilbert and Flinders rivers in the southern Gulf of Carpentaria based on inference from otolith $^{87}\text{Sr}/^{86}\text{Sr}$ profiles.....	47

## List of figures

Figure 1. Satellite imagery of the southern Gulf of Carpentaria, 8 January 2021. ....	5
Figure 2. Map of the northern (NGoC) and southern (SGoC) Gulf of Carpentaria barramundi genetic stocks and commercial fishery reporting grids. ....	8
Figure 3. Map of the regions from which otoliths were selected, including logbook grids (hatched) and relevant river flow gauging stations. ....	13
Figure 4. Captured image (16x magnification, reflected light) of a thin-sectioned barramundi otolith. ....	14
Figure 5. Reported commercial catch and nominal catch rate for barramundi from the Mid sub-stock (13°S to 16°S) of the southern Gulf of Carpentaria. ....	24
Figure 6. Observed length-at-age for legal size barramundi from the Mid sub-stock (13° to 16°S) of the southern Gulf of Carpentaria. ....	25
Figure 7. Estimated age-frequencies (percent) of barramundi from the Mid sub-stock of the southern Gulf of Carpentaria monitored by Fisheries Queensland, 2001–2018 displayed. ....	26
Figure 8. Visualisation of relative year-class strength index of barramundi from the Mid sub-stock. ....	27
Figure 9. Estimated age composition of the commercial barramundi catch per unit effort (CPUE) per calendar year for the Mid sub-stock (13°S to 16°S) of the southern Gulf of Carpentaria. ....	28
Figure 10. Estimated contribution per year-class (YC), to annual commercial barramundi catches (2000–2018) for the Mid sub-stock (13°S to 16°S) of the southern Gulf of Carpentaria. ....	28
Figure 11. Reported commercial catch and nominal catch rate for barramundi from the South sub-stock (16°S to the Queensland/Northern Territory border) of the southern Gulf of Carpentaria. ....	30
Figure 12. Observed length-at-age for legal size barramundi from the South sub-stock (16°S to the Queensland/Northern Territory border) of the southern Gulf of Carpentaria between 2000 and 2018 inclusive. ....	31
Figure 13. Estimated age-frequencies (percent) of barramundi from the South sub-stock of the southern Gulf of Carpentaria monitored by Fisheries Queensland, 2001–2018 displayed. ....	32
Figure 14. Visualisation of relative year-class strength index of barramundi from the South sub-stock. ....	33
Figure 15. Estimated age composition of the commercial barramundi catch per unit effort (CPUE) per year for the South sub-stock (16°S to the Queensland/Northern Territory border) of the southern Gulf of Carpentaria. ....	34
Figure 16. Estimated contribution per year-class (YC) to the commercial barramundi catch (2000–2018) for the South sub-stock (16°S to Queensland/Northern Territory border) of the southern Gulf of Carpentaria. ....	34
Figure 17. Relative frequency histogram of barramundi otolith edge type per month. ....	38

Figure 18. Total river discharge (in ML) per wet season in (a) the Mitchell, (b) the Gilbert and (c) the Flinders region, and (d) Madden–Julian Oscillation (MJO) and (e) Southern Oscillation Index (SOI) summer intensities. ....	40
Figure 19. Predicted mean ( $\pm 95\%$ confidence intervals) otolith increment width for the Mitchell (a) to (e), the Gilbert River (f) to (i) and the Flinders River (j) to (m). ....	44
Figure 20. Difference in cumulative otolith widths of juvenile barramundi in the Mitchell region under the current flow scenario (blue) and under modified flow Scenario X (red)..	45
Figure 21. Freshwater–marine mixing curve of dissolved strontium isotopes ( $^{87}\text{Sr}/^{86}\text{Sr}$ ) across the salinity gradient for rivers of the south-eastern Gulf of Carpentaria, based on observed water samples. ....	46
Figure 22. Otolith $^{87}\text{Sr}/^{86}\text{Sr}$ profiles (5-point smoothed) of ablation transects (core to proximal edge displayed) of barramundi caught in the Mitchell River estuary.....	48
Figure 23. Annual (wet-season year) flow for the (a) Mitchell, (b) Gilbert and (c) Flinders rivers in the southern Gulf of Carpentaria.....	49
Figure 24. Monthly flows across the wet-season year for the (a) Mitchell, (b) Gilbert and (c) Flinders rivers in the southern Gulf of Carpentaria. ....	50
Figure 25. Otolith $^{87}\text{Sr}/^{86}\text{Sr}$ profiles (5-point smoothed) of ablation transects (core to proximal edge displayed) of barramundi from the Gilbert River estuary.....	51
Figure 26. Otolith $^{87}\text{Sr}/^{86}\text{Sr}$ profiles (5-point smoothed) of ablation transects (core to proximal edge displayed) of barramundi from the Flinders River estuary.....	53
Figure 27. Total length modelled as a function of age-class and habitat class (freshwater or non-freshwater). ....	54
Figure 28. Total length modelled as a function of age-class and habitat class (freshwater, intermediate or estuary). ....	55

## Acronyms

AIC.....	Akaike information criterion
AICc .....	second-order Akaike information criterion
CSIRO .....	Commonwealth Scientific and Industrial Research Organisation
DAF.....	Department of Agriculture and Fisheries (Queensland)
ENSO .....	El Niño Southern Oscillation
EOS .....	end-of-system
FRDC.....	Fisheries Research and Development Corporation
GL.....	gigalitre (1,000,000 L)
GLM.....	generalised linear model
GoC .....	Gulf of Carpentaria
GOCIFFF .....	Gulf of Carpentaria Inshore Fin Fish Fishery
log.....	natural logarithm, unless otherwise specified
MJO .....	Madden–Julian Oscillation
ML.....	megalitre (1,000 L)
ppt .....	parts per thousand
SOI.....	Southern Oscillation Index
Sr .....	strontium
YCS .....	year-class strength



## Acknowledgements

We thank the many people who have contributed time, effort and samples that have made this piece of work possible. This includes Fisheries Monitoring staff of Fisheries Queensland (collection, processing and ageing of samples), the seafood processors, and commercial and recreational fishers (past and present) who donated fish/frames to the long-term monitoring program of the Gulf of Carpentaria Inshore Fin Fish Fishery, without which we could not have undertaken such a temporally extensive study of barramundi in Queensland Gulf of Carpentaria rivers.

For growth work, Water Observations from Space were provided by Geoscience Australia's Digital Earth Australia program ([www.ga.gov.au/dea](http://www.ga.gov.au/dea)). Digital Earth Australia makes data from the United States and European Commission readily available to Australian government and industry. Thanks to Dr Claire Krause of Geoscience Australia for making the product available to us, querying the database and disseminating the results; Chris Ndehedehe for access to trial use of GRACE (Gravity Recovery and Climate Experiment) and SWS (Space Weather Services) remotely sensed datasets to support this work.

For otolith microchemistry work, we thank the Department of Environment and Science (Queensland) QCatchments team, who collected most of the water samples and kindly provided access to the cation and trace metal water chemistry results. We thank Michele Burford, Stephen Faggotter (Griffith University) and Rob Kenyon (CSIRO) for collection of estuarine water samples. We thank Kowanyama Rangers John Clark, Anzac, Fitzroy and Tommy for sharing their knowledge and assisting us to collect water and fish samples from the Mitchell region.

This project is jointly funded through the Department of Agriculture and Fisheries (Queensland) and the Northern Australia Environmental Resources Hub of the Australian Government's National Environmental Science Program.

## Executive summary

Barramundi were used as an indicator species for the effects of river flows on estuaries because they use a variety of aquatic habitats (marine to freshwater) and are an iconic fisheries species of significance in northern Australia. The Fisheries Queensland commercial catch logbook and monitoring data for length, age and reproductive data provide a long-term data series of this estuarine-dependent species in the Gulf of Carpentaria (GoC).

Analysis of catch and age data identified highly variable recruitment of GoC barramundi that is significantly related to river flow. Patterns in catch-at-age highlighted the importance of the sequential pattern of river flow over multiple years for barramundi population dynamics. As a long-lived species (maximum observed age of 22 years in the GoC), with female maturity occurring on average at 7 years, barramundi are an indicator of long-term ecological health, integrating inter-annual patterns in the relationship between estuarine production (in the broadest sense) and river flows in catchments of the GoC.

Growth rates of juvenile barramundi, derived from the Queensland Department of Agriculture and Fisheries' historic collection of otoliths (i.e. fish ear bones), were significantly and positively related to wet-season river flow in the Mitchell, Gilbert and Flinders rivers. Modelling of barramundi growth rates in the Mitchell River under a major water development scenario (i.e. 6,000 GL total extraction from three nodes, with a low pump-start threshold and a zero allocation to end-of-system, considered by the Northern Australian Water Resource Assessment) indicated that by 3 years of age, juvenile barramundi would be on average about 19% smaller than under base flow conditions. Reduced growth rates leading to smaller fish is likely to result in increased natural mortality for juvenile barramundi. The available time series of river flows for base and existing entitlements under the current Gulf Water Resource Plan were not sufficiently up-to-date to allow a similar analysis for the Gilbert and Flinders rivers, but should be a priority if data become available.

Barramundi is a catadromous species, spawning in marine salinity water, then opportunistically accessing freshwater habitats as juveniles. Strontium<sup>87/86</sup> isotope ratios in otoliths indicated variable use of freshwater habitats by barramundi in the Mitchell, Gilbert, and Flinders rivers. The Mitchell River had the highest freshwater residency (~60%), with residency defined as the type of aquatic habitat inhabited during the dry season. The Flinders River had the highest estuarine residency (~67%), while the Gilbert River had the highest 'intermediate' residency (i.e. brackish, 49%). These results indicate that the geomorphology and inter-annual river flow patterns of the Mitchell, Gilbert and Flinders rivers offer variable opportunities for the spatial and temporal connectivity of aquatic habitats used by barramundi, including the seasonal floodplains.

Water-resource development should aim to minimise the disruption to the frequency and duration of aquatic habitat inundation and connection in order to maintain the natural productivity of GoC catchments that supports barramundi populations. Further work is required to provide catchment-specific estimates of barramundi use of aquatic habitats, particularly in the Gilbert and Flinders catchments, which could be explicitly used in quantitatively assessing the impacts of water development scenarios.

Currently, the long-established Gulf of Carpentaria Inshore Fin Fish Fishery harvests barramundi and other species (e.g. king threadfin) that rely on estuarine productivity (i.e. abundance, age-structure and biomass) supported by a spatial and temporal patchwork of river flows. This concurs with the finding on juvenile banana prawns ([component 1 of this project](#)) that the Mitchell, Gilbert and Flinders rivers all contribute to estuarine fisheries production, with high variability from year to year.

Barramundi is a species well adapted to the inter-annual variation in climate and wet-season rainfall of northern Australia. They are highly fecund (i.e. producing millions of eggs) and capable of very fast growth and high survival under optimal conditions (i.e. successive good wet seasons with river flows facilitating access to a range of aquatic habitats). However, the GoC and associated catchments are prone to extremes in climate. Successive poor wet seasons, such as occurred between 2013 and 2015, result in the reduced spatial extent of aquatic habitats. This in turn results in reduced barramundi recruitment, growth and survival. We suggest barramundi population dynamics are most sensitive to altered patterns of river flow during and immediately after successive years of below median flow. Water-resource development and planning in the Mitchell, Gilbert and Flinders rivers should aim to not exacerbate or prolong the impacts of climate variability on GoC barramundi populations.

The current study was a component of a [larger project](#) that examined the link between river flows, flood-driven productivity and fisheries of the southern GoC to inform water-resource planning and development. It also complements [another Hub project](#) that examined the impact of water-resource development on migratory shorebirds. That project identified the potential for water-resource development in GoC rivers to impact nutrient inputs and availability of food resources for migratory shorebirds. Together, these projects provide consistent evidence that freshwater flows in GoC estuaries and floodplains are essential for these ecosystems and their associated fauna. Impacts of modified river flows on multiple aspects of the ecosystem (e.g. prawns, fish, shorebirds) should be explicitly considered during water planning.

# 1. Introduction

Barramundi (*Lates calcarifer*) is an iconic fishery species and a key predator in aquatic habitats of the Gulf of Carpentaria (GoC). It is a major component of the inshore commercial net fishery in the region, with an average harvest of about 626 tonnes per year for 2009–2018, and average gross value of production beach price of about \$17 million per year). Barramundi is also a target species for recreational fishing tourism in the southern GoC and is important to Indigenous communities (BDO EconSearch 2020).

Facultative (i.e. non-essential) catadromy has been demonstrated for barramundi and there are alternate theories as to the reasons for this variability (Pender and Griffin 1996; de Lestang et al. 2000; Milton and Chenery 2005; Milton et al. 2008; Halliday et al. 2012; Crook et al. 2016).

Indices of barramundi recruitment have been previously considered during water-resource planning for Gulf rivers (Bayliss et al. 2014). The difficulty in representatively sampling young-of-the year barramundi often results in a recruitment index that is hindcast from the age-structure of fish harvested by the commercial fishery. This index, often referred to as year-class strength (YCS), has been modelled against river flows in various locations, and several mechanisms have been speculated (Staunton-Smith et al. 2004; Halliday et al. 2012; Crook et al. 2016). Further understanding of these theorised mechanisms that link YCS to river flows is ongoing (e.g. Chan et al. 2012).

The overall aim of [this project](#) was to examine the links between river flow, flood-driven productivity and fisheries of the southern GoC, to inform water-resource planning and development. To this end, component 4 of this project undertook three tasks:

1. an analysis of Queensland Department of Agriculture and Fisheries (DAF) barramundi catch and age information against available data of river flows, as a proxy for floodplain inundation and primary production, given that the latter two were not available as time series
2. an analysis of juvenile barramundi growth with river flows, using otolith increment widths as a proxy for somatic growth
3. an analysis of the microchemistry of barramundi otoliths to obtain a population perspective of how barramundi use aquatic habitats in the rivers of the southern GoC and how facultative catadromy is related to hydrologic opportunity.

Results are discussed in the context of the consequences for barramundi recruitment, growth and fisheries productivity.

## 1.1 Rivers of interest

The Mitchell, Gilbert and Flinders rivers and associated catchments occur within the wet-dry tropics of northern Australia (Warfe et al. 2011). Summary information derived from the National Australia Sustainable Yields Project (CSIRO 2009) is included (Table 1) to provide context to the current work, and to highlight similarities and differences between GoC rivers in regard to a catadromous species such as barramundi. The lower reaches of the rivers include parts of the Gulf Plains bioregion, with the marine plains dominating the coastal edges of the catchments.

Table 1. Summary rainfall/flow information (1930–2007).

Region	Daly	Roper	South-west	Flinders-Leichardt	South-east	Mitchell
Catchments	Daly	Koolatong Walker Roper Towns Limmen Bight Rosie	McArthur Robinson Calvert Settlement Nicholson	Leichardt Morning Inlet <sup>WR</sup> Flinders	Norman Gilbert Staaten <sup>WR</sup>	Mitchell
Area (km <sup>2</sup> )	54,423	128,518	111,890	145,223	122,094	72,229
Rainfall coefficient of variation	0.25	0.30	0.39	0.42	0.38	0.29
Mean annual (Sep–Aug) rainfall (mm)	1,019	843	670	493	750 <sup>A</sup>	965 <sup>A</sup>
Mean annual rainfall deficit (mm)	–902	–1,085	–1,291	–1,446	–1,230	–940
Volume of streamflow (GL/year)	8,653	14,394	9,958	6,390	14,430	14,301
Major perennial rivers	yes	yes	yes	no	no	yes

Regions derived from the Northern Australia Sustainable Yields Project (CSIRO 2009) for comparative purposes. Note: 1930 to 2007 does not include the rainfall/flow/flood events of 2009, 2011 or 2019 which occurred in the Mitchell, Gilbert and Flinders rivers. <sup>WR</sup> designated 'wild river' with limited potential for development; <sup>A</sup> excludes coastal floodplain rainfall.

### 1.1.1 Mitchell River

The Mitchell River has a catchment area of 72,229 km<sup>2</sup> and a length of about 500 km. The lower catchment includes the Mitchell River Fan Aggregation, which is listed in the Directory of Important Wetlands in Australia. Wet-season river flows from the Mitchell River distribute across these wetlands, which extend along ~125 km of coastline, from the Nassau River in the south to the Mitchell and Alice Rivers and Yanko Creek in the north. The 715,000 ha of alluvial plain wetlands provide diverse and extensive areas of seasonal, semi-permanent and permanent aquatic habitats including 'deep' water habitats (EHP 2015). The Mitchell River has perennial river flow because of wet-season flows and year-round groundwater discharge from local and regional aquifers.

### 1.1.2 Gilbert River

The Gilbert River has a catchment area of 46,354 km<sup>2</sup>, which contains the Gilbert, Einasleigh and Etheridge rivers. The extensive coastal delta of the Gilbert River includes the nationally listed Smithburne-Gilbert Fan Aggregation wetland, which contains the greatest concentration of coastal floodplain lagoonal wetlands in western Cape York Peninsula and, along with the Mitchell River delta, is the largest landform feature of this type in the state of Queensland (EHP 2015). The Gilbert River plays an important role in distributing wet-season

river flows to seasonal wetlands between the Norman River and the Staaten River (i.e. along ~150 km of coastline). Figure 1 illustrates the floodwater pathways of the Gilbert River system during a 'moderate' flood as classified by the Australian Bureau of Meteorology. The floodwater pathway is a much broader area than the main Gilbert River channel considered by hydrological modelling during water-resource planning. The Gilbert River Formation of the Great Artesian Basin provides groundwater to upper reaches of the Norman and Gilbert rivers, extending base flows into the dry season. However, large parts of the Gilbert River system are ephemeral and cease-to-flow on average for 105 to 175 days per year (Petheram et al. 2013a: gs 917111A Minnies dip, Einsaleigh River, gs 917001A Rockfields Gilbert River).

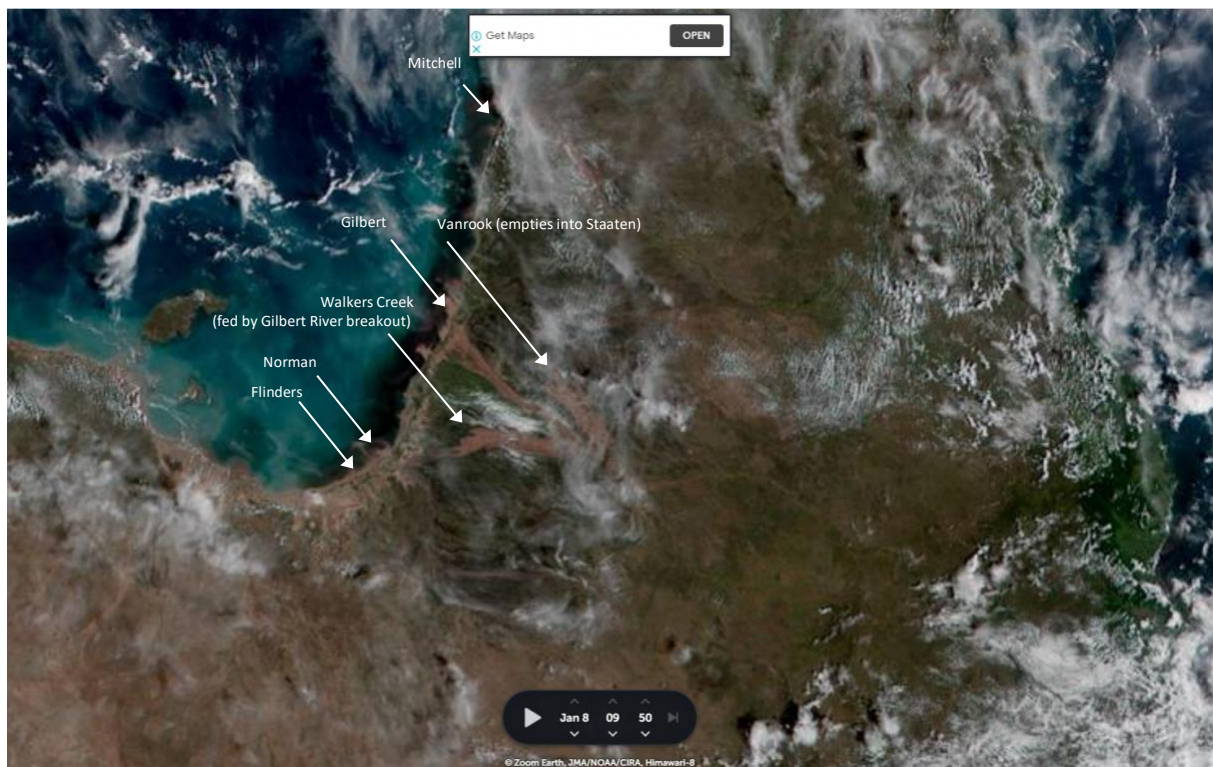


Figure 1. Satellite imagery of the southern Gulf of Carpentaria, 8 January 2021.

### 1.1.3 Flinders River

The Flinders River has a catchment area of 108,182 km<sup>2</sup>, and a length of ~1,000 km, being the sixth-longest river in Australia. The coastal delta of the Flinders River is part of the Southern Gulf Aggregation, which is an estuarine wetland covering 546,000 ha, extending from west of Burketown to the northeast of Karumba. It is the largest continuous estuarine wetland aggregation of its type in northern Australia (EHP 2015). Wet-season river flows from the Flinders River inundate these estuarine wetlands, which can extend along ~70 km of coastline. Tidal inundation, especially during the high 'spring' tides of summer, and freshwater flooding during the wet season are dominant influences on the productivity of this wetland. Within the Aggregation, wetlands can range from marine to brackish, and the majority are seasonal.

River flow in the Flinders River is dominated by wet-season rainfall, which runs off into the river channel or infiltrates into the alluvial aquifer. As river levels drop, groundwater then discharges from the alluvial aquifer into the river, until the groundwater level falls below that of the riverbed – when ‘the river runs dry’. The Flinders River system is highly ephemeral and ceases-to-flow on average for about 230 days per year (Petheram et al. 2013b: gs 915003A Walkers Bend, Flinders River). Permanent or near-permanent waterholes exist because of wet-season surface flows (Wallace et al. 2017), rather than groundwater contributions (CSIRO 2009), although Great Artesian Basin springs do occur in some areas of the Flinders catchment.

## 2. Methodology

### 2.1 Catch and age

#### 2.1.1 Catch and age data

The positive influence of river flows on barramundi has been common knowledge for a long time (e.g. Dunstan 1959). Multiple studies have reported relationships between catch and rainfall or river flow; for example, for the Fitzroy River, Queensland east coast (Robins et al. 2005); Princess Charlotte Bay (Balston et al. 2009a,b); all of Queensland (Meynecke et al. 2006); and the Daly River, Northern Territory (Bayliss et al. 2008). The analysis of fish age-structure underlying commercial harvest data (e.g. Staunton-Smith et al. 2004) has provided insights into likely causes of increases in catch, which result from increased catchability (an immediate effect) and increased recruitment success (a delayed effect).

The aim of this task was to analyse historic barramundi catch and age data held by DAF against available river flow data (gauged and/or modelled), as a proxy for floodplain inundation and primary production. Age-frequency data were derived from the DAF Fisheries Monitoring program, which began in 2000. This standardised program was designed to provide annual representative sampling of the length, reproductive condition and age of barramundi harvested by commercial and recreational fishers of the GoC to provide population-level data suitable for use in stock status evaluations and stock assessments (Campbell et al. 2017; Streipert et al. 2019). The collection is underpinned by stratified spatial and temporal sampling and ageing protocols (Fisheries Queensland 2010, 2012). The ageing protocols have a quality assurance approach that requires annual age-reader training, testing against a reference collection (as recommended by Campana 2005) and quality assurance procedures for accuracy and precision, including an index of average percent error that must be less than 5%. The Queensland DAF barramundi ageing protocols are based on known-age specimens (Russell et al. 2015) as well as reference specimens (Stuart and McKillop 2002).

In the GoC, barramundi spawn over spring and summer (i.e. October to March), with a peak in December/January (Davis 1985). The 1st of January is the nominal Queensland birth date for Queensland GoC barramundi. Year-class (i.e. birth-year) was assigned based on spawning year; for example, fish spawned between October 2008 and March 2009 are allocated to the 2009 year-class. The age-frequencies considered in the current study are relative frequencies, as sample sizes vary between collection years, and are equivalent to an age-specific catch per unit effort (Morrongiello et al. 2014).

There are two genetic stocks of barramundi within the Queensland section of the GoC – a northern stock and a southern stock (Jerry et al. 2013; Loughnan et al. 2019). Fisheries Queensland monitors barramundi at the genetic stock level, with length, age and reproductive samples collected for the southern GoC stock ([www.daf.qld.gov.au/business-priorities/fisheries/monitoring-compliance/monitoring-reporting/commercial-fisheries/species-specific/barramundi-from-the-gulf-of-carpentaria](http://www.daf.qld.gov.au/business-priorities/fisheries/monitoring-compliance/monitoring-reporting/commercial-fisheries/species-specific/barramundi-from-the-gulf-of-carpentaria)). The southern GoC barramundi stock extends across numerous catchments (Figure 2), which have inter-annual differences in the timing, duration, magnitude and frequency of freshwater flow events. The long-term age-frequency data held by Fisheries Queensland is not always sufficient for analyses at the spatial scale of individual rivers (i.e. Mitchell, Gilbert and Flinders). Therefore, in the current



analysis, age-frequencies were analysed at a sub-stock level, where (i) the ‘Mid’ sub-stock was defined as between 13°S and 16°S, with the major river influence being the Mitchell River; and (ii) the ‘South’ sub-stock was defined as between 16°S and the border between Queensland and the Northern Territory, with the major river influences being the Flinders and Gilbert rivers. The South sub-stock is also influenced by freshwater flows from the Staaten, Norman, Leichardt, and Nicholson rivers (Figure 2).

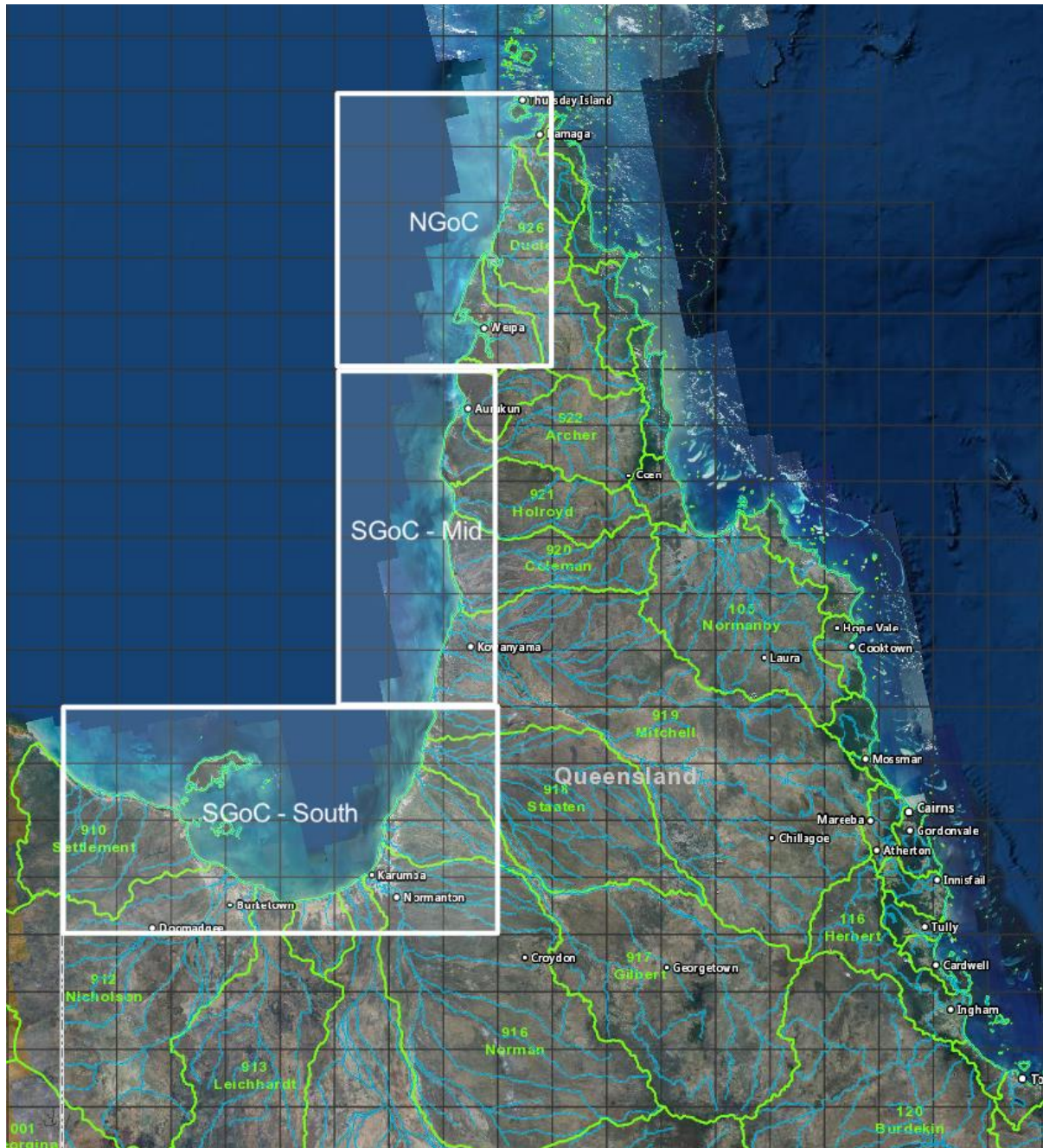


Figure 2. Map of the northern (NGoC) and southern (SGoC) Gulf of Carpentaria barramundi genetic stocks and commercial fishery reporting grids.

Harvest data for barramundi and associated effort data (days fished) were derived from the Fisheries Queensland commercial catch logbook CFISH database (data request number 2830).

### **2.1.2 Year-class strength**

Indices of recruitment were based on a catch-curve approach (Maceina 1997), using the sampled age-frequencies. We adopted a catch-curve approach for consistency and comparison with previous work (Halliday et al. 2012, Bayliss et al. 2014). The annual age-frequencies of barramundi harvested by the inshore net fishery (i.e. Gulf of Carpentaria Inshore Fin Fish Fishery [GOCIFFF], N3 symbol) were used to generate a longer time series with broader spatial representation of barramundi from the rivers of the southern GoC than previously considered.

The catch-curve approach of Maceina (1997) assumes that the deviations (i.e. studentised residuals) from the modelled abundance of age-frequencies (log transformed), after fitting age, is an index of relative recruitment strength of sampled year-classes. Large positive residuals indicate strong year-classes and large negative residuals indicate weak year-classes (Maceina 1997; Honsey et al. 2016). The approach assumes constant mortality and consistency in the age-classes that are fully recruited (i.e. available) to the fishery. We note that for barramundi in the GoC, mortality is likely to vary over time and that age-at-recruitment to the fishery (but not size-at-recruitment) is likely to vary over time. However, the catch-curve approach is considered robust to breaches of such assumptions (Telzaff et al. 2011) and generates a relative index of variation in YCS that can be linked to environmental factors such as river flows.

The analyses were restricted to a subset of available age-classes to reflect the selectivity of fish harvested (Staunton-Smith et al. 2004). In the GOCIFFF, barramundi harvest is regulated by a minimum legal size of 580 mm total length, and a maximum legal size of 1200 mm. Mesh sizes of the set gill nets used in this fishery are restricted to between 162.5 mm and 245 mm, with greater than 80% of the harvest since 2000 being caught in 6–6½ inch mesh gill nets (Streipert et al. 2019).

In the current study, analyses considered 19 sequential years of barramundi age-frequencies sampled between 2000 and 2018 (inclusive). We considered age-classes between 3 and 9 years of age to be fully available to the fishery, reflecting the mesh sizes used in the fishery. The studentised residuals from the linear model –  $\ln(\text{age-frequencies}) \sim \text{age} + \text{sample year}$  – were calculated and plotted against time to provide a visualisation of YCS.

We assumed that the fishery harvest of barramundi, given the relatively stable fishing regulations over the sampling years and consistency in mesh size of gill nets used, provided a relatively stable window into variation in age-frequencies over the sample years (Mais 1981). We assumed the length and age samples collected by Fisheries Queensland were representative of the harvest and that the harvest and effort data are accurately reported in the commercial catch logbook (CFISH), with errors randomly distributed across fishers over time and space.

### **2.1.3 Catch-at-age**

As an extension to standard YCS indices, we combined age-frequency data with reported harvest and effort data to derive a catch-at-age frequency per unit effort (Mais 1981). Catch-at-age is appropriate for barramundi from the southern GoC stock because harvest is size-selective not age-selective (Streipert et al. 2019). Consistency in management arrangements suggest that variation in age-frequency should be predominantly related to recruitment variability rather than variation in size-based selectivity. The catch-at-age matrix was assumed to be representative; that is, the reported harvest (after adjusting for effort) was accurate and proportional to population abundance. Ageing error was assumed to be small in comparison to variation in recruitment.

### **2.1.4 Flow data**

Multiple rivers discharge into the Queensland GoC, potentially influencing the southern GoC barramundi stock (Table 2). It was beyond the resources of the current study to generate suitable river flow and floodplain metrics for all rivers. The analyses use data for the Mitchell, Gilbert and Flinders rivers, which are major contributors of river flows to the GoC. Adjacent river systems are likely to influence barramundi populations but are not accounted for in the catch and age analyses presented herein.

We considered multiple sources of river flow data available, including gauged river flows from the Queensland Water Monitoring Information Panel ([water-monitoring.information.qld.gov.au](http://water-monitoring.information.qld.gov.au)) and the Bureau of Meteorology ([www.bom.gov.au/waterdata](http://www.bom.gov.au/waterdata)) and modelled end-of-system (EOS) discharge volumes from the Flinders and Gilbert Agricultural Resource Assessment and Northern Australia Water Resource Assessment. All data sources had limitations, such as missing data or a time series that was insufficient for the age-frequency-based analyses. At the outset of the current study, it was envisaged that a time series of floodplain inundation could be generated and used in analyses of fisheries data. It is possible that metrics of floodplain inundation may better capture the effects of river flows on fisheries production than discharge, which is a volumetric rate of river flow measured in litres per unit of time (i.e. per day, month, quarter or year). Estimating floodplain productivity and inundation using remote sensing has limitations, and recent work suggests that river discharge is a suitable indicator of hot spots of biomass accumulation (Ndehedehe et al. 2020; Ndehedehe et al. 2021). As such, and in the absence of a robust time series of floodplain inundation for the Mitchell, Gilbert and Flinders catchments (which we recommend should be generated), we used river discharge in the analyses of catch and age.

For analyses of YCS, we used modelled EOS flow for the Mitchell, Gilbert and Flinders rivers, provided by the CSIRO via the Fisheries Research and Development Corporation (FRDC) project 2018/079 ('Ecological modeling of the impacts of water development in the Gulf of Carpentaria with particular reference to impacts on the Northern Prawn Fishery').

Table 2. Major rivers and creeks in the Mid and South regions of the southern Gulf of Carpentaria barramundi genetic stock area.

Region and rivers	Potential data sources
<b>South SGoC barramundi sub-stock</b>	
Settlement Creek	No data
Nicholson	GS912101A @ Gregory Downs; AMTD 104 km; catchment area = 12,690 km <sup>2</sup>
Albert	No data
Leichardt	GS913007B @ Floraville Homestead; AMTD 100 km; catchment area = 23,660 km <sup>2</sup>
Morning Inlet	No data
<b>Flinders</b>	<b>GS915003A @ Walkers Bend; AMTD 103 km; catchment area = 106,300 km<sup>2</sup></b> <b>CSIRO – FGARA updated EOS*</b>
Norman	GS9160001B @ Glenore Weir; AMTD 102 km; catchment area = 39,360 km <sup>2</sup>
Walkers Creek	No recent data
<b>Gilbert*</b>	<b>GS917001D @ Rockfields; AMTD 276 km; catchment area = 10,990 km<sup>2</sup></b> <b>GS917014A @ Burke Development Road; AMTD 102 km; catchment area = 39,100 km<sup>2</sup></b> <b>CSIRO – FGARA updated EOS*</b>
Staaten	GS918003A @ Dorunda; AMTD 95 km; catchment area = 6,789 km <sup>2</sup>
<b>Mid SGoC barramundi sub-stock</b>	
Nassau	No data
<b>Mitchell</b>	<b>GS919009B @ Dunbar; AMTD 139 km; catchment area = 45,870 km<sup>2</sup></b> <b>CSIRO – AWRA-R EOS states non-routing, node 9190000*</b>
Coleman	No recent data
Edward	No data
Holroyd	No recent data
Archer**	GS922001A @ Telegraph Crossing; AMTD 203 km; catchment area = 2,828 km <sup>2</sup>
Watson**	GS923001A @ Jackin Creek; AMTD 62 km; catchment area = 1,001 km <sup>2</sup>

\* modelled flow data supplied by CSIRO via FRDC project 2018/079; \*\* time series of data insufficient due to missing data; 'catchment area' reports area that is upstream of the gauge. AMTD = adopted middle thread distance; AWRA-R = Australian Water Resources Assessment – River; EOS = end-of-system; FGARA = Flinders and Gilbert Agricultural Resource Assessment. Rivers of interest in bold.

### 2.1.5 Analysis with flow

Relationships between replicate samples of age-frequencies over time and potential explanatory river flow variables were analysed using a generalised linear model (GLM) of the form:

$$\ln(\text{age-frequency}) \sim \text{age-class} + \text{sample year} + \ln(\text{flow variables} + 1)$$

Typically, flow in the birth-year occurs during the first year of life and is standard in YCS analyses (see Morrongiello et al. 2014; Jenkins et al. 2015; Stoessel et al. 2018; Sullivan et al. 2018; Tonkin et al. 2020). As the purpose of the analysis was to inform planning for water development scenarios, analyses were conducted for flows for each river system, with  $F_M$

indicating Mitchell River flow,  $F_G$  indicating Gilbert River flow and  $F_F$  indicating Flinders River flow.

Flow data was aggregated into that occurring within the 'birth-year', noted in YCS analyses as  $F_0$ , aggregated by: (i) month (e.g.  $F_{0\_Jan}$  being flow in the birth-year for the month of January); and (ii) quarter, with quarters being October to December ( $F_{0\_OND}$ ), January to March ( $F_{0\_JFM}$ ), April to June ( $F_{0\_AMJ}$ ) and July to September ( $F_{0\_JAS}$ ).

The patterns in the catch-at-age data for barramundi observed during the current study highlighted that the age-structure of barramundi harvested in the southern GoC was the consequence of river flow in the birth-year ( $F_0$ ), as well as the sequential pattern of river flow over subsequent years. To account for the influence of river flows over sequential years on YCS and catch-at-age, flow variables were also constructed for: (iii) quarterly flows that occurred between the first and second birthday ( $F_{1\_OND}$ ,  $F_{1\_JFM}$ ,  $F_{1\_AMJ}$  and  $F_{1\_JAS}$  occurring during the second year of life); (iv) quarterly flows that occurred between the second and third birthday ( $F_{2\_OND}$ ,  $F_{2\_JFM}$ ,  $F_{2\_AMJ}$ , and  $F_{2\_JAS}$ , occurring during the third year of life); and (v) flows occurring between the third birthday and when an age-class was captured (i.e.  $F_{3\_to\_Capture}$ ). Sample year was forced as a categorical factor in the GLM as is standard practice (Staunton-Smith et al. 2004; Morrongiello et al. 2014).

## 2.2 Growth

The barramundi growth models presented herein, and their interpretation, are preliminary. Refined analyses using EOS river discharge provided by the CSIRO can be found in Leahy and Robins (2021), available at [era.daf.qld.gov.au/id/eprint/8174](http://era.daf.qld.gov.au/id/eprint/8174)

### 2.2.1 Otolith data

Barramundi harvests in the southern GoC have been routinely monitored for length, age and gender by DAF's Fisheries Queensland for assessment purposes since 2000. This includes annual collection and preparation of thin-sectioned sagittal otoliths, used for age-frequency purposes, with spatial sub-sampling from commercial and recreational fishers, seafood processors and research projects across the stock. Barramundi otoliths were sourced from this archive for the collection years between 2000 and 2018. Catch location had varying levels of precision, depending on the sample source. For consistency, spatial location was allocated using Queensland commercial fishery logbook grids ([www.business.qld.gov.au/industries/farms-fishing-forestry/fisheries/monitoring-reporting/requirements/logbook-maps](http://www.business.qld.gov.au/industries/farms-fishing-forestry/fisheries/monitoring-reporting/requirements/logbook-maps)). To ensure adequate sample sizes, individuals from the Flinders region were captured from the Flinders River or the grid AD18 (Figure 3). Individuals from the Gilbert region were captured from the Gilbert River, grid AC16 or the Smithburne River, which is within the floodplain of the Gilbert River but diverges from the main channel about 100 km from the coast (Whitehouse 1943). Individuals from the Mitchell region were captured from the Mitchell River, grids AB13 or AC14, or the Nassau River, which is within the floodplain of the Mitchell, but diverges from the main channel about 100 km from the coast and is fed by lateral flows (Whitehouse 1943). Sample sizes for the Flinders and Mitchell regions were supplemented using barramundi collected by FRDC research project 2007/002 (a collaborative project with the Tropical Rivers and Coastal Knowledge program), between March 2008 and January 2011 (Halliday et al. 2012).

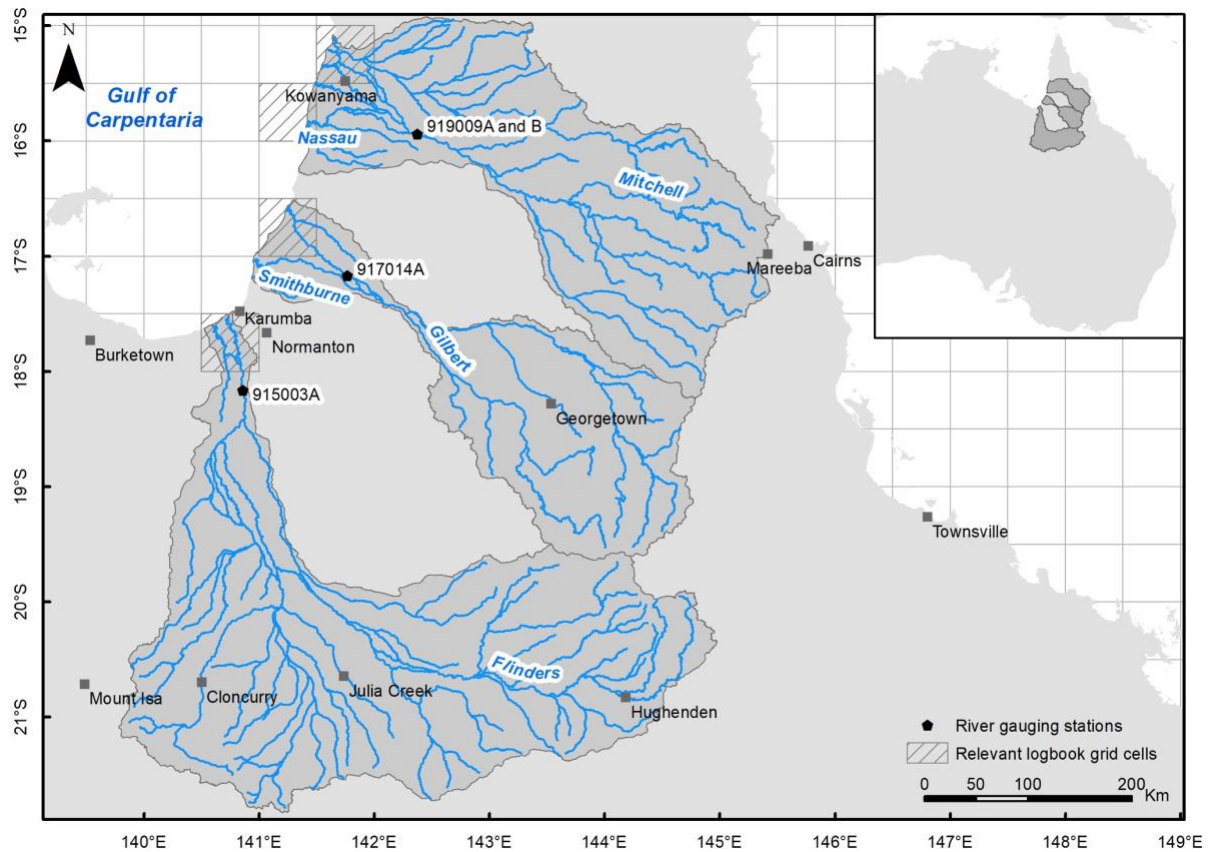


Figure 3. Map of the regions from which otoliths were selected, including logbook grids (hatched) and relevant river flow gauging stations.

Sagittal otoliths had been removed and sectioned as per Fisheries Queensland (2010) standard protocols. Age and increment width measurements were taken from still images of transverse otolith sections viewed using reflected LED light at 16x magnification on a Leica MZ6 microscope and captured on a Leica DFC295 camera (Leica-Microsystems, Germany). When viewed using reflected light, annual increments in barramundi otoliths appear as pairs of wide translucent and narrow opaque zones (Fisheries Queensland 2012). In the GoC, barramundi growth rates are fastest during the hot wet season from approximately October to March (Xiao 1999), when the wide translucent zone is formed in the otolith. In northern Australia, barramundi growth rates slow during the cool dry season from approximately April to September (Xiao 1999). The narrow opaque zone is likely formed during this season, as recorded for barramundi on the east coast of Australia (Stuart and McKillop 2002; Staunton-Smith et al. 2004). The nominal birth date for barramundi in Queensland (Fisheries Queensland 2012) is the 1st of January. Year-class was assigned based on sample year and age-class.

Age-class, which is a combination of increment count, edge classification and date-of-capture as per its age-allocation matrix (Fisheries Queensland 2012). Increment count and edge classification was estimated from two readings in separate sessions by a single reader (S. Leahy). The index of average percent error was < 3%, which is considered sufficiently precise (Chilton and Beamish 1982; Robertson and Morison 1999). If the age-class estimate for an individual fish differed between reading sessions, the otolith was read a third time by the same reader and the consensus age-class was used for year-class determination.

Otolith increment widths were measured for the first 3 'years' of growth (i.e. age 0+, 1+ and 2+), which captures the period of most rapid somatic growth in barramundi (Stuart and McKillup 2002). This period is the ontogenetic stage in which growth rates are most strongly influenced by freshwater nursery habitat availability (Russell et al. 2015; Roberts et al. 2019) and/or increased food availability from productivity responses to freshwater flows (Davies et al. 2008; Pettit et al. 2017). Therefore, we expected inter-annual differences in freshwater availability and subsequent growth rates (using the proxy of otolith increment widths) to be most apparent and influential in these first 3 years of life.

Barramundi otoliths do not have a perfectly linear growth axis (Figure 4) that is present in some species (e.g. Stocks et al. 2011; Godiksen et al. 2012; Ong et al. 2015; Barrow et al. 2018). Therefore, otolith increment widths were measured using a polyline along the clearest path near the ventral edge of the *sulcus acusticus*, perpendicular to the axis of increment formation (Figure 4), similar to Matta et al. (2010), Morrongiello et al. (2014), Katayama (2018) and Martino et al. (2019). Measurements were taken from the otolith core to the area of peak luminosity (i.e. most opaque area) in the first opaque zone (i.e. increment) to capture the fast summer and slow winter growth experienced by the fish in its first year of life. The distance between the area of peak luminosity in the first opaque zone and the area of peak luminosity in the second opaque zone represented growth in a fish's second year of life, and so on for growth in a fish's third year of life. The area of peak luminosity was used for replicability of the results and to minimise the subjectivity inherent in visual assessment of the transition area between opaque and translucent zones at minute spatial scales. Measurements were taken in Image-Pro Plus 7.0 (Media Cybernetics, USA).

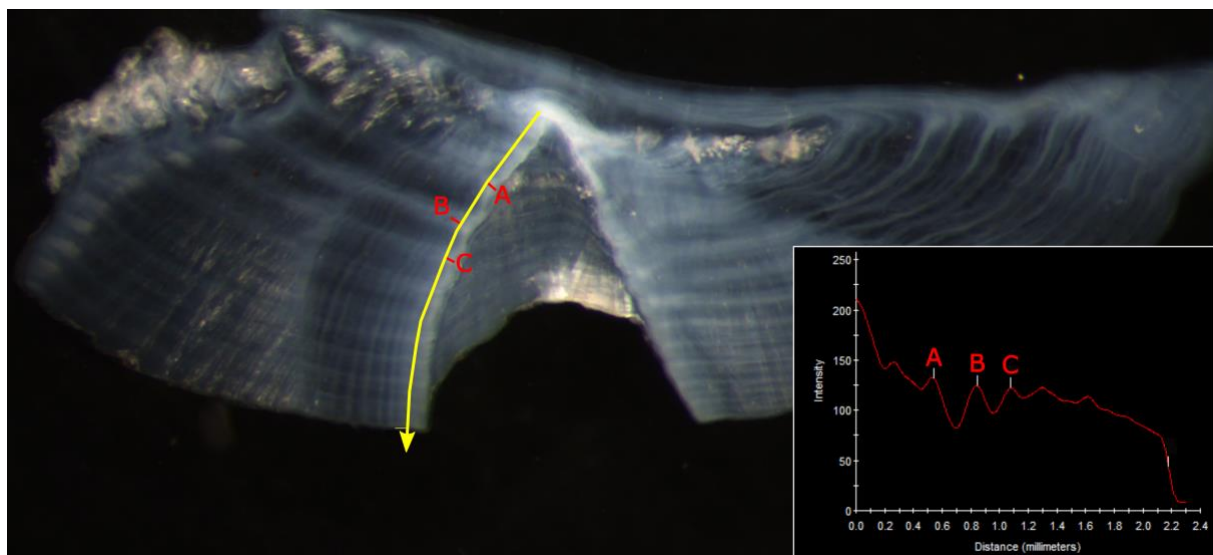


Figure 4. Captured image (16x magnification, reflected light) of a thin-sectioned barramundi otolith.

Placement of the polyline (in yellow) and the increment markers (in red). Inset: light intensity of the polyline transect, including placement of the increment markers to coincide with peak luminosity (i.e. light intensity). Otolith ID: QLc1016, from the Mitchell region.

Measurements of small morphometric characteristics are disproportionately vulnerable to measurement-effect errors (Yezerinac et al. 1992). We considered annual otolith increment widths in barramundi (in this study, mean = 0.496 mm, 0.310 mm, 0.221 mm for increments 1, 2, and 3, respectively) to be vulnerable to this source of error. Consequently, stringent quality control measures were adopted to maximise the statistical power of subsequent data analyses (Yezerinac et al. 1992). Sectioned otoliths were excluded from the dataset if they were unreadable (i.e. received a readability score of 1; Fisheries Queensland 2012). Measurements were taken twice by a single reader in separate measuring sessions. If the difference between the first and second measurement sessions for each of the three increments of any given otolith was  $\leq 15\%$ , then the final value of each increment width was calculated as the mean of the two measuring sessions. If any increment widths differed by  $>15\%$  between the two measuring sessions, then the otolith was measured a third time. As above, where the difference between the first and third session for each of the three increments was  $\leq 15\%$ , the value of each increment width was calculated as the mean of the first and third measuring sessions, and similarly for agreement between the second and third measuring sessions. Finally, if the measurements of any increments differed by  $>15\%$  between all three combinations of measuring sessions, then the otolith was excluded from the dataset. This quality control procedure resulted in an increment width dataset of increments 1 to 3 for: (i) 860 individuals in the Flinders region, (ii) 283 individuals in the Gilbert region, and (iii) 325 individuals in the Mitchell region.

### **2.2.2 Environmental data**

#### **Water availability**

Seasonal flooding is an important driver of barramundi population dynamics, as evidenced in growth rates (Robins et al. 2006), YCS (Staunton-Smith et al. 2004; Halliday et al. 2012), exploitable biomass (Tanimoto et al. 2012) and subsequently commercial catch (Robins et al. 2005). The exact mechanisms underpinning this are speculated to be the result of flow-stimulated increases in the biological productivity of estuarine habitats and the connection of seasonal nursery habitats used by juvenile barramundi (Halliday et al. 2012).

*In situ* river discharge data in the GoC are spatially and temporally patchy. For this reason, *in situ* river gauge datasets (DNRME 2018) were supplemented with modelled EOS or node-based river flow products from the CSIRO (Hughes et al. 2017) and Queensland Department of Environment and Science (Gilbert and Flinders, Queensland Hydrology unit, unpublished data). Hydrodynamic models are designed for evaluating water development scenarios and provide modelled daily river discharge data that include historical and current water abstraction in each region.

#### **Mitchell region**

An *in situ* river gauge dataset of daily river discharge was available from July 1995 to June 2018 by pooling the records from the Koolatah (919009A) and Dunbar (919009B) gauging stations. Modelled flow data were available from January 1900 to December 2015 at the mouth of the Mitchell River (node 9190000, i.e. EOS) and node 9190090, equivalent to the Dunbar gauging station. *In situ* and modelled datasets showed strong agreement ( $r > 0.82$ ). For temporal consistency, modelled flow data from the EOS node was used for all further analyses on barramundi growth rates in the Mitchell region.



## **Gilbert region**

*In situ* river gauge data suitably low in the catchment was only available from February to August 2015, and then again from February 2016 to June 2018 (station 917014A, ~102 km from the mouth of the Gilbert). Draft hydrological modelled river flow data were available from January 1970 to February 2016 at the EOS node for the Gilbert catchment (Queensland Hydrology unit, unpublished data). *In situ* and modelled datasets showed strong agreement, although overlapping data points were sparse ( $r = 0.82$ ,  $n = 24$ ). The EOS modelled dataset for the Gilbert River was more temporally complete and was therefore selected for use in all further analyses on barramundi growth rates in the Gilbert region.

## **Flinders region**

*In situ* river gauge data near the EOS were available from July 1995 to July 2018, but with temporal gaps in 1996, 1997, 1998, 2004, 2005 and 2010 (Walkers Bend, gauging station 915003A). Modelled river flow data were available from July 1889 to June 2011 at the node equivalent to the *in situ* gauge (Queensland Hydrology unit, unpublished data). *In situ* and modelled datasets showed excellent agreement ( $r = 0.94$ ). Therefore, modelled river flow data were used to infill minor gaps in the *in situ* gauge time series using an optimised polynomial function, derived using the *basicTrendline* package in R (Mei 2019):

$$y = -1.1363 * 10^{-6}x^2 + 1.551x + 161.99 \quad \text{Eq. 1}$$

where  $y$  is the *in situ* gauge-measured river discharge volume, and  $x$  is the modelled flow at that location. The infill model had an  $R^2$  of 0.897, and the infilled dataset was used in all further analyses on barramundi growth rates in the Flinders region.

## **Flow variables**

Peak growth rates in barramundi occur in summer (approximately October to March, Xiao 1999), and do not coincide with the calendar year. Calendar months were therefore reclassified into hydrological years starting in October and ending the following September. Total river discharge per month was calculated for each region, in each year for which concurrent barramundi otolith increment data were available. River flow was minimal or absent in July, August and September for all study years; therefore, those months were excluded from further analyses. Data exploration indicated that total discharge in each month was highly collinear between months, with coarse similarity groupings in October–November–December, January–February–March and April–May–June. Total discharge was therefore summed by quarter, with flow in October–November–December ( $F_{\text{OND}}$ ) representing an early start to the wet season, January–February–March ( $F_{\text{JFM}}$ ) capturing peak wet-season flow and April–May–June ( $F_{\text{AMJ}}$ ) capturing a late end to the wet season, including natural draining of each catchment. Total discharge per quarter was natural log transformed to improve variable distribution.

Measures of wet-season maximum flow and flow duration were produced in case these might prove more influential than total discharge on barramundi growth rates: (1) maximum weekly average discharge encountered at any point between October and June the following year, and (2) duration (in weeks) of flows in the 60th percentile and above between October and June the following year. However, both variables were discarded due to redundancy with log-transformed total discharge in one or more quarters. Peak discharge was highly collinear with total discharge in the January–February–March quarter, and the duration of >60th

percentile flows was somewhat collinear with October–November–December and April–May–June quarterly discharge.

## Temperature

Temperature is a fundamental determinant of growth rates in fish, with potentially large effects on otolith growth (Gillanders et al. 2012). However, final growth models did not include any temperature variables due to: (1) a shortage of *in situ* water temperature records for the study regions and time frames of interest; (2) vulnerability of remotely sensed measures of water temperature to cloud cover (e.g. MODIS); and (3) collinearity between available historical water temperature and measures of wet-season flood extent, duration and flow volume.

## Atmospheric indices

Regional or continental-scale atmospheric indices can be related to fish growth rates (Martino et al. 2019) and catch rates (Balston 2009a,b). Atmospheric indices can be a proxy for a conglomerate of local environmental conditions over an extended period. In some cases, they can serve as better predictors of ecological processes than direct measures of local conditions (Hallett et al. 2004). In the current study, relationships between two atmospheric indices and barramundi growth rates were explored as an alternative to river discharge volume. They were the Southern Oscillation Index (SOI) and the Madden–Julian Oscillation (MJO), which have previously been used to model ecological processes in northern Australia.

The SOI is an indicator of El Niño and La Niña events. In northern Australia, El Niño (i.e. sustained SOI values less than –8) is associated with hotter and drier than normal conditions, while La Niña (i.e. sustained SOI values greater than +8) is associated with cooler and wetter than usual conditions (Bureau of Meteorology 2012). Monthly SOI values were accessed via the Australian Bureau of Meteorology ([bom.gov.au](http://bom.gov.au)) and were classified into ‘summers’ starting in October and ending in March, to align with annual patterns in barramundi growth and the northern wet season. Monthly SOI values were averaged within each summer.

The MJO describes an eastward moving body of moist air that results in locally increased sub-equatorial cloud cover and rainfall in a 30-to-60-day recurring cycle (Madden and Julian 1972). Phases 4 and 5 of the MJO capture the intensity of the MJO roughly over the GoC region (Wheeler and Hendon 2004). Phase 4 (centred on longitude 140°E) was selected, as it captures enhanced convective activity on the eastern side of the GoC. MJO intensity values in the Phase 4 region were available every 5 days from the US National Weather Service ([cpc.ncep.noaa.gov/products/precip/CWlink/daily\\_mjo\\_index/pentad.html](http://cpc.ncep.noaa.gov/products/precip/CWlink/daily_mjo_index/pentad.html)). MJO values were averaged for January to March as an index of MJO intensity during the peak of the wet season.

### 2.2.3 Growth rate modelling

A linear mixed-effects model was used to test the hypothesis that otolith increment widths in juvenile barramundi were influenced by quarterly river discharge:

$$\ln(w_{i\text{FishID}}) = \ln(i) * \ln(F_{OND}) + \ln(i) * \ln(F_{JFM}) + \ln(i) * \ln(F_{AMJ}) \\ + \ln(\text{Age at capture}) + (1|\text{FishID})$$

Eq. 2

where  $w$  is measured otolith increment width for increment number  $i$  of fish<sub>FishID</sub>;  $i$  is the increment number of the measured increment;  $F_{OND}$  is the total river discharge in October, November and December;  $F_{JFM}$  is the total river discharge in January, February and March; and  $F_{AMJ}$  is the total river discharge in April, May and June. Age-at-capture was included as a covariate to account for possible age selectivity bias in the samples resulting from individuals with rapid or slow growth occurring in the dataset at disproportionately younger or older ages respectively (Doubleday et al. 2015). *FishID* was included as a random intercept to account for repeated measures (increments 1, 2 and 3) on the same fish. Random slope effects could not be included due to limitations with model convergence.

A separate linear mixed-effects model was used to test the hypothesis that atmospheric indices could be used instead of river discharge to model growth rates in juvenile barramundi:

$$\ln(w_{i\text{FishID}}) = \ln(i) * SOI + \ln(i) * MJO + \ln(\text{Age at capture}) + (1|\text{FishID}) \quad \text{Eq. 3}$$

Models were built using the *lme4* package (Bates et al. 2018) in R (RStudio Team 2018). Separate models were built for each region, as the period for which sufficient otolith data were available ( $\geq 10$  increment widths per year per region) was not consistent across study regions (Table 3). Predictor variables were inspected for data range, distribution and collinearity prior to inclusion in the models (Zuur et al. 2013), and were standardised using the default conditions of the *scale* function in the *base* R package to clarify the interpretation and comparison of model coefficients.

Model selection on the fixed-effects structure of each model used the *MuMIn* package in R (Barton 2018). Models were ranked by AICc (second-order Akaike information criterion) and selected using a maximum likelihood approach (Zuur et al. 2009). Parameter coefficients and estimates of model fit are reported for the top ( $\leq 2$  AICc) river discharge and atmospheric index models for each region, which were refitted using a restricted maximum likelihood approach (Zuur et al. 2009).

Table 3. Data availability for key data types used in this study.

	Mitchell	Gilbert	Flinders
Barramundi year-classes	1997–2008	2006–2012	1997–2013
Barramundi growth years	1997–2009	2006–2013	1997–2014
<i>In situ</i> river gauge data	1995–2018	2015, 2016–2018	1995–2018
Modelled river discharge data	1900–2015	1970–2016	1889–2011
Hydrological years	1997–2009	2006–2013	1997–2014

## 2.2.4 Scenario testing

Multiple water development scenarios have been proposed for the Mitchell region, with modelled flow available from the CSIRO (Hughes et al. 2017). A single, large impact scenario (hereafter referred to as Scenario X) was used to assess whether changes in juvenile barramundi growth rates could be detected under a large water development scenario. Scenario X involves a total annual extraction of 6,000 GL from three nodes within the Mitchell catchment, with a low pump-start threshold (200 ML/day) and zero allocation to EOS flow. Data were accessed using the Northern Australia Water Resource Assessment portal ([nawra-river.shinyapps.io/river](http://nawra-river.shinyapps.io/river)) on 24 October 2019.

To produce juvenile barramundi growth estimates under Scenario X that are directly comparable to the existing flow scenario, a simulation of barramundi growth rates was constructed for the same period that was used to produce the linear mixed-effects growth models (1997 to 2009, Table 3). For simulation purposes, 100 unique individuals were allocated to each year-class between 1997 and 2008, resulting in a total of 1,300 unique simulated barramundi. An age-at-capture was assigned to each individual using a random subset from the original otolith dataset from the Mitchell region, with replacement. Total quarterly river discharge was calculated for each growth year between 1997 and 2009. All model variables were transformed to match those used for the linear mixed-effects growth models, including application of identical variable centring and scaling terms.

## 2.3 Otolith microchemistry

Barramundi are facultatively catadromous, that is, spawned in approximately marine salinity water with a variable proportion of the population using/moving to freshwater habitats for a variable period. It has been suggested that barramundi that migrate into freshwater habitats are more likely to grow faster and survive better, thus providing more recruits to the fishery than individuals that remained in estuarine habitats (Milton 2009; Roberts et al. 2019). As such, variability in recruitment, as indexed by YCS, may be related to hydrologic opportunity, that is, opportunities for barramundi to move up- and downstream through connectivity provided by the seasonal river flows in GoC catchments, and the benefits that come from accessing freshwater habitats.

Analysis and interpretation of otolith microchemistry assumes that: (i) elements are temporally stable once deposited in the otolith, and (ii) the influence of maternal effects is temporally limited to the core of the otolith. Milton and Chenery (2001), Elsdon and Gillanders (2005), and Lowe et al. (2009) indicate that changes in elemental concentrations in water of an aquatic habitat are not immediately reflected in otolith chemistry; rather, it takes days to weeks for changed elemental chemistry to be reflected in fish otoliths.

### 2.3.1 Otolith sample selection

Barramundi otoliths were drawn from the DAF Fisheries Monitoring collection, which at the time of sample selection contained ~9,500 sagittal otoliths. The otoliths processed for microchemistry were the second whole sagittal otolith that remained after its matching partner had been previously thin-sectioned by DAF for ageing.

Spatially, otoliths were selected if they were caught in the Mitchell, Gilbert or Flinders rivers or associated estuarine areas. While some samples had detailed location information, other

samples were allocated to one of the above rivers based on the commercial fishery logbook grid from which they were harvested ([www.business.qld.gov.au/industries/farms-fishing-forestry/fisheries/monitoring-reporting/requirements/logbook-maps](http://www.business.qld.gov.au/industries/farms-fishing-forestry/fisheries/monitoring-reporting/requirements/logbook-maps)). Grid AB13 was considered as part of the Mitchell River estuarine area, grid AC16 was considered as part of the Gilbert River estuarine area and grid AD18 was considered as part of the Flinders River estuarine area (Figure 3).

A long-term aim for research on Queensland barramundi populations has been to better understand how habitat use influences recruitment strength, fish growth and fishery production. Given the temporal variability in river flow in catchments of the GoC, we adopted a year-class approach, whereby samples for otolith microchemistry were selected for different year-classes from each river based on: (i) sample availability, and (ii) river flow sequences experienced by the available year-class samples in the historic otolith collection. Available data were examined to identify years of low, median, high or extreme wet-season river flow. Samples from year-classes from a range of these conditions were selected to provide contrast in the opportunity for flow enabled movement. From the DAF barramundi otolith collection, samples were also selected on the basis of: (i) age-class, such that for any year-class, fish of all harvested ages were represented; (ii) length-class (50 mm total length bins), such that fish of all harvested lengths-at-capture were represented; and (iii) gender (male or female where data available, otherwise unknown), such that male and female fish were represented gender proportionally to their presence in the barramundi otolith collection (Table 4). Samples were supplemented for the Flinders and Mitchell rivers with barramundi that meet the above criteria collected during FRDC research project 2007/002 (a collaborative project with the Tropical Rivers and Coastal Knowledge program). Some samples had been previously analysed for otolith microchemistry using trace metal to calcium ratios (Halliday et al. 2012).

Table 4. Summary information of samples selected for  $^{87}\text{Sr}/^{86}\text{Sr}$  analysis from the DAF barramundi otolith collection.

	Mitchell River	Gilbert River	Flinders River
<i>Number analysed</i>	106	94	202
<i>Age-class range</i>	1 to 8	2 to 10	1 to 7
<i>Total length range (mm)</i>	580 to 1,010	600 to 1,100	580 to 1,070
<i>Capture method</i>	commercial fishery recreational/Indigenous line	commercial fishery	commercial fishery
<i>Gender</i>	37% male 9% female 53% unknown	67% male 33% female	38% male 5% female 57% unknown
<i>Capture years</i>	2005, 2006, 2008, 2009, 2010	2010, 2011, 2015	2003 to 2015
<i>Year-classes</i>	2002, 2003, 2005, (2006 <sup>A</sup> )	2006, 2008, 2011	2002, 2003, 2005, 2006, 2008
<i>Wet-season years</i>	2002 to 2010	2006 to 2015	2002 to 2015

<sup>A</sup> utilising samples and data available from FRDC project 2007/002 (Halliday et al. 2012).

### **2.3.2 Otolith sample preparation**

Selected whole barramundi otoliths were blocked in clear casting resin. All plastic-ware used was washed with 10% nitric acid for 24 hours and rinsed with Millipore water. Blocked otoliths were sectioned transversely through the core (= primordium) using a low-speed Buehler® Isomet™ saw lubricated with Millipore water. Each 400 µm section was hand polished with 1500 grit wet and dry paper moistened with Millipore water. Polished sections were stored in acid-washed plastic vials until mounted. The exposed polished surface of the otoliths was wiped with tissue and 0.5M nitric acid. Up to 10 thin sections were mounted on microscope slides using clear casting resin. Air-dried slides were stored in individual plastic bags before analysis.

### **2.3.3 Laser ablation – strontium isotopes**

Thin-sectioned otoliths were ablated and measured for strontium isotope ratios ( $^{87}\text{Sr}/^{86}\text{Sr}$ ) using a Nu Plasma MC-ICP-MS (Nu Instruments, Wrexham, UK) coupled to an Australian Scientific Instruments RESOLUTION laser ablation system with a Laurin Technic (Canberra, ACT, Australia) ablation cell and Compex 110 excimer laser (Lambda Physik, Gottingen, Germany) operating at 193 nm, as described in Woodhead et al. (2005).

The ablation track for each otolith thin section was marked using GeoStar ver 6.14 software (Resonetics, Nashua, NA, USA) and a 400x objective coupled to a video imaging system. Ablation tracks were preferentially run from the distal edge, through the core to the proximal edge adjacent to the *sulcus acusticus*, thus being approximately perpendicular to the longest axis of growth. In some samples, the ablation track was shortened, running from the core to the proximal edge. The laser system was operated in routine 'spot' mode, with a fluency target of  $\sim 3 \text{ J/cm}^2$  and a repetition rate of 5 Hz (Crook et al. 2016). This corresponded to a spot size of  $\sim 40 \text{ }\mu\text{m}$ , with the laser moving at  $\sim 10 \text{ }\mu\text{m/s}$ .

The ablation track for each sample was examined using a Leica MZ6 stereo microscope at 16x magnification, with calibrated images captured with a Leica DFC295 camera (Leica-Microsystems, Germany) using reflected ring lighting on a black background. The exposed surface of the ablated otolith (which are highly reflective) was covered with a drop of water to improve image contrast and enhance the visual appearance of opaque zones. The ablation track was measured on the still images using Image-Pro Plus (version 7, Media Cybernetics, Rockville, MD, USA); distances from distal edge to core, and between each opaque zone and proximal edge were measured. Features of the otoliths (i.e. edges, core, opaque zones) were matched to the ablated  $^{87}\text{Sr}/^{86}\text{Sr}$  data by calibration of the measured distance with the ablation rate (i.e. time elapsed).

### **2.3.4 Water chemistry**

Water samples were obtained from freshwater and estuarine reaches of the rivers of interest, with additional samples collected from adjacent rivers (Table 5). Water samples were collected as per the standard protocols of the Queensland Department of Environment and Science Chemistry Centre, including filtration with 0.45 µm Sartorius Minisart® hermetically sealed filters, acidification with  $\sim 1\%$  v/v metal-free 70% nitric acid, and storage at  $\leq 4^\circ\text{C}$  in nitric acid-aged, pre-treated plastic bottles. Water samples were analysed for soluble cations (calcium) and soluble metals (including strontium and barium) by the Queensland Chemistry Centre as per National Association of Testing Authorities accredited analysis. Water samples

were analysed for  $^{87}\text{Sr}/^{86}\text{Sr}$  and strontium concentrations by the Isotope Geoscience Group of the University of Melbourne.

Novel mixing models of  $^{87}\text{Sr}/^{86}\text{Sr}$  across the salinity gradient for the Mitchell, Gilbert and Flinders rivers were developed using the approach of Fry (2002), with an upstream freshwater endmember and a downstream estuarine endmember. The freshwater site in the main channel with the lowest salinity was used as the upstream freshwater endmember (Crook et al. 2016), while water samples collected in each estuary in October 2017 were used as the estuarine endmember. Mixing curves were developed for adjacent rivers (e.g. the Norman River) to provide spatial context for results, as the lower delta of many southern GoC rivers are connected by extensive flooding during the wet season. Only the Mitchell River has been studied previously for selected trace element water chemistry (Batlle-Aguilar et al. 2014), in this case for freshwater reaches at least ~139 km (adopted middle thread distance) from the river mouth (i.e. Dunbar gs details, [water-monitoring.information.qld.gov.au](http://water-monitoring.information.qld.gov.au)). Additional water samples were collected upstream of the upper limit of tidal influence in each of the rivers of interest to provide a seasonal replicate and to determine how closely the hypothetical mixing curves represented the water chemistry in lower habitats. These additional water samples were collected and processed according to the same procedures as detailed above, with results given in Appendix 2. Barramundi were sampled at the same time by line fishing in collaboration with recreational fishers and Kowanyama Rangers in October 2018. This was the end of the dry season, when there had been limited opportunity for barramundi to move due to the lack of river flows within the previous 3 months.

Table 5. Site details and chemistry of water samples used to develop conservative mixing curves of  $^{87}\text{Sr}/^{86}\text{Sr}$  to infer salinity and likely habitat residency of barramundi in south-eastern Gulf of Carpentaria rivers.

River <sup>a</sup> , site, latitude/longitude (°S, °E)	Collection date	Salinity (ppt) <sup>b</sup>	$^{87}\text{Sr}/^{86}\text{Sr}$	Sr (µg/L)
<b>Mitchell River</b>				
Gordon Arthur Crossing, 16.30, 143.973	08/09/2017	0.04	0.73158	16.8
Estuary main channel, 15.218, 141.608	09/11/2017	31.00	0.70924	3,330.2
<b>Gilbert River</b>				
Burke Development Road, 17.168, 141.764	08/10/2017	0.12	0.72451	183.4
Estuary main channel, 16.651, 141.269	11/11/2017	37.00	0.70917	4,843.8
<b>Flinders River</b>				
Yambore Creek, 20.282, 142.027	21/10/2017	0.19	0.70846	438.1
Eastern Creek, 20.843, 141.748	23/10/2017	0.19	0.70615	640.3
Estuary main channel, 17.610, 140.618	14/11/2017	39.00	0.70923	5,698.1
<b>Norman River</b>				
Moonlight Creek, 18.263, 142.196	07/10/2017	0.03	0.76359	6.5

<sup>a</sup> unless otherwise noted, samples are from the main river channel; <sup>b</sup> salinity derived from measured conductivity (ppt: parts per thousand).

### **2.3.5 $^{87}\text{Sr}/^{86}\text{Sr}$ profile classification**

The  $^{87}\text{Sr}/^{86}\text{Sr}$  profile for each sample was classified for habitat use depending on the strontium isotope values during slow-growth opaque zones (Roberts et al. 2019), which coincides approximately with the cooler dry season in the southern GoC. To be classed as freshwater,  $^{87}\text{Sr}/^{86}\text{Sr}$  ablation values needed to indicate a salinity of  $\leq 1$  parts per thousand (ppt) derived from the mixing curve for at least one growth season (i.e. an opaque zone and following translucent zone  $\cong 1$  year). To be classed as estuarine,  $^{87}\text{Sr}/^{86}\text{Sr}$  ablation values needed to indicate a salinity of  $>5$  ppt for all opaque zones. Strontium isotope profiles with  $^{87}\text{Sr}/^{86}\text{Sr}$  ablation values during opaque zones of  $>1$  ppt but  $\leq 5$  ppt were classified as intermediate. This was a conservative approach to habitat use classification based on  $^{87}\text{Sr}/^{86}\text{Sr}$  profiles, where a fish needed at least one dry season with  $^{87}\text{Sr}/^{86}\text{Sr}$  ablation values indicative of residency in water of  $\leq 1$  ppt salinity to be classified as freshwater. Other studies have used a binary classification of habitat use (i.e. freshwater or estuarine). However,  $^{87}\text{Sr}/^{86}\text{Sr}$  profiles in the current rivers of interest (especially the Mitchell and Gilbert rivers) clearly had a profile class that was neither freshwater nor full estuarine/marine; an 'intermediate' classification was therefore needed.

### **2.3.6 Total length as related to habitat class**

Growth in barramundi is highly seasonal (Xiao 1999, 2000; Russell et al. 2015), resulting in large variability in length-at-age (Staunton-Smith et al. 2004). Davis and Kirkwood (1984) were unable to estimate a reliable average growth curve for barramundi from five rivers in northern Australia, postulating that environmental conditions were probably a major factor in growth variability. These authors also noted variable growth between years within individual river systems.

Anecdotal reports from commercial and recreational fishers suggest that barramundi grow faster in freshwater habitats than in saltwater habitats, with freshwater fish often noted as being heavier (i.e. 'fatter') for the same total length (Dunstan 1959). Several studies have linked increased growth rates to river flow to the estuary (Sawynok 1998; Robins et al. 2005) or freshwater residency (Roberts et al. 2019). However, targeted research using tag-recapture of barramundi released into different habitats suggests factors affecting growth are more complex than simply fresh or salt water and likely related to prey availability (Russell et al. 2015).

In the current analysis, we investigated whether 'faster' growth, as indexed by length-at-age, was associated with freshwater habitat use and whether this was consistent across the Mitchell, Gilbert and Flinders rivers. Preliminary analyses, given sample size constraints, used a linear model (RStudio 2018) to predict total length (at capture) as a function of age-class (at capture, natural log transformed) and habitat class (initially two classes: freshwater; and non-freshwater, i.e. intermediate and estuarine). Further analyses considered additional habitat classes, relevant to each river, as well as year-class to further understand how barramundi growth in each river system might vary.



## 3. Results

### 3.1 Catch and age

Commercial harvest and effort for barramundi from the southern GoC stock has been variable over time. Visual inspection of the data was restricted to harvest years 2000 to 2018, for which there is catch, effort, length-frequency and age-frequency information. The influence of major management changes during this period are minimal (see Streipert et al. 2019 for details).

#### 3.1.1 Mid sub-stock (Mitchell River)

##### Catch

Regional commercial catch and nominal catch rate (kg/day fished) for barramundi in the Mid sub-stock varied between years, with the lowest reported catch in 2015 and the lowest reported catch rate in 2005. The highest reported catch was in 2008, and the highest nominal catch rate in 2012 (Figure 5).

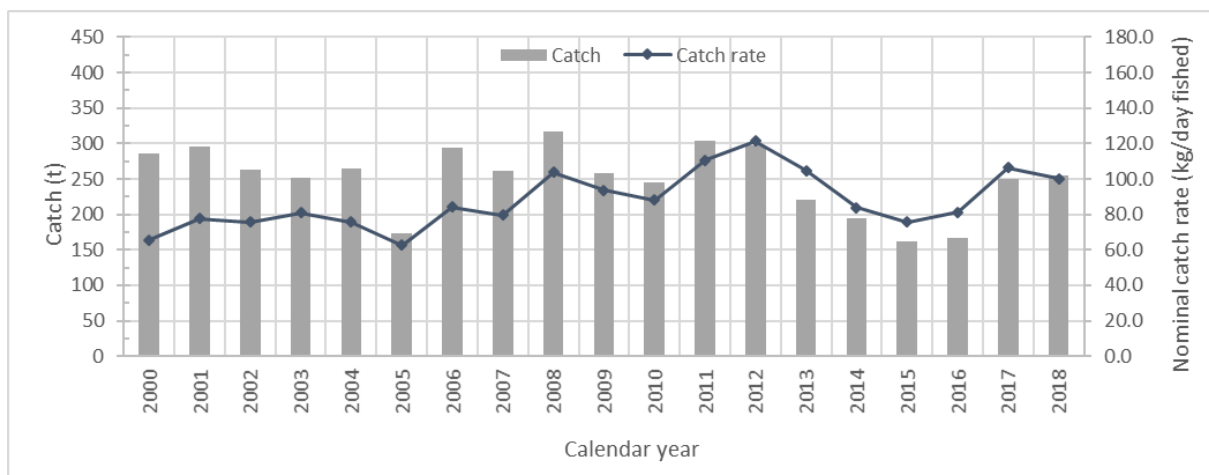


Figure 5. Reported commercial catch and nominal catch rate for barramundi from the Mid sub-stock (13°S to 16°S) of the southern Gulf of Carpentaria.

##### Age-frequency and catch-at-age

Barramundi from the Mid sub-stock of the southern GoC displayed highly variable length-at-age (Figure 6), with variable total length for any given age-class, indicative of large variability in growth.

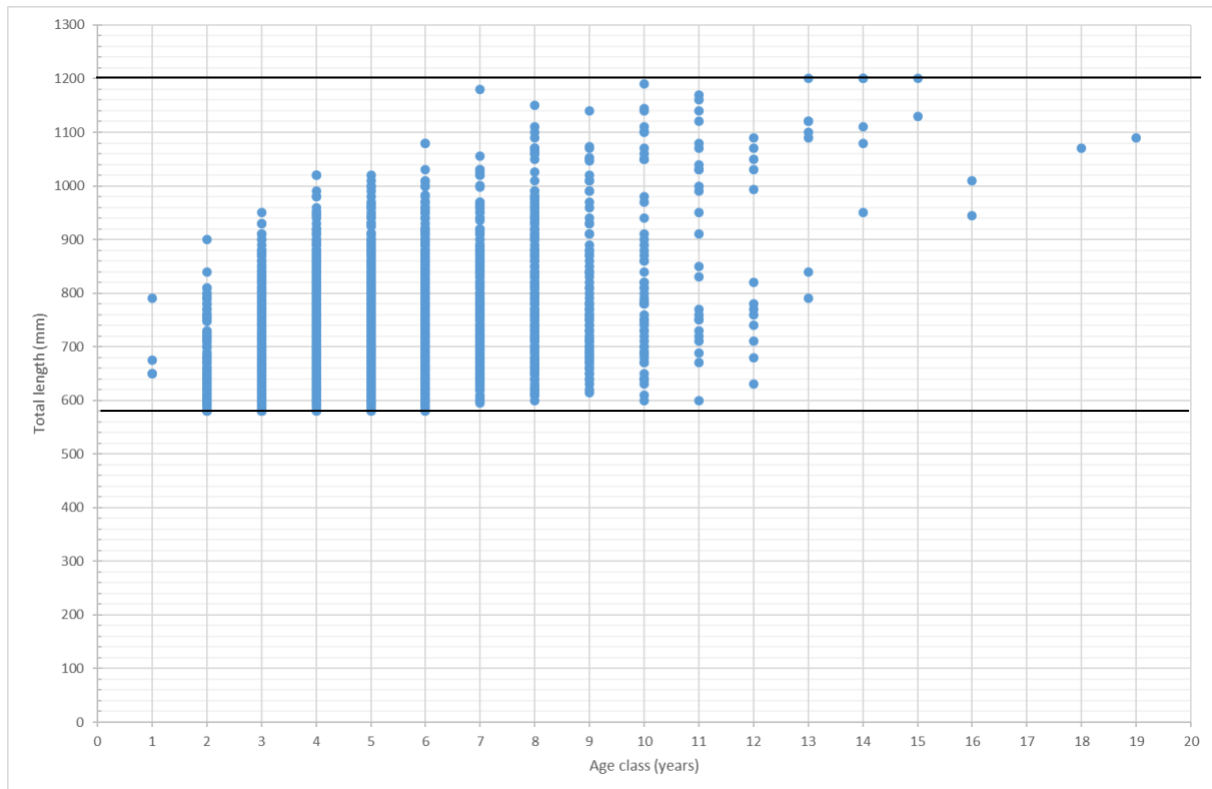


Figure 6. Observed length-at-age for legal size barramundi from the Mid sub-stock (13° to 16°S) of the southern Gulf of Carpentaria. Samples are from the DAF Fishery Monitoring program collected between the years 2000 and 2018 inclusive ( $n=4,140$ ), noting the minimum legal size of barramundi in Queensland is 580 mm total length and the maximum legal size is 1,200 mm as indicated by the black lines.

There was considerable variation between years in the age-frequencies of barramundi from the Mid sub-stock (Figure 7), suggesting variable recruitment between year-classes. Although the current study used a broader spatial scale, and samples were predominantly derived from a different fishing sector (i.e. commercial net fishery compared to recreational line fishery), between-year variation in age-frequencies was similar to the patterns reported by Halliday et al. (2012) for the Mid sub-stock.

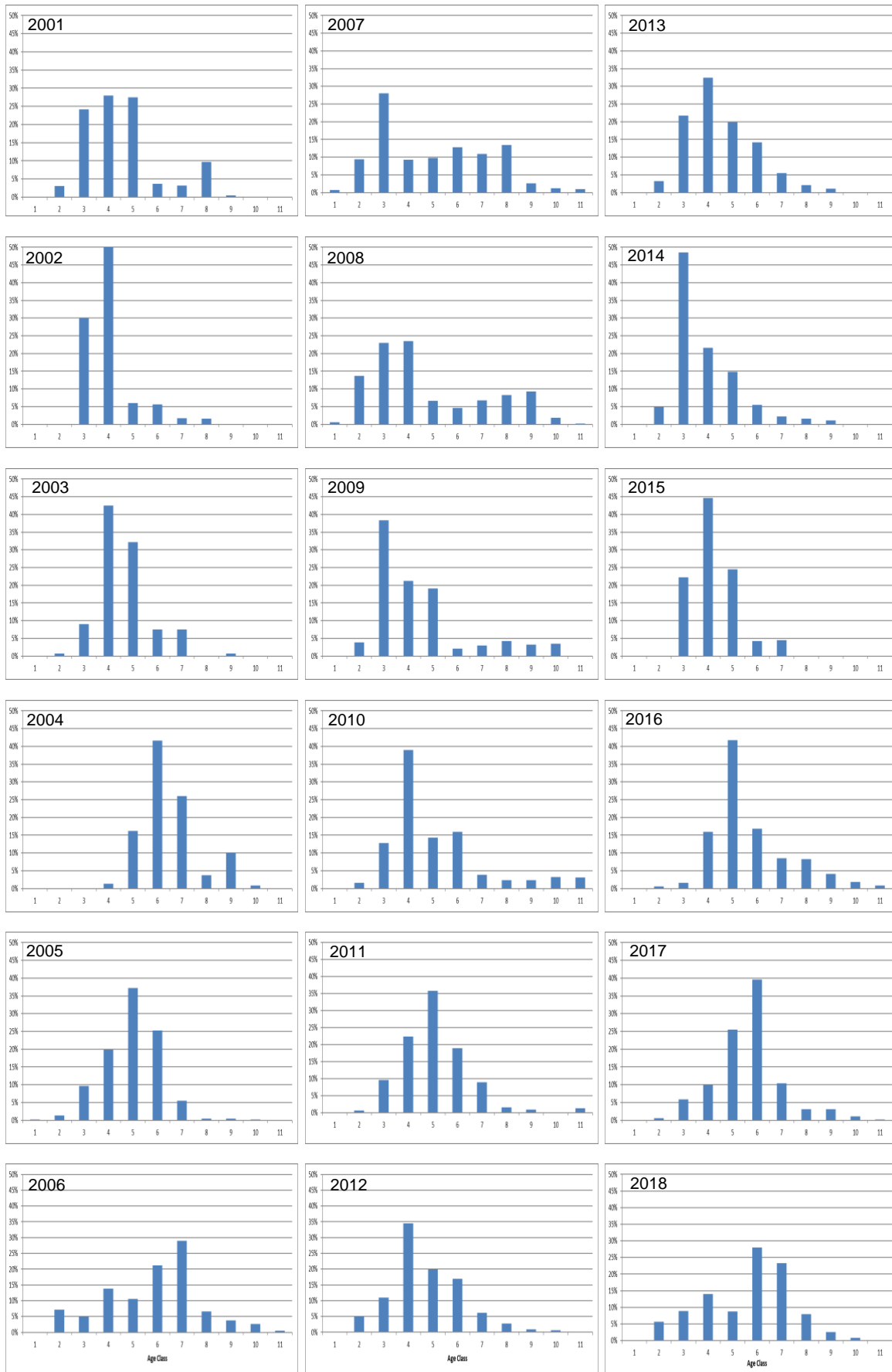


Figure 7. Estimated age-frequencies (percent) of barramundi from the Mid sub-stock of the southern Gulf of Carpentaria monitored by Fisheries Queensland, 2001–2018 displayed.

Age-class accounted for about 45% of the variation in  $\ln(\text{age-frequency})$  (Table 6). The inclusion of sample year in the model (main effect, factor) was not significant, and therefore was not included in further model fitting. The base model containing only age-class highlights relative recruitment strength compared to the average recruitment over the 19 sampling years. Model fits for alternate base models for the Mid sub-stock are included in Appendix 1.

Standardised residuals from the catch-curve regression ( $\ln(\text{age-frequency}) \sim \text{age-class}$ ) were averaged and plotted to aid in the visualisation of relative YCS of barramundi (Figure 8). For the Mid sub-stock, nine of the 25 year-classes were considered to be relatively weak (i.e. residuals  $\leq -0.5$ ; years: 1991, 1992, 1994, 1995, 2002, 2003, 2013, 2014 and 2015), six year-classes were considered to be relatively strong (i.e. residual  $\geq 0.5$ ; years 1998, 1999, 2000, 2010, 2011 and 2012), and the remaining 10 years were considered neither weak nor strong (i.e. 'average').

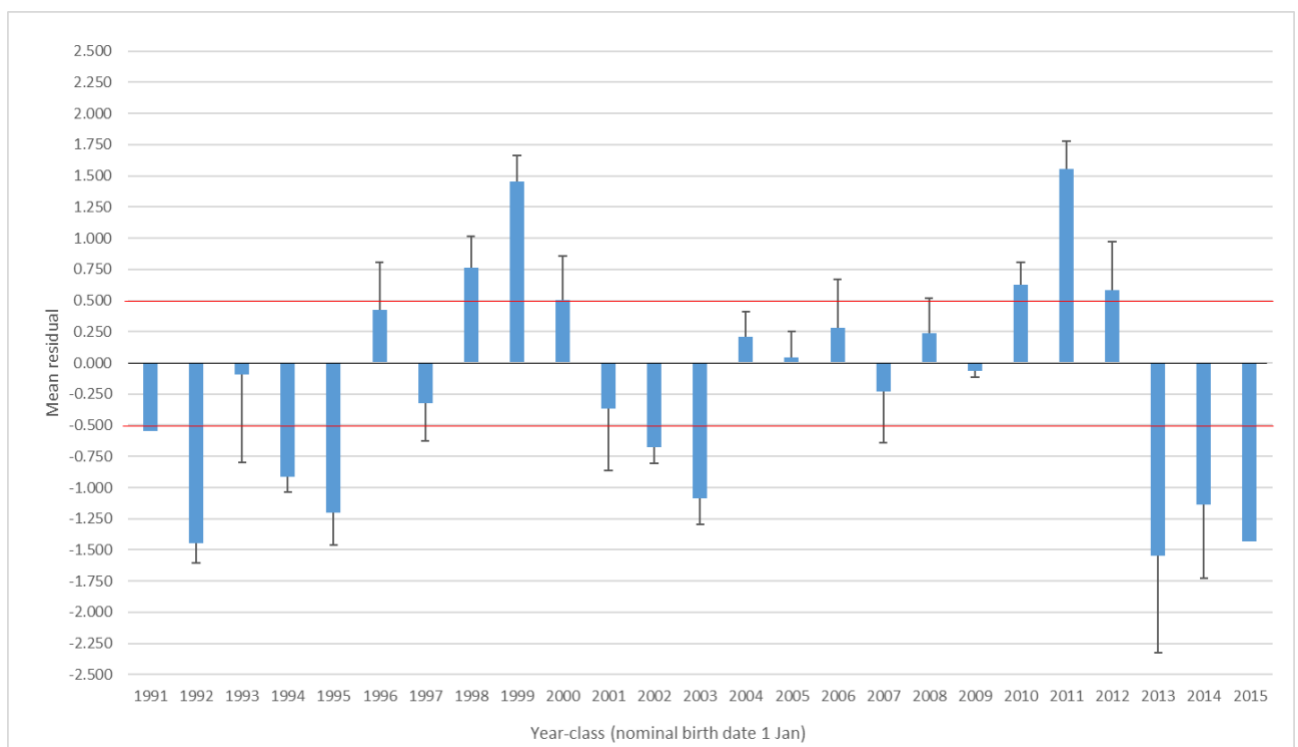


Figure 8. Visualisation of relative year-class strength index of barramundi from the Mid sub-stock. Mean residuals ( $\pm$  standard error) are from the catch-curve regression ( $\ln(\text{age-frequency}) \sim \text{age-class}$ ) of barramundi sampled between 2000 and 2018 ( $n=8,581$ ) from the Mid sub-stock ( $13^{\circ}\text{S}$  to  $16^{\circ}\text{S}$ ) of the southern Gulf of Carpentaria. Mean residual values  $\geq 0.5$  are considered indicative of relatively strong year-classes. Mean residual values  $\leq -0.5$  are considered indicative of relatively weak year-classes.

The estimated age composition of the commercial barramundi harvest was variable for the Mid sub-stock region (Figure 9). The fishery harvest in this region is usually dominated by 4- to 6-year-old fish, but sometimes younger fish were important in the harvest (e.g. 2008, 2014) and sometimes older fish were important in the harvest (e.g. 2018). The estimated contribution per year-class to the fishery harvest (Figure 10) further highlights the variable productivity of different year-classes. In addition to the strong year-classes identified from the catch-curve regression (Figure 8), the year-classes between 2004 and 2008 made an important contribution to the fishery harvest (Figure 10), although were considered as 'average' year-classes in Figure 8.

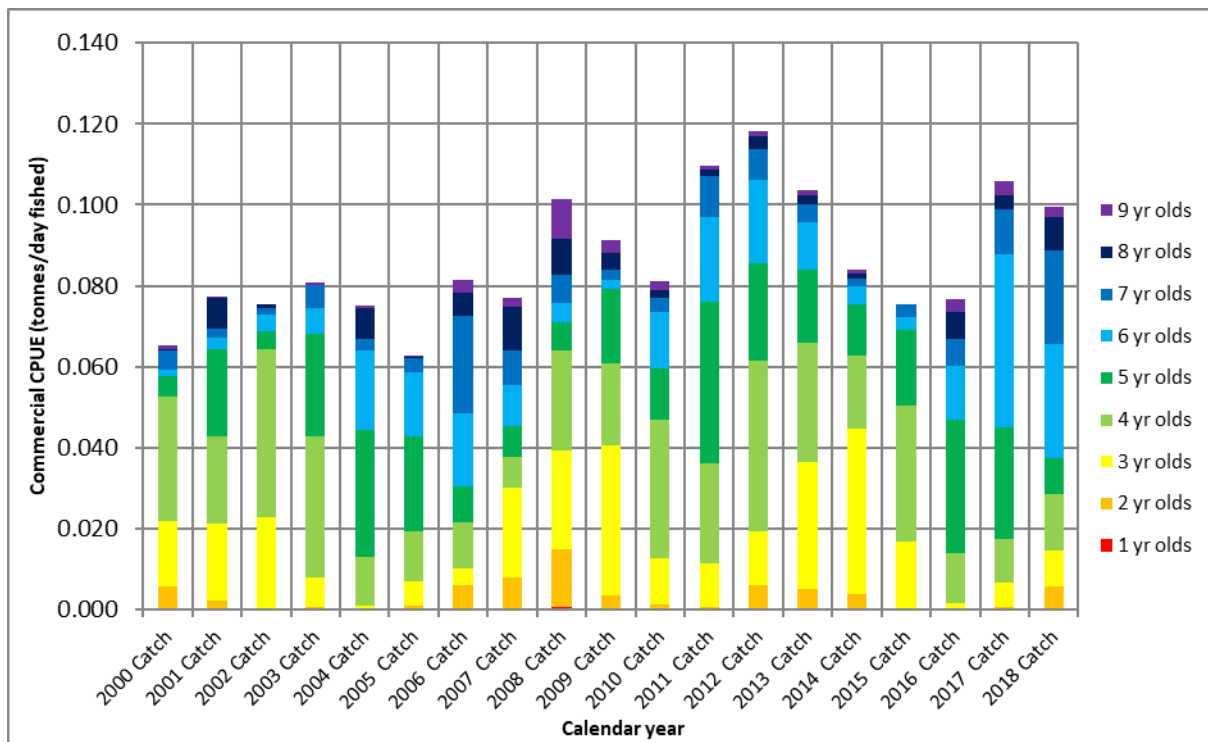


Figure 9. Estimated age composition of the commercial barramundi catch per unit effort (CPUE) per calendar year for the Mid sub-stock (13°S to 16°S) of the southern Gulf of Carpentaria.

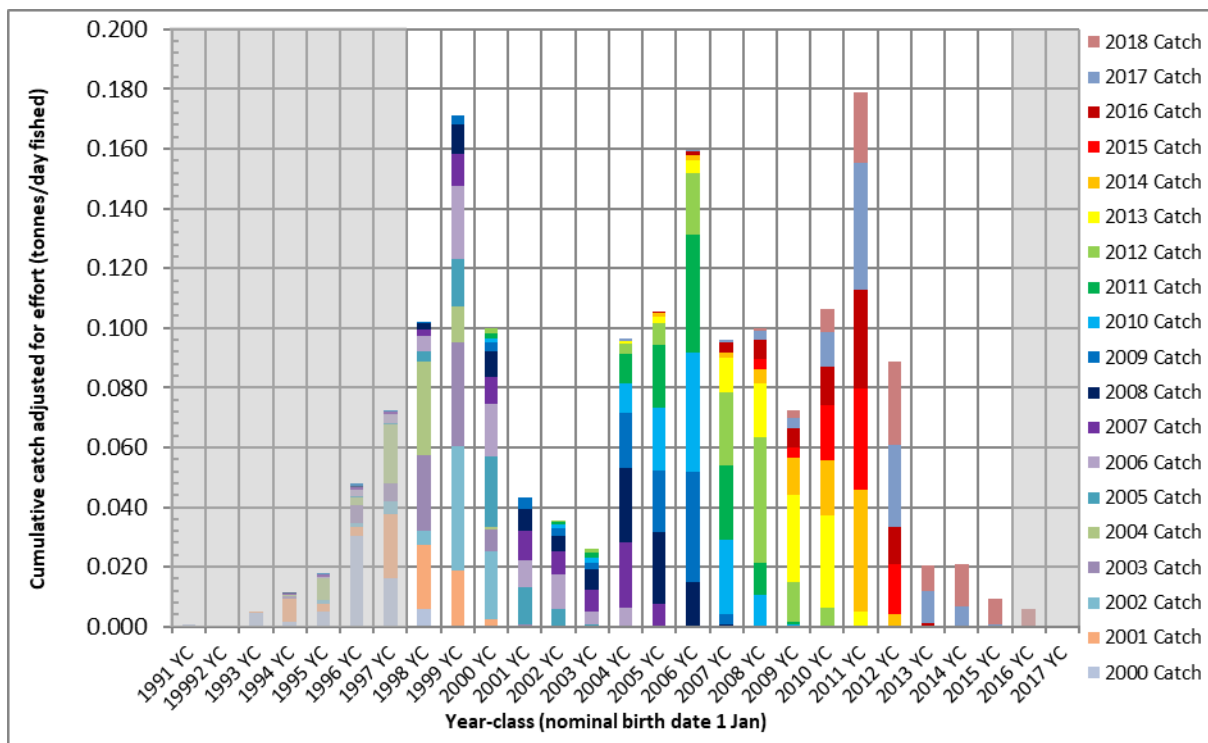


Figure 10. Estimated contribution per year-class (YC), to annual commercial barramundi catches (2000–2018) for the Mid sub-stock (13°S to 16°S) of the southern Gulf of Carpentaria.

Greyed regions contain insufficient data for interpretation or analysis.

## Analysis with flow

Ideally, all components of the hydrograph would be incorporated into modelling river flow effects on the variability in fish age-frequency, as barramundi are exposed to multiple aspects of river flows, given their opportunistically catadromous life history. Simple to complex multi-term models were fitted, including the 'full model' that represents all components of the hydrograph, albeit coarsely as aggregated discharge. The 'top' models, presented in Table 6 were selected based on having a high adjusted  $R^2$ , a low AIC (Akaike information criterion) and being consistent with barramundi biology in GoC rivers.

The top model for monthly flows during the birth-year for Mitchell River barramundi accounted for 62.5% of variation in  $\ln(\text{age-frequency})$  and included flows in December, January and April. All flow terms were statistically significant and positive in effect. The top model for quarterly Mitchell River flows in the birth-year accounted for 58.5% of variation in age-frequency and included  $F_{M0\_OND}$ ,  $F_{M0\_JFM}$ , and either  $F_{M0\_JAS}$  or  $F_{M0\_AMJ}$ .

The top model for quarterly flows in the Mitchell River from birth-year until capture accounted for 68.5% of the variation in  $\ln(\text{age-frequency})$  and included the quarterly flows in the birth-year (i.e.  $F_{M0}$ ) as well as quarterly flows in the second year of life (i.e. after the first birthday,  $F_{M1}$ ), flows in the third year of life (i.e. after the second birthday,  $F_{M2}$ ) and flows from the third birthday to capture (i.e.  $F_{M3\_to\_Capture}$ ). Including flows from the second and third years of life, as well as flows in the years-to-capture significantly improved model fit. Coefficients for the top models are provided in Appendix 1.

Flow terms were also fitted to the standardised residuals from the catch-curve regression as described in Bayliss et al. (2014). Models for the YCS index mirrored those in Table 6; with fitted coefficients are available on request.

Table 6. Results of the all-subsets generalised linear models predicting the abundance of barramundi age-classes (3 to 9 years) for the Mid sub-stock (13°S to 16°S) of the southern Gulf of Carpentaria with Mitchell River flow ( $F_M$ ).

Model type	Model structure	Df	Adj. $R^2$	AIC	$\Delta$ AIC
<b>Birth-year monthly flows</b>					
Base	Age-class <sup>#</sup>	2	45.4	191.63	55.81
Top	Age-class <sup>#</sup> , $F_{M0\_Dec}$ , $F_{M0\_Jan}$ , $F_{M0\_Apr}$	5	62.5	135.82	0.00
Full	Age-class <sup>#</sup> , $F_{M0\_Oct}^{**}$ , $F_{M0\_Nov}^{**}$ , $F_{M0\_Dec}$ , $F_{M0\_Jan}$ , $F_{M0\_Feb}^*$ , $F_{M0\_Mar}^{**}$ , $F_{M0\_Apr}$ , $F_{M0\_May}^{**}$ , $F_{M0\_Jun}^{**}$ , $F_{M0\_Jul}^*$ , $F_{M0\_Aug}^{**}$ , $F_{M0\_Sep}^*$	14	61.9	147.00	11.18
<b>Birth-year quarterly flows</b>					
Base	Age-class <sup>#</sup>	2	45.4	195.20	56.35
Top	Age-class <sup>#</sup> , $F_{M0\_OND}$ , $F_{M0\_JFM}$ , $F_{M0\_JAS}$	5	58.5	138.85	0.00
Top alt	Age-class <sup>#</sup> , $F_{M0\_OND}$ , $F_{M0\_JFM}$ , $F_{M0\_AMJ}$	5	58.3	138.91	0.06
Full	Age-class <sup>#</sup> , $F_{M0\_OND}$ , $F_{M0\_JFM}$ , $F_{M0\_AMJ}^*$ , $F_{M0\_JAS}^*$	6	58.6	139.00	0.15
<b>Birth-year quarterly <math>F_{M0}</math>, plus quarterly <math>F_{M1}</math>, plus quarterly <math>F_{M2}</math>, plus <math>F_{M3\_to\_Capture}</math></b>					
Base	Age-class <sup>#</sup>	2	45.4	244.51	94.95
Top	Age-class <sup>#</sup> , $F_{M0\_OND}$ , $F_{M0\_JFM}$ , $F_{M1\_OND}$ , $F_{M1\_AMJ}$ , $F_{M2\_OND}$ , $F_{M2\_JAS}^*$ , $F_{M3\_to\_Capture}$	8	68.5	149.56	0.00
Top alt	Age-class <sup>#</sup> , $F_{M0\_OND}$ , $F_{M0\_JFM}$ , $F_{M1\_OND}$ , $F_{M1\_AMJ}$ , $F_{M2\_JAS}$ , $F_{M3\_to\_Capture}$	7	67.9	151.09	1.53
Full	Age-class <sup>#</sup> , $F_{M0\_OND}$ , $F_{M0\_JFM}$ , $F_{M0\_AMJ}$ , $F_{M0\_JAS}^*$ , $F_{M1\_OND}$ , $F_{M1\_JFM}^{**}$ , $F_{M1\_AMJ}$ , $F_{M1\_JAS}^{**}$ , $F_{M2\_OND}^*$ , $F_{M2\_JFM}^*$ , $F_{M2\_AMJ}^*$ , $F_{M2\_JAS}^*$ , $F_{M3\_to\_Capture}$	14	69.2	167.76	20.01

\* variable not significant; # variable with negative coefficient.

### 3.1.2 South sub-stock (including Flinders and Gilbert rivers)

#### Catch

Variation in the commercial catch and nominal catch rate (kg/day fished) in the South sub-stock was similar to the Mid sub-stock but not the same. The lowest total catch for this region was reported in 2015, with the lowest catch rate in 2003 (Figure 11). The highest total catch was reported in 2011, which was also the year with the highest catch rate.

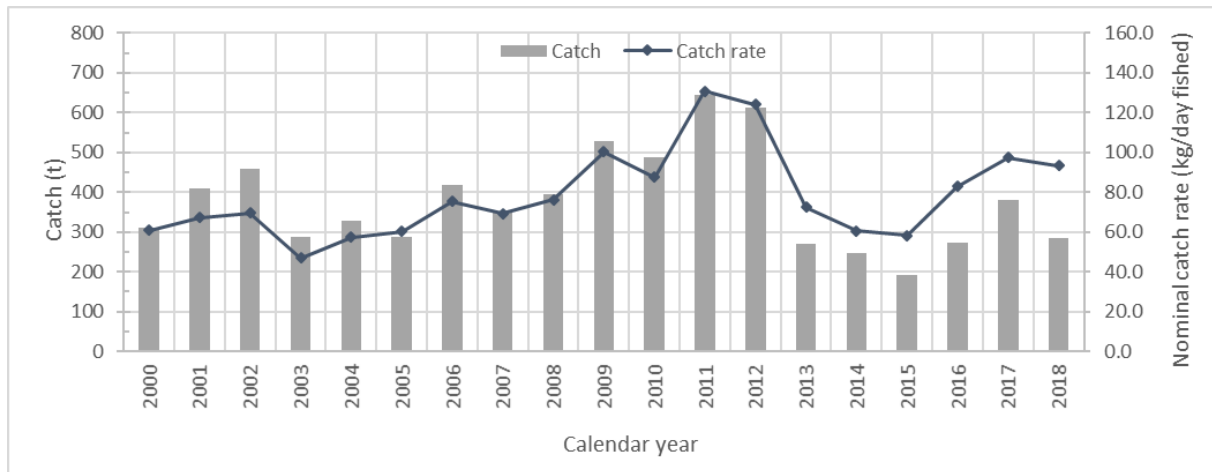


Figure 11. Reported commercial catch and nominal catch rate for barramundi from the South sub-stock (16°S to the Queensland/Northern Territory border) of the southern Gulf of Carpentaria.

## Age-frequency and catch-at-age

Barramundi sampled from the South sub-stock displayed highly variable length-at-age (Figure 12), which is typical for barramundi in Queensland.

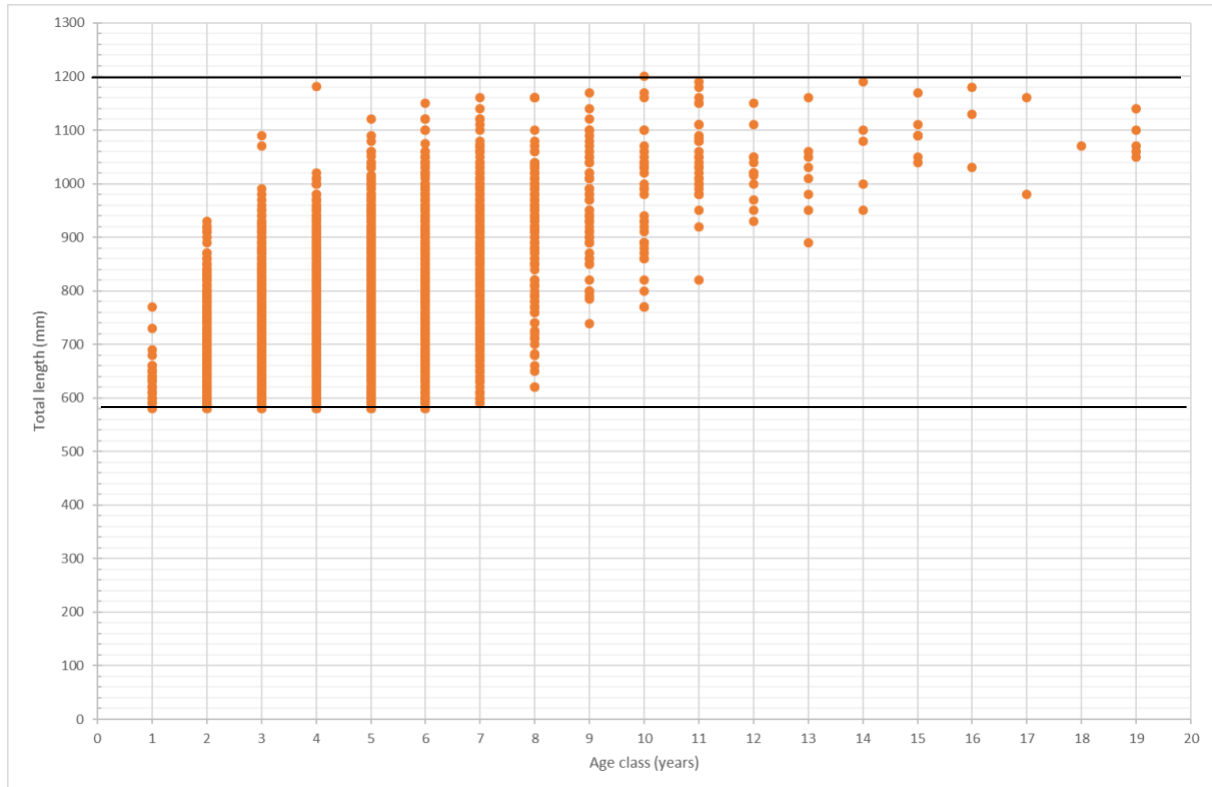


Figure 12. Observed length-at-age for legal size barramundi from the South sub-stock (16°S to the Queensland/Northern Territory border) of the southern Gulf of Carpentaria, between 2000 and 2018 inclusive. Samples are from the DAF Fishery Monitoring program collected between the years 2000 and 2018 inclusive ( $n=5,708$ ), noting the minimum legal size of barramundi in Queensland is 580 mm total length and the maximum legal size is 1,200 mm as indicated by the black lines.

Age-frequencies of barramundi from the South sub-stock of the southern GoC showed considerable variation between years (Figure 13), suggesting variable recruitment between year-classes. Although the current study used a broader spatial scale and samples were derived from a larger number of fishing operators, between-year variation in age-frequencies was similar to the patterns reported by Halliday et al. (2012).



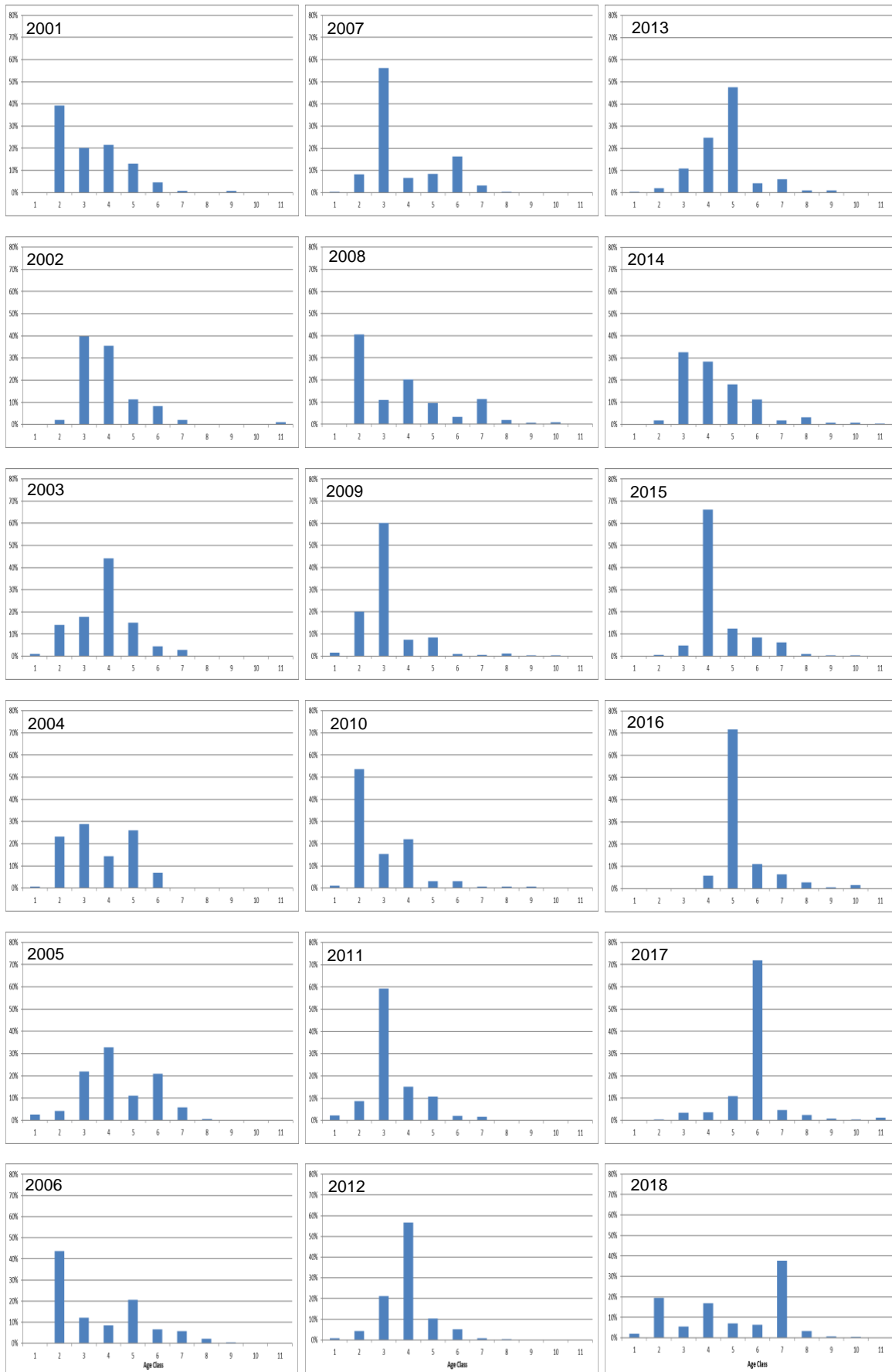


Figure 13. Estimated age-frequencies (percent) of barramundi from the South sub-stock of the southern Gulf of Carpentaria monitored by Fisheries Queensland, 2001–2018 displayed.

Age-class accounted for about 59% of the variation in  $\ln(\text{age-frequency})$  (Table 7). Including sample year in the model (main effect, factor) did not significantly improve the base model fit. The base model containing only age-class highlights relative recruitment strength compared to the average recruitment over the 19 sampling years. Model fits for alternate base models for the South sub-stock are included in Appendix 1.

Standardised residuals from the catch-curve regression ( $\ln(\text{age-frequency}) \sim \text{age-class}$ ) were averaged and plotted to aid in the visualisation of relative YCS (Figure 14). For the South sub-stock, eight of the 25 year-classes were relatively weak (i.e. residual  $\leq -0.5$ ; years: 1992, 1994, 1995, 2002, 2003, 2013, 2014 and 2015), four year-classes were relatively strong (i.e. residual  $\geq 0.5$ ; years: 1998, 1999, 2008 and 2011), and the remaining 13 year-classes, were neither weak nor strong (i.e. 'average').

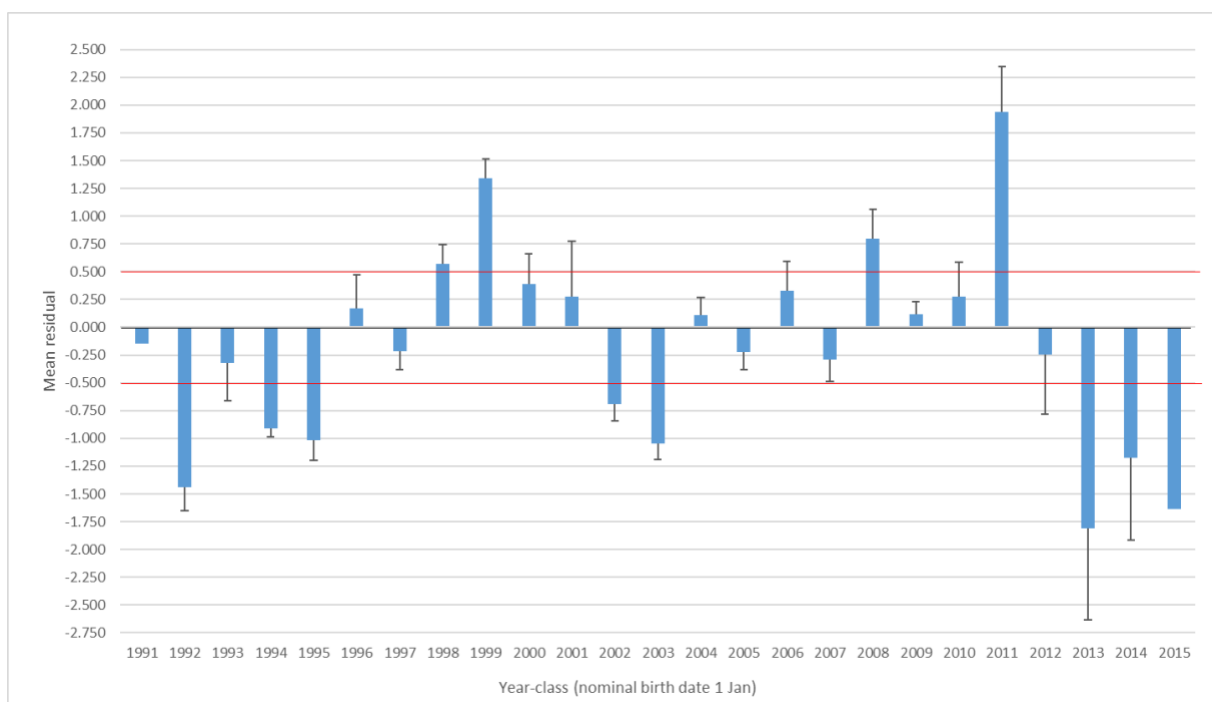


Figure 14. Visualisation of relative year-class strength index of barramundi from the South sub-stock. Mean residuals ( $\pm$  standard error) are from the catch-curve regressions ( $\ln(\text{age-frequency}) \sim \text{age-class}$ ) of barramundi sampled (2000–2018,  $n = 14,618$ ) from the South sub-stock (16°S to Queensland/Northern Territory border) of the southern Gulf of Carpentaria. Mean residual values  $\geq 0.5$  are considered indicative of relatively strong year-classes. Mean residual values  $\leq -0.5$  are considered indicative of relatively weak year-classes.

Visual inspection of the catch-at-age of the commercial catch highlights cycles in age-structure of barramundi from the South sub-stock (Figure 15). The fishery harvest is usually dominated by 3- to 4-year-old fish, but sometimes younger fish were important in the harvest (e.g., 2010) and sometimes older fish were important in the harvest (e.g. 2016 and 2017). Some of the variation in the age-structure results from between-year differences in fishing practices (i.e. the location in the estuaries and coastal foreshores where nets are set), but underlying recruitment variability is likely to be the main driver.

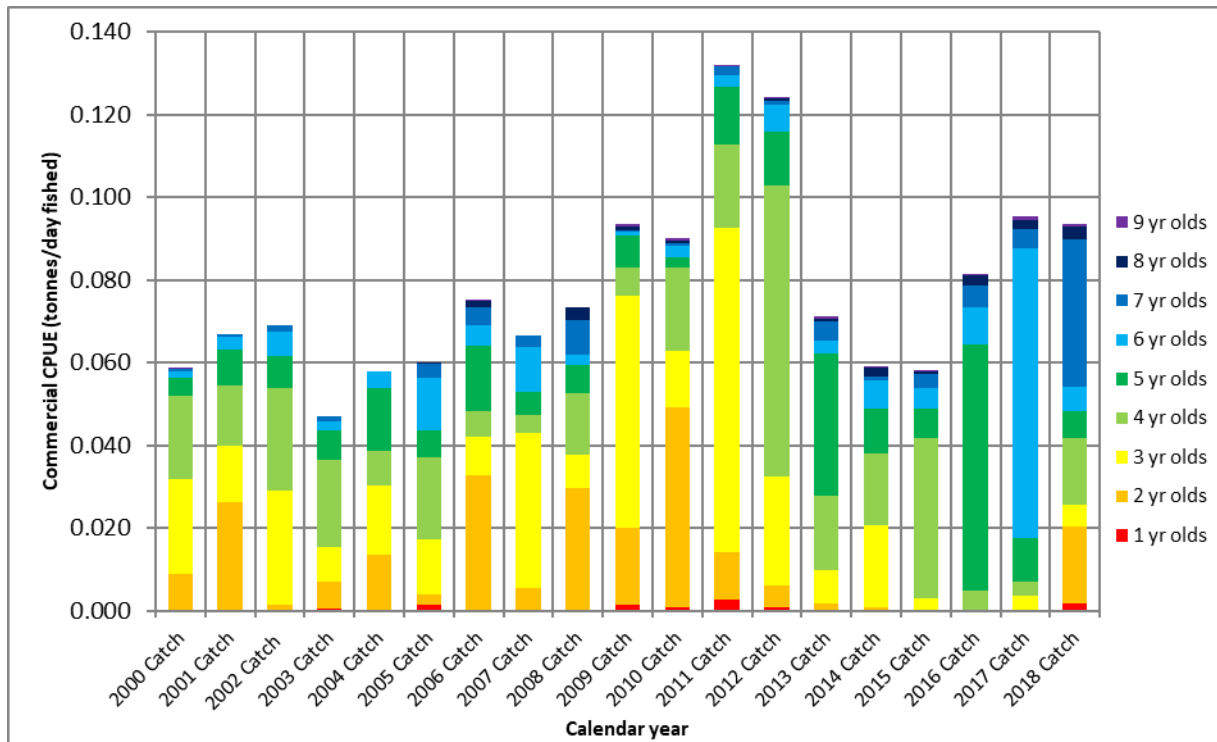


Figure 15. Estimated age composition of the commercial barramundi catch per unit effort (CPUE) per year for the South sub-stock (16°S to the Queensland/Northern Territory border) of the southern Gulf of Carpentaria.

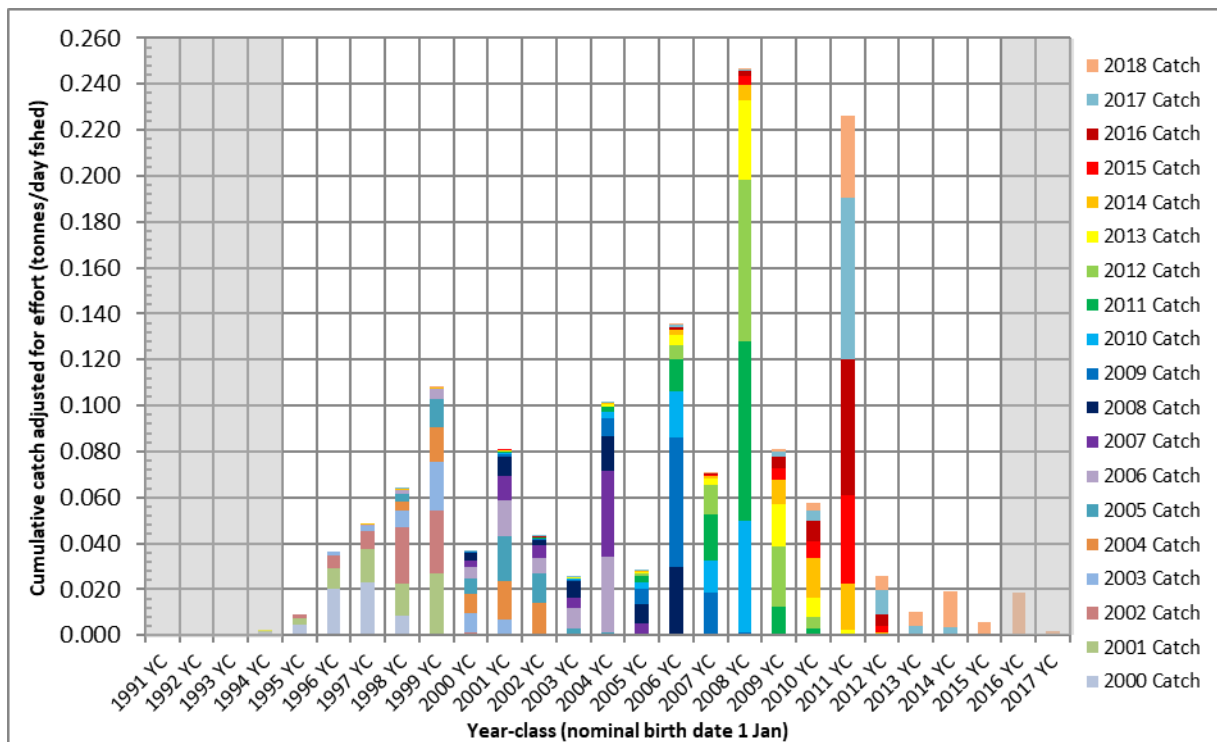


Figure 16. Estimated contribution per year-class (YC) to the commercial barramundi catch (2000–2018) for the South sub-stock (16°S to Queensland/Northern Territory border) of the southern Gulf of Carpentaria. Greyed regions contain insufficient data for interpretation or analysis.

## Analysis with flow

Ideally, all components of the hydrograph would be incorporated into modelling river flow effects on the variability in fish abundance-at-age. Simple to complex, multi-term models were fitted, including the ‘full model’ that represents all components of the hydrograph. The ‘top’ model(s) were selected based on the adjusted  $R^2$ , low AIC and consistency with barramundi biology in GoC rivers. Models were built to explore the relationship between the relative age-frequency of barramundi and flow from: (i) only the Flinders River, (ii) only the Gilbert River, and (iii) both the Flinders and Gilbert rivers.

### Only Flinders River flows

The top model for monthly, birth-year Flinders River flows accounted for 73.3% of variation in age-frequency and included flows in December, January and March (Table 7). All flow terms were statistically significant and positive in effect. The top model for quarterly, birth-year Flinders River flows accounted for 68.0% of variation in age-frequency and included  $F_{F0\_OND}$  and  $F_{F0\_JFM}$ . The top model for quarterly flows in the Flinders River from birth-year until capture accounted for about 76.9% of the variation in age-frequency and included the quarterly flows in the birth-year (i.e.  $F_{F0}$ ) as well as quarterly flows in the third year of life (i.e. after the second birthday,  $F_{F2}$ ) and flows from the third birthday to capture (i.e.  $F_{F3\_to\_Capture}$ ). Coefficients for the top models are provided in Appendix 1.

Table 7. Results of the all-subsets generalised linear models predicting the abundance of barramundi age-classes (3 to 9 years) for the South sub-stock (16°S to Queensland/Northern Territory border) of the southern Gulf of Carpentaria with Flinders River flow.

Model type	Model structure	Df	Adj R <sup>2</sup>	AIC	ΔAIC
<b>Birth-year monthly flow (<math>F_{F0}</math>)</b>					
Base	Age-class <sup>#</sup>	2	58.9	204.12	63.00
Top	Age-class <sup>#</sup> , $F_{F0\_Dec}$ , $F_{F0\_Jan}$ , $F_{F0\_Mar}$	5	73.3	141.12	0.00
Full	Age-class <sup>#</sup> , $F_{F0\_Oct}^{*#}$ , $F_{F0\_Nov}^*$ , $F_{F0\_Dec}^{*#}$ , $F_{F0\_Jan}$ , $F_{F0\_Feb}^{\#}$ , $F_{F0\_Mar}^*$ , $F_{F0\_Apr}^{*#}$ , $F_{F0\_May}^{*#}$ , $F_{F0\_Jun}^*$ , $F_{F0\_Jul}^{*#}$ , $F_{F0\_Aug}^*$ , $F_{F0\_Sep}^*$	14	73.1	147.00	5.88
<b>Birth-year quarterly flow (<math>F_{F0}</math>)</b>					
Base	Age-class <sup>#</sup>	2	58.9	173.37	35.41
Top	Age-class <sup>#</sup> , $F_{F0\_OND}$ , $F_{F0\_JFM}$	4	68.0	138.15	0.00
Top alt	Age-class <sup>#</sup> , $F_{F0\_OND}$ , $F_{F0\_JFM}$ , $F_{F0\_AMJ}^*$	5	68.4	138.91	0.96
Full	Age-class <sup>#</sup> , $F_{F0\_OND}$ , $F_{F0\_JFM}$ , $F_{F0\_AMJ}^*$ , $F_{F0\_JAS}^{*#}$	6	68.2	139.00	0.85
<b>Birth-year quarterly <math>F_{F0}</math>, plus quarterly <math>F_{F1}</math>, plus quarterly <math>F_{F2}</math>, plus <math>F_{F3\_to\_Capture}</math></b>					
Base	Age-class <sup>#</sup>	2	58.9	237.79	97.62
Top	Age-class <sup>#</sup> , $F_{F0\_OND}$ , $F_{F0\_AMJ}$ , $F_{F2\_OND}$ , $F_{F2\_JFM}^{\#}$ , $F_{F3\_to\_Capture}$	7	76.9	140.17	0.00
Full	Age-class <sup>#</sup> , $F_{F0\_OND}$ , $F_{F0\_JFM}^{*#}$ , $F_{F0\_AMJ}$ , $F_{F0\_JAS}^{*#}$ , $F_{F1\_OND}^{*#}$ , $F_{F1\_JFM}$ , $F_{F1\_AMJ}^{*#}$ , $F_{F1\_JAS}^*$ , $F_{F2\_OND}$ , $F_{F2\_JFM}^{\#}$ , $F_{F2\_AMJ}^{*#}$ , $F_{F2\_JAS}^{*#}$ , $F_{F3\_to\_Capture}$	15	77.0	148.00	7.83

\* variable not significant; # variable with negative coefficient.

### Only Gilbert River flows

The top model for monthly, birth-year Gilbert River flows accounted for 72.4% of variation in age-frequency and included flows in December, January and March (Table 8). All flow terms were statistically significant and positive in effect. The top model for quarterly, birth-year Gilbert River flows accounted for 69.7% of variation in age-frequency and included  $F_{G0\_OND}$ , and either  $F_{G0\_AMJ}$  or  $F_{G0\_JFM}$ . The top model for quarterly flows in the Gilbert River from birth-year until capture accounted for 76.0% of the variation in age-frequency and included the quarterly flows in the birth-year (i.e.  $F_{G0}$ ) as well as quarterly flows in the second year of life (i.e. after the first birthday,  $F_{G1}$ ) and flows from the third birthday to capture (i.e.  $F_{G3\_to\_Capture}$ ). Coefficients for the top models are provided in Appendix 1.

Table 8. Results of the all-subsets generalised linear models predicting the abundance of barramundi age-classes (3 to 9 years) for the South sub-stock (16°S to Queensland/Northern Territory border) of the southern Gulf of Carpentaria with Gilbert River discharge.

Model type	Model structure	Df	Adj R <sup>2</sup>	AIC	ΔAIC
<b>Birth-year monthly <math>F_{G0}</math></b>					
Base	Age-class <sup>#</sup>	2	58.9	204.12	63.99
Top	Age-class <sup>#</sup> , $F_{G0\_Dec}$ , $F_{G0\_Jan}$ , $F_{G0\_Mar}$	5	72.4	140.98	0.00
Full	Age-class <sup>#</sup> , $F_{G0\_Oct}^{*#}$ , $F_{G0\_Nov}^{*#}$ , $F_{G0\_Dec}^{*#}$ , $F_{G0\_Jan}$ , $F_{G0\_Feb}^{*#}$ , $F_{G0\_Mar}^{*#}$ , $F_{G0\_Apr}^{*#}$ , $F_{G0\_May}^{*#}$ , $F_{G0\_Jun}^{*#}$ , $F_{G0\_Jul}^{*#}$ , $F_{G0\_Aug}^{*#}$ , $F_{G0\_Sep}^{*#}$	14	73.2	147.00	6.02
<b>Birth-year quarterly <math>F_{G0}</math></b>					
Base	Age-class <sup>#</sup>	2	58.9	182.26	44.67
Top	Age-class <sup>#</sup> , $F_{G0\_OND}$ , $F_{G0\_AMJ}$	4	69.7	137.59	0.00
Top alt	Age-class <sup>#</sup> , $F_{G0\_OND}$ , $F_{G0\_JFM}$	4	69.4	138.81	1.22
Full	Age-class <sup>#</sup> , $F_{G0\_OND}$ , $F_{G0\_JFM}^{*#}$ , $F_{G0\_AMJ}^{*#}$ , $F_{G0\_JAS}^{*#}$	6	69.8	139.00	1.41
<b>Birth-year quarterly <math>F_{G0}</math>, plus quarterly <math>F_{G1}</math>, plus quarterly <math>F_{G2}</math>, plus <math>F_{G3\_to\_Capture}</math></b>					
Base	Age-class <sup>#</sup>	2	58.9	286.89	109.19
Top	Age-class <sup>#</sup> , $F_{G0\_OND}$ , $F_{G0\_JFM}$ , $F_{G1\_OND}$ , $F_{G1\_AMJ}$ , $F_{G3\_to\_Capture}$	7	76.0	162.70	0.00
Full	Age-class <sup>#</sup> , $F_{G0\_OND}$ , $F_{G0\_JFM}^{*#}$ , $F_{G0\_AMJ}^{*#}$ , $F_{G0\_JAS}^{*#}$ , $F_{G1\_OND}^{*#}$ , $F_{G1\_JFM}^{*#}$ , $F_{G1\_AMJ}^{*#}$ , $F_{G1\_JAS}^{*#}$ , $F_{G2\_OND}$ , $F_{G2\_JFM}^{*#}$ , $F_{G2\_AMJ}^{*#}$ , $F_{G2\_JAS}^{*#}$ , $F_{G3\_to\_Capture}$	15	79.7	148.00	14.70

\* variable not significant; # variable with negative coefficient.

### Both Flinders and Gilbert River flows

The top model for monthly, birth-year flows from the Flinders and Gilbert rivers accounted for 77.4% of variation in age-frequency and included flows between December and April from either the Flinders or Gilbert rivers (Table 9). All flow terms were statistically significant, and all were positive in effect, except for  $F_{F0\_Feb}$ . There was high correlation between monthly river flows in the Flinders and Gilbert rivers (Appendix 1). However, the top model did not contain flows in the same month from both rivers.

The top model for quarterly, birth-year flows from the Flinders and Gilbert rivers accounted for 70.7% of variation in age-frequency and included  $F_{F0\_JFM}$ ,  $F_{G0\_OND}$ , and  $F_{G0\_AMJ}$ .

The top model for quarterly flows in the Flinders and Gilbert rivers from birth-year until capture accounted for 77.7% of the variation in age-frequency and included the quarterly flows in the birth-year (i.e.  $F_{G0}$ ) as well as quarterly flows in the second year of life (i.e. after the first birthday,  $F_{G1}$ ) and flows from the third birthday to capture (i.e.  $F_{G3\_to\_Capture}$ ). Coefficients for the top models are provided in Appendix 1.

Table 9. Results of the all-subsets generalised linear models predicting the abundance of barramundi age-classes (3 to 9 years) for the South sub-stock (16°S to Queensland/Northern Territory border) of the southern Gulf of Carpentaria with Flinders ( $F_F$ ) and Gilbert ( $F_G$ ) rivers flow

Model type	Model structure	Df	Adj R <sup>2</sup>	AIC	ΔAIC
<b>Flinders and Gilbert birth-year monthly flow (<math>F_{F0}</math> and <math>F_{G0}</math>)</b>					
Base	Age-class <sup>#</sup>	2	58.9	242.11	102.11
Top	Age-class <sup>#</sup> , $F_{F0\_Jan}$ , $F_{F0\_Feb}$ <sup>#</sup> , $F_{F0\_Mar}$ , $F_{G0\_Dec}$ , $F_{G0\_Jan}$ , $F_{G0\_Apr}$	8	77.4	140.00	0.00
Full	Age-class <sup>#</sup> , $F_{F0\_Dec}$ <sup>**</sup> , $F_{F0\_Jan}$ , $F_{F0\_Feb}$ <sup>#</sup> , $F_{F0\_Mar}$ <sup>*</sup> , $F_{F0\_Apr}$ <sup>*</sup> , $F_{G0\_Dec}$ , $F_{G0\_Jan}$ , $F_{G0\_Feb}$ <sup>*</sup> , $F_{G0\_Mar}$ <sup>*</sup> , $F_{G0\_Apr}$ <sup>*</sup>	12	77.2	145.00	1.00
<b>Flinders and Gilbert quarterly flow (<math>F_{F0}</math> and <math>F_{G0}</math>)</b>					
Base	Age-class <sup>#</sup>	2	58.9	182.26	44.39
Top	Age-class <sup>#</sup> , $F_{F0\_JFM}$ , $F_{G0\_OND}$ , $F_{G0\_AMJ}$	5	70.7	137.87	0.00
Full	Age-class <sup>#</sup> , $F_{F0\_OND}$ <sup>*</sup> , $F_{F0\_JFM}$ <sup>*</sup> , $F_{F0\_AMJ}$ <sup>*</sup> , $F_{F0\_JAS}$ <sup>**</sup> , $F_{G0\_OND}$ , $F_{G0\_JFM}$ <sup>*</sup> , $F_{G0\_AMJ}$ <sup>**</sup> , $F_{G0\_JAS}$ <sup>*</sup>	10	70.7	143.00	5.13
<b>Flinders and Gilbert birth-year quarterly flows (<math>F_{F0}</math> and <math>F_{G0}</math>), wet-season flows <math>F_{F1\_Oct\_to\_Mar}</math>, wet-season flows <math>F_{F2\_Oct\_to\_Mar}</math>, and annual flows<math>F_{G3\_to\_Capture}</math></b>					
Base	Age-class <sup>#</sup>	2	58.9	248.49	107.88
Top	Age-class <sup>#</sup> , $F_{F0\_OND}$ , $F_{F0\_AMJ}$ , $F_{F0\_JAS}$ <sup>**</sup> , $F_{G0\_OND}$ , $F_{F1\_Oct\_to\_Mar}$ , $F_{F3\_to\_Capture}$ <sup>*</sup> , $F_{G3\_to\_Capture}$	9	77.7	143.61	0.00
Full	Age-class <sup>#</sup> , $F_{F0\_OND}$ , $F_{F0\_JFM}$ <sup>**</sup> , $F_{F0\_AMJ}$ , $F_{F0\_JAS}$ <sup>**</sup> , $F_{F1\_Oct\_to\_Mar}$ , $F_{F2\_Oct\_to\_Mar}$ <sup>#</sup> , $F_{F3\_to\_Capture}$ <sup>**</sup> , $F_{G0\_OND}$ , $F_{G0\_JFM}$ <sup>#</sup> , $F_{G0\_AMJ}$ <sup>*</sup> , $F_{G0\_JAS}$ <sup>**</sup> , $F_{G1\_Oct\_to\_Mar}$ <sup>*</sup> , $F_{G2\_Oct\_to\_Mar}$ <sup>*</sup> , $F_{G3\_to\_Capture}$	16	78.0	149.00	5.39

\* variable not significant; # variable with negative coefficient.

The results from the GLMs confirm the importance of birth-year flows in determining relative recruitment of barramundi, but also demonstrate the importance of rivers flows in subsequent years. The top models can be used for quantitatively considering the relative risk of alternate water development scenarios as per McGregor et al. (2018) and Bayliss et al. (2014).

## 3.2 Growth

### 3.2.1 Timing of increment formation

The edge interpretation of the long-term otolith dataset was opportunistically used to assess the timing of opaque zone formation in the wider Gulf and in each study region. Pooled across all regions, the formation of an opaque band (edge type = 'new') was generally associated with the austral winter but was observed as early as February in 5.8% of fish sampled, all of which were from the southernmost Flinders region. 'New' edge types were increasingly common over the following months, with more than 50% of fish having a new increment by September (Figure 17).

A latitudinal gradient was apparent once samples were separated by region (Figure 17), although this may be influenced by the unequal sample numbers from each region in each month. The formation of a new edge was observed earliest in the southernmost region (February, in the Flinders), a month later at the intermediate region (Gilbert), and not until another month later at the northernmost region (Mitchell). Similarly, more than 50% of fish displayed a new increment by June in the southernmost Flinders region, by July in the intermediate Gilbert region, and by September in the northernmost Mitchell region.

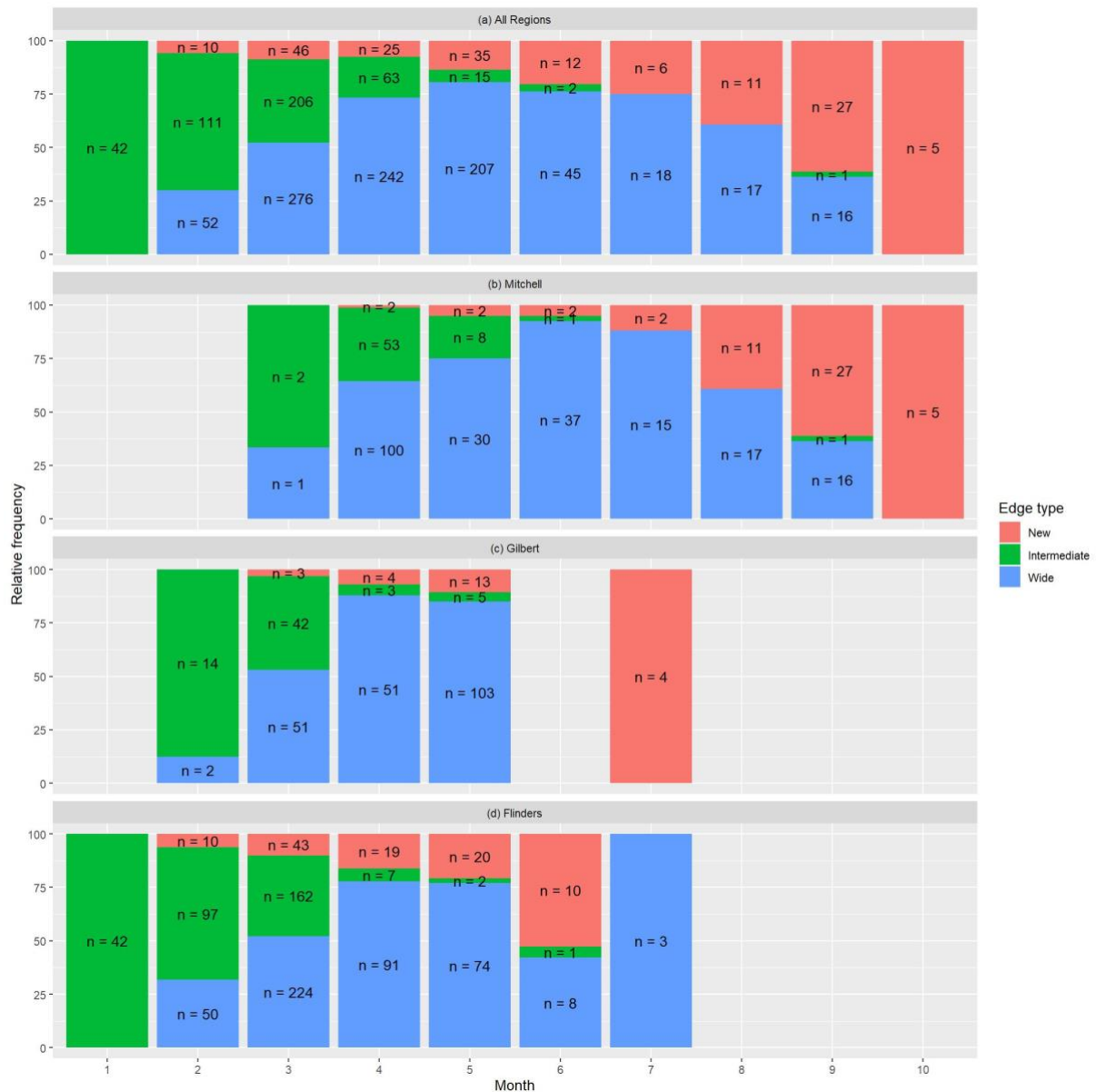


Figure 17. Relative frequency histogram of barramundi otolith edge type per month. (a) All regions combined ( $n=1,491$ ), (b) Mitchell region ( $n=332$ ), (c) Gilbert region ( $n=295$ ) and (d) Flinders region ( $n=864$ ). Samples are sparse in October and unavailable in November and December due to annual fishery closure between 7 October and 1 February. Samples collected in January are from research sampling.

### 3.2.2 River and atmospheric index patterns

Peak river discharge occurred in January–February–March in almost all regions and years, although important flows were occasionally observed earlier (October–November–December) or later (April–May–June) (Figure 18). Minimum and maximum river discharge volumes differed greatly between river systems, with consistently larger river discharges observed from the Mitchell River compared with the Gilbert and Flinders rivers (Figure 18).

Mean MJO intensity in the period from January to March each year demonstrated little variation in most years, with occasional large positive (e.g. 1998) or negative (e.g. 2007,

2013, 2014) pulses. MJO was positively correlated with October–November–December flows, and particularly strongly with January–February–March flows in all three study regions ( $0.329 < r < 0.452$ ; Table 10).

Mean summer SOI across the study period (Figure 18) aligned with known El Niño Southern Oscillation (ENSO) events, for example, the 1998 El Niño summer, and 2010 and 2011 La Niña summers (Bureau of Meteorology 2012). SOI was positively correlated with early, mid and late wet-season river discharge volumes in all three study regions ( $0.187 < r < 0.577$ ; Table 10). Although the relationship between MJO and SOI appeared to be inconsistent across the study regions, this is an artefact of sub-setting the MJO and SOI datasets to the period for which barramundi growth data is available for each region. Barramundi growth data were available for the longest period in the Flinders region (1997–2014; Table 10, Figure 18). Therefore, the correlation coefficient calculated between MJO and SOI in the Flinders region ( $r = -0.106$ ) should be considered the most accurate representation of the relationship between those two variables.

Table 10. Pearson correlation coefficients between river flow variables and atmospheric indices for each study region.

<b>Mitchell</b>	<b>F<sub>OND</sub></b>	<b>F<sub>JFM</sub></b>	<b>F<sub>AMJ</sub></b>	<b>MJO</b>	<b>SOI</b>
<b>F<sub>OND</sub></b>					
<b>F<sub>JFM</sub></b>	0.201				
<b>F<sub>AMJ</sub></b>	-0.226	0.118			
<b>MJO</b>	0.455	0.329	-0.116		
<b>SOI</b>	0.258	0.270	0.382	-0.171	
<b>Gilbert</b>	<b>F<sub>OND</sub></b>	<b>F<sub>JFM</sub></b>	<b>F<sub>AMJ</sub></b>	<b>MJO</b>	<b>SOI</b>
<b>F<sub>OND</sub></b>					
<b>F<sub>JFM</sub></b>	0.815				
<b>F<sub>AMJ</sub></b>	0.400	0.027			
<b>MJO</b>	0.333	0.452	-0.037		
<b>SOI</b>	0.577	0.545	0.552	0.262	
<b>Flinders</b>	<b>F<sub>OND</sub></b>	<b>F<sub>JFM</sub></b>	<b>F<sub>AMJ</sub></b>	<b>MJO</b>	<b>SOI</b>
<b>F<sub>OND</sub></b>					
<b>F<sub>JFM</sub></b>	0.445				
<b>F<sub>AMJ</sub></b>	0.404	0.359			
<b>MJO</b>	0.124	0.398	-0.007		
<b>SOI</b>	0.378	0.315	0.187	-0.106	

F<sub>OND</sub> = total river discharge in October–November–December; F<sub>JFM</sub> = total river discharge in January–February–March; F<sub>AMJ</sub> = total river discharge in April–May–June; MJO = mean Phase 4 Madden–Julian Oscillation from January to March; SOI = mean Southern Oscillation Index from October to March.



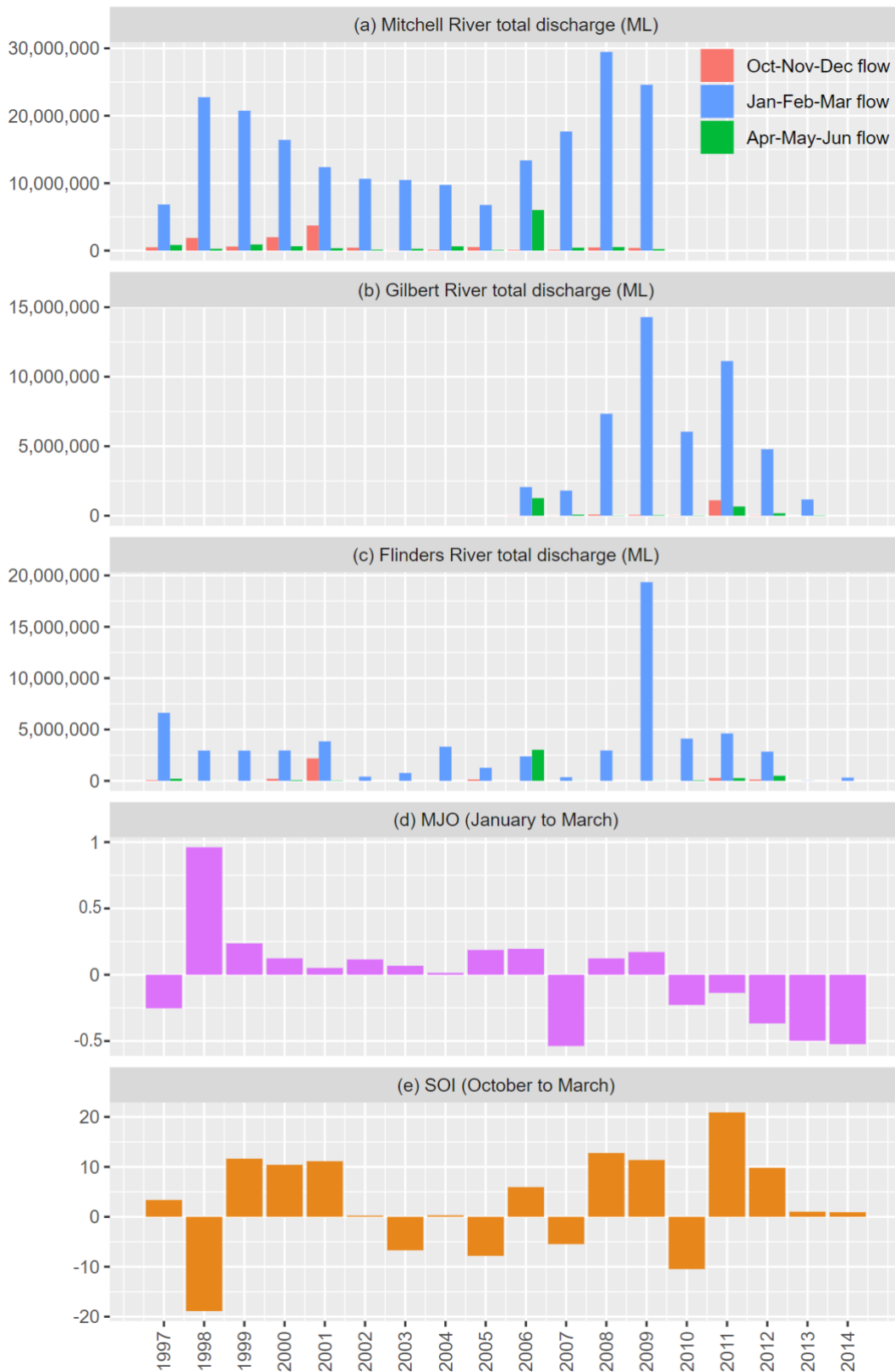


Figure 18. Total river discharge (in ML) per wet season in (a) the Mitchell, (b) the Gilbert and (c) the Flinders region, and (d) Madden-Julian Oscillation (MJO) and (e) Southern Oscillation Index (SOI) summer intensities.

### 3.2.3 Drivers of otolith increment width

Increment number and age-at-capture were consistently included in all top models describing otolith increment width in 0- to 3-year-old barramundi (Table 11). In all cases, increment number had the strongest effect on increment width by an order of magnitude (coefficients  $< -0.30$ ), due to the decrease in increment width with age. The weaker negative effect of the age-at-capture covariate (coefficients generally  $< -0.02$ ) indicates that individuals captured at an older age had narrower early growth increments (i.e. slower growers are captured older) than fish captured at a younger age (i.e. faster growers are captured younger).

#### **Mitchell region**

The model selection process identified two top models describing the effects of river discharge on otolith increment width in the Mitchell region, and two top models describing the effects of atmospheric indices (Table 11). Marginal and conditional  $R^2$  values were similarly high for all models. Conditional  $R^2$  accounts for both fixed and random effects, whereas marginal  $R^2$  accounts for the fixed effects alone (Nakagawa and Schielzeth 2013). The high  $R^2$ , both conditional and marginal, indicates that the random effect of FishID (the repeated measure component) accounted for very little of the total variation in the increment width dataset.

The two top river discharge models proposed that total flow in each of the three wet-season periods (October–November–December, January–February–March, April–May–June) was significantly and positively related to juvenile barramundi growth rates (Table 11). Some interaction effects were present and had similarly large coefficients to the main effects. A positive interaction between increment number and flow in January–February–March indicates that older juveniles benefit more from high flow volumes at the peak of the wet season than do young-of-the-year barramundi (Figure 19). Conversely, a negative interaction effect between increment number and flow in April–May–June indicates that younger juveniles benefit more from high flow volumes at the end of the wet season than do older juveniles (Figure 19). This effect may in part be driven by the extended 2006 wet season (Figure 18).

The top atmospheric models indicated that both MJO and SOI have strong positive effects on juvenile barramundi growth rates in the Mitchell region; the largest otolith increment widths were seen in La Niña (strongly positive SOI) and intensely monsoonal (high MJO) wet seasons (Table 11, Figure 19).

#### **Gilbert region**

The model selection process identified three top models describing the effects of river discharge on juvenile barramundi growth rates in the Gilbert region (Table 11), noting that total flow in October–November–December was excluded from analyses due to strong collinearity with January–February–March flow, and that only 8 years of otolith growth data were available for analysis (Figure 18). Total river discharge volume in January–February–March had a strong and highly significant effect on juvenile barramundi growth rates. This effect demonstrated a positive interaction with increment number (Table 11), such that older juveniles were more strongly influenced by high flow rates than were young-of-the-year juveniles (Figure 19). A positive main effect of flow in April–May–June was also observed.

Two similar top atmospheric models were identified by the model selection process, with both indicating a positive main effect of SOI on juvenile barramundi growth rates, and a positive interaction between MJO and increment number (Table 11, Figure 19). The interaction is driven by a negative relationship between MJO and growth within the first increment, but a positive relationship between MJO and growth in the third increment.

### **Flinders region**

The model selection process identified three top models describing the effects of river discharge on otolith increment width in the Flinders region (Table 11). All models included a strong positive effect of January–February–March flow on barramundi growth rates, and a strong interaction with increment number, wherein older juvenile barramundi were positively impacted by high January–February–March flows and young-of-the-year (i.e. 0+) juveniles experienced little, or slightly negative, influence on their growth rates (Figure 19). A weak positive effect of early wet-season flows (October–November–December) was observed in the Flinders region, as was a negative interaction with increment number, such that older juvenile barramundi were not affected by early wet-season flows, but young-of-the-year juveniles were positively affected by early wet-season flows (Figure 19). This interaction appeared to be largely constrained to low flow volumes, with the greatest effect of October–November–December flows observed below 500,000 ML.

A single model best described the effects of atmospheric indices on otolith increment width in the Flinders region (Table 11). The model indicated a strong positive relationship between SOI and juvenile barramundi growth rates for the Flinders region (Figure 19), and a strong interactive effect of MJO and increment number, such that young-of-the-year barramundi were negatively impacted by an intense MJO, but older juveniles experienced greater growth rates under those same conditions (Figure 19).

Table 11. Linear mixed model design, parameter coefficients and statistical significance of fixed effects included in the top ( $\leq 2\text{AICc}$ ) models for river flow variables and atmospheric indices for the Mitchell, Gilbert and Flinders rivers.

Mitchell													
Intercept	Age-at-capture	Increment	F <sub>OND</sub>	F <sub>JFM</sub>	F <sub>AMJ</sub>	Inc. F <sub>OND</sub>	Inc. F <sub>JFM</sub>	Inc. F <sub>AMJ</sub>	df	AICc	Rel. weight	Marg. R <sup>2</sup>	Cond. R <sup>2</sup>
-1.096***	-0.032***	-0.327***	0.017***	0.010*	0.014**		0.010*	-0.010*	10	-1230.8	0.696	0.877	0.897
-1.096***	-0.032***	-0.327***	0.018***	0.009	0.014**	-0.003	0.011*	-0.011*	11	-1229.1	0.304	0.877	0.897
Intercept	Age-at-capture	Increment	MJO	SOI	Inc. MJO	Inc. SOI			df	AICc	Rel. weight	Marg. R <sup>2</sup>	Cond. R <sup>2</sup>
-1.094***	-0.037***	-0.329***	0.018***	0.022***		-0.008			8	-1242.8	0.677	0.878	0.899
-1.095***	-0.036***	-0.329***	0.016***	0.023***					7	-1241.3	0.323	0.878	0.898
Gilbert													
Intercept	Age-at-capture	Increment	F <sub>OND</sub>	F <sub>JFM</sub>	F <sub>AMJ</sub>	Inc. F <sub>OND</sub>	Inc. F <sub>JFM</sub>	Inc. F <sub>AMJ</sub>	df	AICc	Rel. weight	Marg. R <sup>2</sup>	Cond. R <sup>2</sup>
-1.124***	-0.020***	-0.303***	N/a	0.028***	0.012*	N/a	0.014*	0.010	9	-908.4	0.504	0.837	0.859
-1.127***	-0.017***	-0.306***	N/a	0.029***		N/a	0.017***		7	-907.1	0.265	0.836	0.858
-1.127***	-0.019***	-0.304***	N/a	0.029***	0.007	N/a	0.015**		8	-906.9	0.230	0.836	0.858
Intercept	Age-at-capture	Increment	MJO	SOI	Inc. MJO	Inc. SOI			df	AICc	Rel. weight	Marg. R <sup>2</sup>	Cond. R <sup>2</sup>
-1.121***	-0.017**	-0.308***	<0.001	0.015*	0.037***				8	-913.9	0.62	0.837	0.861
-1.122***	-0.016**	-0.308***	<0.001	0.014*	0.040***	-0.006			9	-913.0	0.38	0.837	0.861
Flinders													
Intercept	Age-at-capture	Increment	F <sub>OND</sub>	F <sub>JFM</sub>	F <sub>AMJ</sub>	Inc. F <sub>OND</sub>	Inc. F <sub>JFM</sub>	Inc. F <sub>AMJ</sub>	df	AICc	Rel. weight	Marg. R <sup>2</sup>	Cond. R <sup>2</sup>
-1.106***	-0.022***	-0.325***	0.006*	0.015***		-0.007*	0.020***		9	-2867.6	0.557	0.871	0.878
-1.106***	-0.022***	-0.325***	0.006	0.015***	0.001	-0.006	0.020***		10	-2865.8	0.230	0.870	0.878
-1.105***	-0.021***	-0.325***	0.005	0.016***			0.017***		8	-2865.6	0.213	0.870	0.878
Intercept	Age-at-capture	Increment	MJO	SOI	Inc. MJO	Inc. SOI			df	AICc	Rel. weight	Marg. R <sup>2</sup>	Cond. R <sup>2</sup>
-1.107***	-0.026***	-0.327***	0.002	0.014***	0.011***				8	-2776.7	1.000	0.865	0.873

\*  $p < 0.05$ , \*\*  $p < 0.005$ , \*\*\*  $p < 0.001$ . F<sub>OND</sub> = total river discharge in October–November–December; F<sub>JFM</sub> = total river discharge in January–February–March; F<sub>AMJ</sub> = total river discharge in April–May–June; ‘Inc. X’ = interaction effect between increment number and the specified variable; df = degrees of freedom; AICc = second-order Akaike information criterion; ‘Rel. weight’ = model relative weight; ‘Marg. R<sup>2</sup>’ = marginal R<sup>2</sup> (fixed effects only); ‘Cond. R<sup>2</sup>’ = conditional R<sup>2</sup> (fixed and random effects); MJO = mean Phase 4 Madden–Julian Oscillation from January to March; SOI = mean Southern Oscillation Index from October to March. Random intercept effect of FishID was included for all models. All variables (except atmospheric indices) were natural log transformed prior to analysis, and all predictor variables were scaled and centred prior to analysis. Variables marked ‘N/a’ were not included in the global model due to collinearity with other fixed effects.

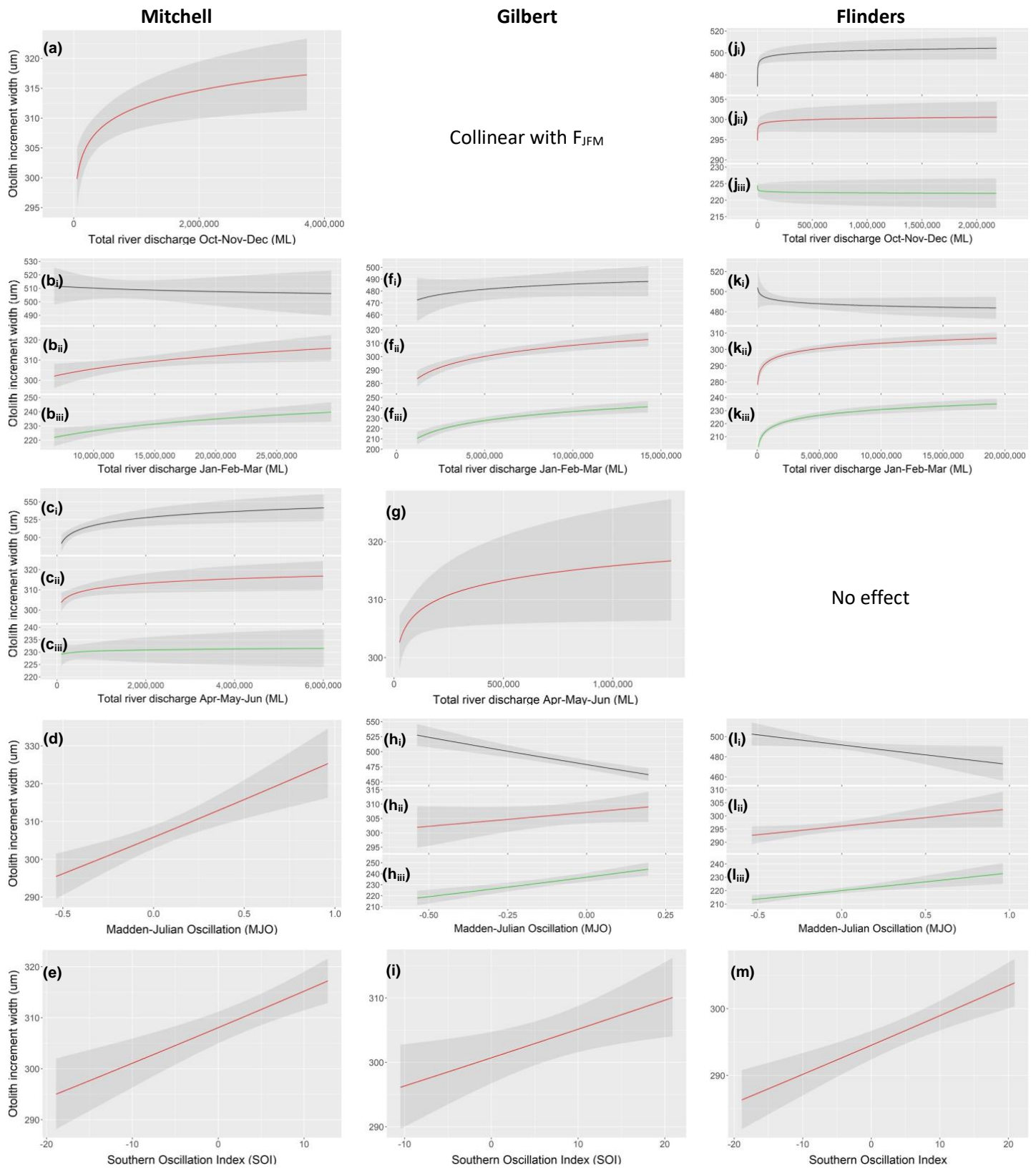


Figure 19. Predicted mean ( $\pm 95\%$  confidence intervals) otolith increment width for the Mitchell (a) to (e), the Gilbert River (f) to (i) and the Flinders River (j) to (m). Based on the single top model for each region with significant ( $p < 0.05$ ) interactive effects illustrated. Black line: increment 1; red line: increment 2; green line: increment 3. Where significant interactions with increment were not present, predicted otolith increment widths are illustrated for increment 2.

### 3.2.4 Scenario testing

Juvenile barramundi growth rates in the Mitchell region were distinctly reduced under flow Scenario X compared with existing flow conditions. Otolith increment widths were reduced by 14.2% to 28.2% under flow Scenario X (Table 12). This resulted in a 19% reduction in cumulative otolith width between the otolith core and third increment. This means that age 2+ juvenile barramundi would be expected to be, on average, about 19% smaller (in total length) under flow Scenario X compared with juvenile barramundi under current flow conditions (Figure 20).

Table 12. Predicted changes in juvenile barramundi growth rates (otolith increment widths) in the Mitchell region for water development Scenario X, relative to current river discharge volumes.

	Percent difference in increment width	Percent difference in cumulative otolith width
<b>Increment 1</b>	-14.2%	-14.2%
<b>Increment 2</b>	-23.1%	-17.6%
<b>Increment 3</b>	-28.2%	-19.3%

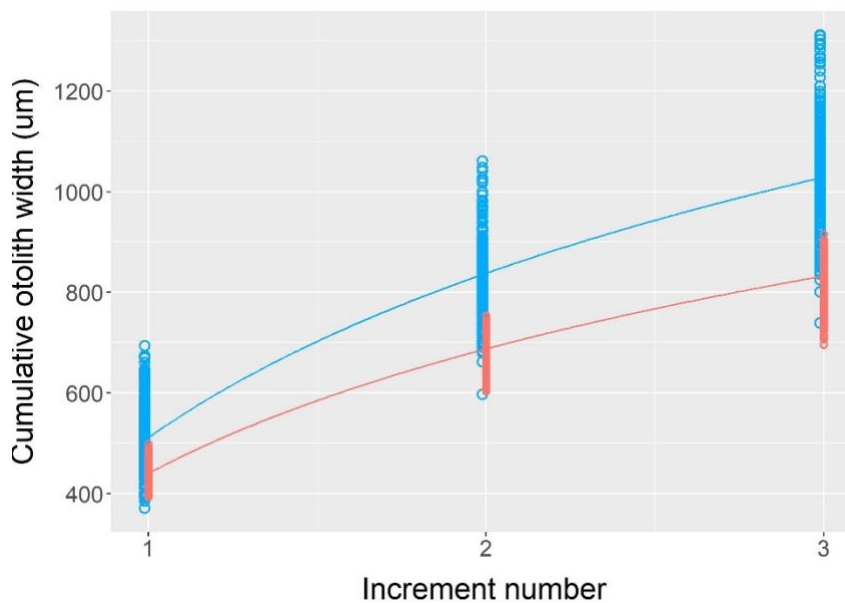


Figure 20. Difference in cumulative otolith widths of juvenile barramundi in the Mitchell region under the current flow scenario (blue) and under modified flow Scenario X (red).

## 3.3 Otolith microchemistry

### 3.3.1 Water chemistry

The steepness and direction of the  $^{87}\text{Sr}/^{86}\text{Sr}$  mixing curves varied between rivers (Figure 21), being more discriminatory between salinities for the Mitchell, Gilbert and Norman rivers, and least discriminatory for the Flinders River. The mixing curve for the Flinders River was very shallow, and inverse to all other rivers sampled. Inverse mixing curves have previously been reported in the literature, such as in the rivers of southern Papua New Guinea (Milton and Chenery 2005).

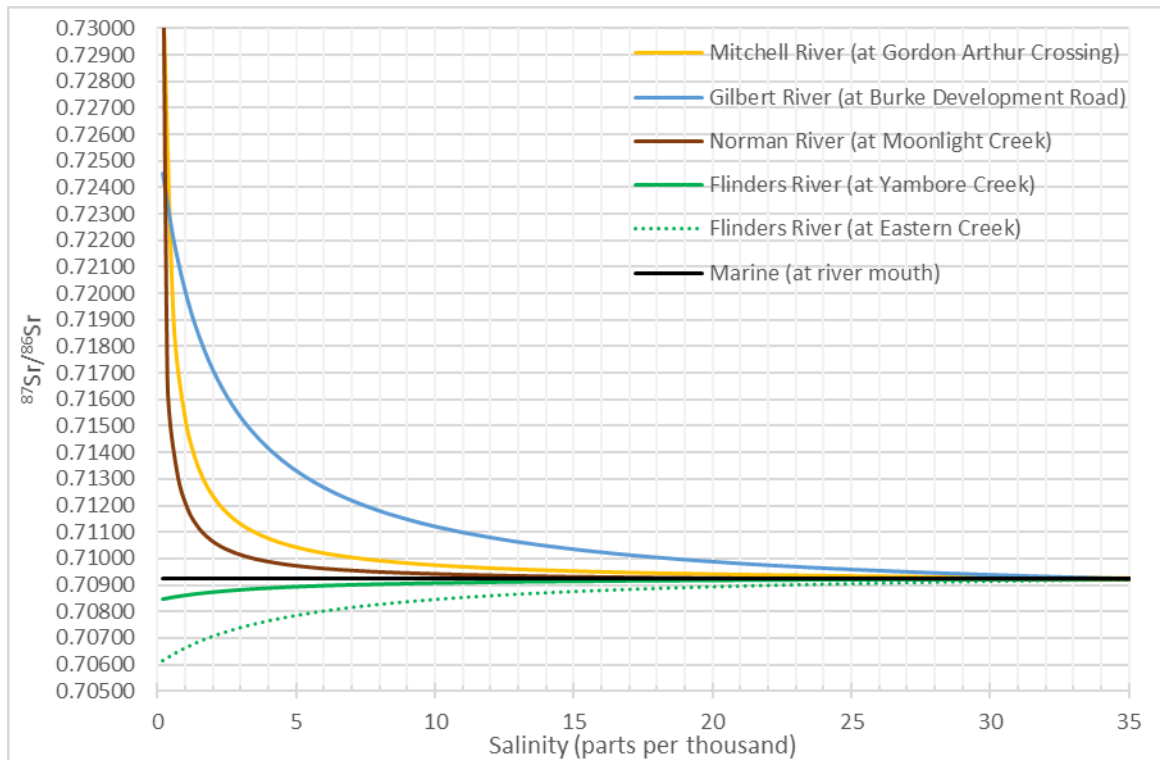


Figure 21. Freshwater–marine mixing curve of dissolved strontium isotopes ( $^{87}\text{Sr}/^{86}\text{Sr}$ ) across the salinity gradient for rivers of the south-eastern Gulf of Carpentaria, based on observed water samples.

The  $^{87}\text{Sr}/^{86}\text{Sr}$  values of additional water samples collected to provide spatial and temporal replicates were closely matched to the hypothetical mixing curves for the Mitchell, Gilbert and Norman Rivers, but were somewhat contrary for the Flinders River (Appendix 2). The results for the Flinders River suggest that the strontium isoscape in this part of the GoC is spatially (and temporally) complex, and concurs with that reported by Adams et al. (2019).

### 3.3.2 Habitat use inferred from $^{87}\text{Sr}/^{86}\text{Sr}$ profile

Each fish analysed for otolith  $^{87}\text{Sr}/^{86}\text{Sr}$  was classified for habitat use inferred from the laser ablation profile values during the slow-growth opaque zone (Roberts et al. 2019), which approximately coincides with the dry season in the southern GoC. Otolith strontium isotope ratios for the Mitchell and Gilbert rivers were relatively easy to classify for habitat use inferred from the  $^{87}\text{Sr}/^{86}\text{Sr}$ , whereas those from the Flinders River were generally more difficult to classify. The shallow freshwater–marine  $^{87}\text{Sr}/^{86}\text{Sr}$  hypothetical mixing curve and spatially complex strontium isoscape for the Flinders River, combined with the ‘scattered’  $^{87}\text{Sr}/^{86}\text{Sr}$  profiles of barramundi from the Flinders River, indicated that results for this river should be considered less certain.

Of the estuaries sampled in the current study, barramundi from the Mitchell River estuary had the highest proportion of fish classified as freshwater habitat use (Table 13). Barramundi from the Gilbert had the highest number of fish classified as ‘intermediate’ and the Flinders had the highest number of fish classified as estuarine habitat use (Table 13). This probably reflects the variable opportunities for diadromous movement in each of the systems, which would be a function of catchment geomorphology and temporal patterns in flow hydrology.

Table 13. Habitat residency of barramundi harvested from estuaries of the Mitchell, Gilbert and Flinders rivers in the southern Gulf of Carpentaria based on inference from otolith  $^{87}\text{Sr}/^{86}\text{Sr}$  profiles.

	Freshwater	Intermediate	Estuary		
<b>Mitchell overall (n=106)</b>	<b>63%</b>	<b>27%</b>	<b>10%</b>		
2002 year-class	66%	28%	6%		
2003 year-class	50%	29%	21%		
2005 year-class	66%	24%	10%		
2006 year-class <sup>A</sup>	43%	43%	14%		
<b>Gilbert overall (n=94)</b>	<b>25%</b>	<b>49%</b>	<b>26%</b>		
2006 year-class	15%	69%	15%		
2008 year-class	26%	43%	31%		
2011 year-class	35%	57%	9%		
<b>Flinders overall (n=202)</b>	<b>33%</b>	<b>0%</b>	<b>67%</b>		
	<b>Fw</b>	<b>Fw<sup>†</sup></b>	<b>Intermediate</b>	<b>Estuary<sup>#</sup></b>	<b>Estuary</b>
<b>Flinders overall subcategories</b>	<b>23%</b>	<b>10%</b>	<b>0%</b>	<b>38%</b>	<b>29%</b>
2002 year-class	12%	17%	0%	12%	59%
2003 year-class	35%	15%	0%	8%	42%
2005 year-class	29%	0%	0%	21%	50%
2006 year-class <sup>A</sup>	19%	10%	0%	48%	24%
2008 year-class	25%	6%	0%	58%	11%

<sup>A</sup> samples derived from Halliday et al. (2012) with habitat class interpretation based on five Mitchell River barramundi with both  $^{87}\text{Sr}/^{86}\text{Sr}$  and trace metal/calcium profiles (i.e. strontium, barium, manganese, magnesium). Fw<sup>†</sup> sub-classification being 'freshwater' but having  $^{87}\text{Sr}/^{86}\text{Sr}$  values indicative of habitat based on water samples from the Flinders River at the Burke Development Road causeway. Estuary<sup>#</sup> sub-classification being 'estuarine' as having estuarine  $^{87}\text{Sr}/^{86}\text{Sr}$  values during all opaque zones but having  $^{87}\text{Sr}/^{86}\text{Sr}$  values indicating salinity <5 parts per thousand during one or more translucent zones.

### Mitchell River

Barramundi caught in the estuary of the Mitchell River could readily be classified by their  $^{87}\text{Sr}/^{86}\text{Sr}$  profile as residing in water with an inferred salinity of  $\leq 1$  ppt (Figure 22). Overall, 63% of barramundi in the Mitchell River had resided in freshwater for at least one dry season, while 10% had resided only in estuarine water of >5 ppt (Table 13). The remainder (27%) were classified as 'intermediate'. The  $^{87}\text{Sr}/^{86}\text{Sr}$  profiles of intermediate-classed fish were commonly cyclical, with inferred salinity values of >1 ppt and <5 ppt during the dry season (Figure 22).



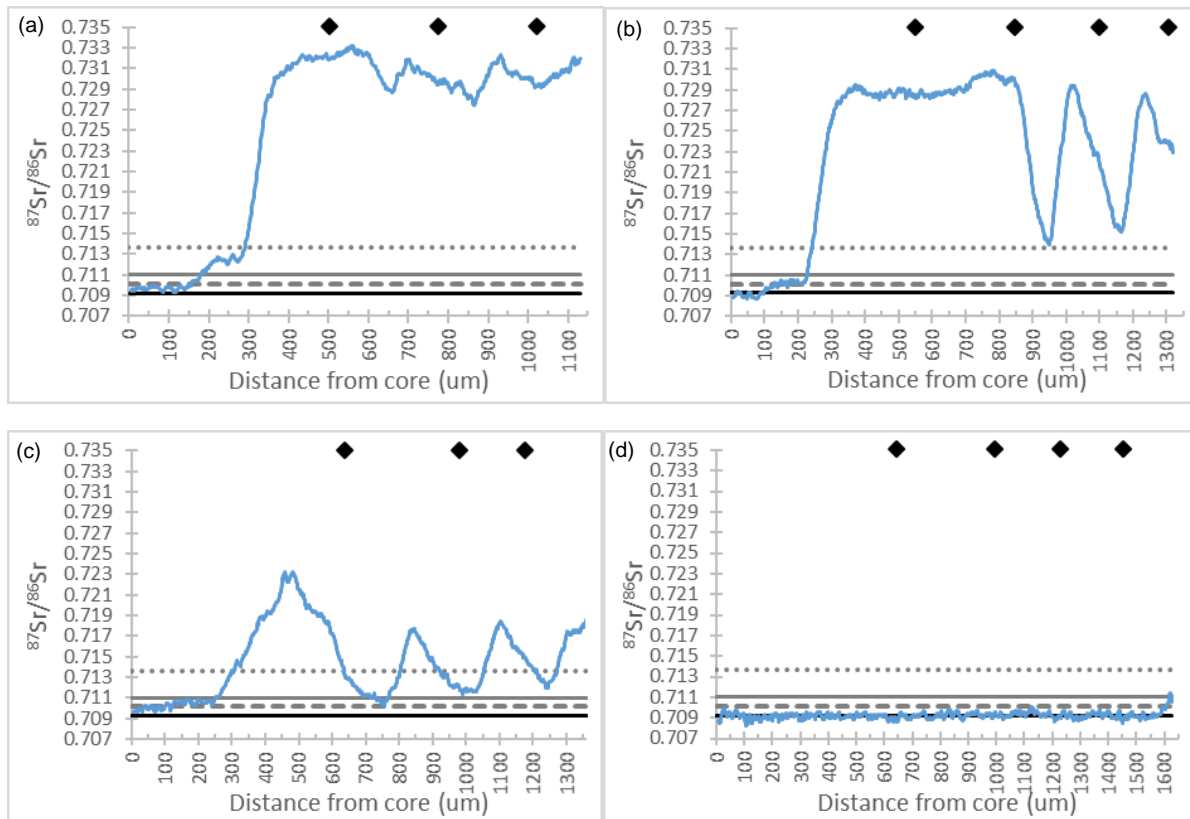


Figure 22. Otolith  $^{87}\text{Sr}/^{86}\text{Sr}$  profiles (5-point smoothed) of ablation transects (core to proximal edge displayed) of barramundi caught in the Mitchell River estuary. The solid black line is the  $^{87}\text{Sr}/^{86}\text{Sr}$  of marine water sampled from the Mitchell River estuary in October 2017. The grey lines are the 1 ppt (dotted) and 5 ppt (dashed) salinity from the mixing curve for the Mitchell River. The grey solid line is the  $^{87}\text{Sr}/^{86}\text{Sr}$  of water sampled from Bull Crossing (freshwater site) in October 2018. Examples illustrate habitat residency classes: freshwater (a) and (b), intermediate (c), and estuarine (d).

There were slight differences in habitat residency between barramundi from different year-classes from the Mitchell River (Table 13). This may reflect differing opportunities for movement up- and downstream based on the size and duration of wet-season flows (Figure 23).

Jardine et al. (2012) notes that barramundi may forage in saltwater for several years before being found in (freshwater) waterholes. Of the barramundi from the Mitchell River that moved into freshwater habitats, the majority (~52%) moved upstream during the wet season associated with their first year of life (i.e. as zero-year-olds or 'young-of-the-year'), and 41% moving during the wet season associated with their second year of life (i.e. as 1-year-olds). Barramundi that moved upstream in the Mitchell River as 1-year-olds were predominantly from the 2005 year-class, which experienced a relatively low flow in the 2005 wet season (Figure 23). Additionally, the monthly flow in 2005 was greatly reduced below the long-term median between February and July, potentially reducing temporal and spatial opportunities for young-of-the-year upstream movement (Figure 24).

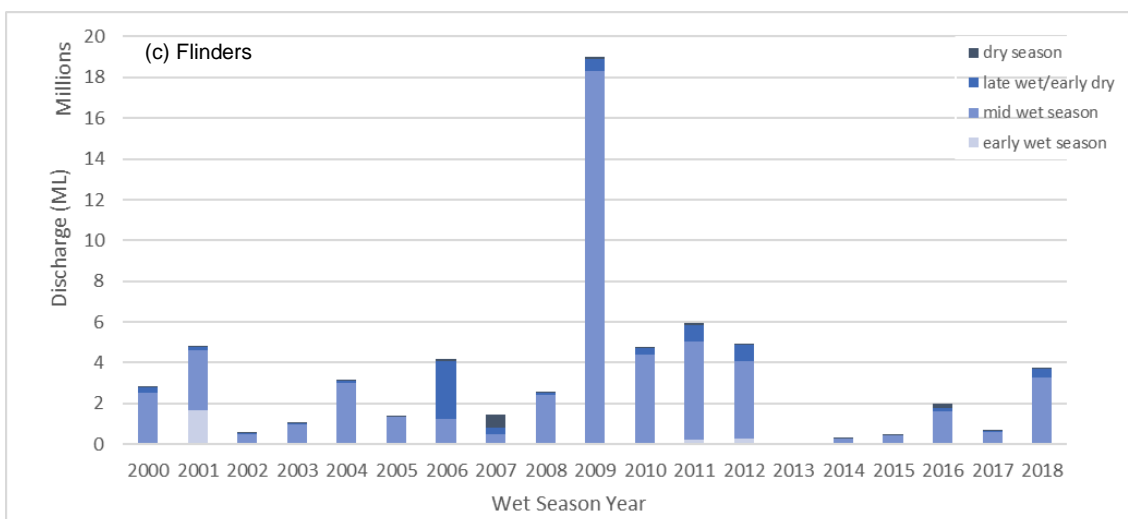
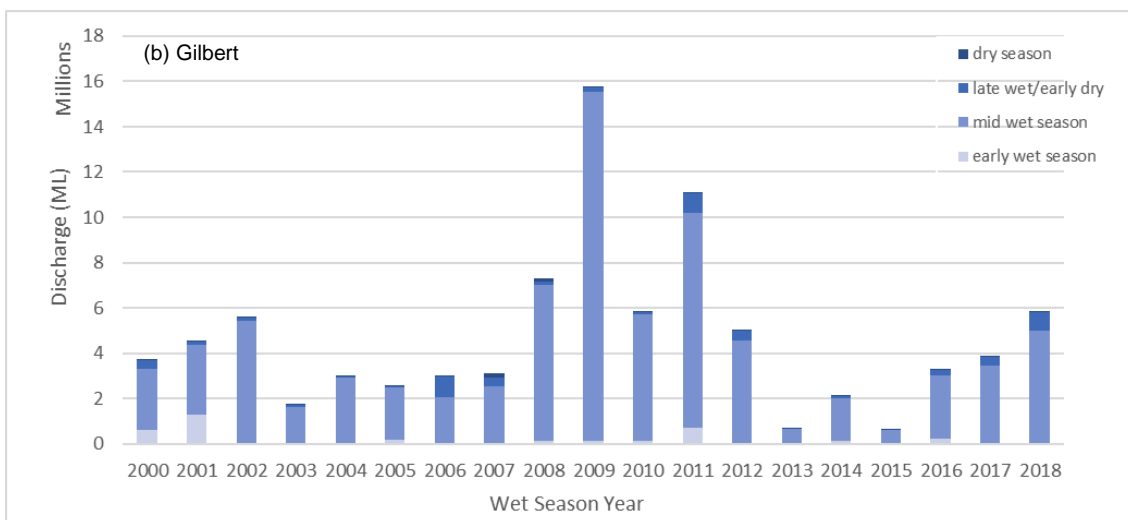
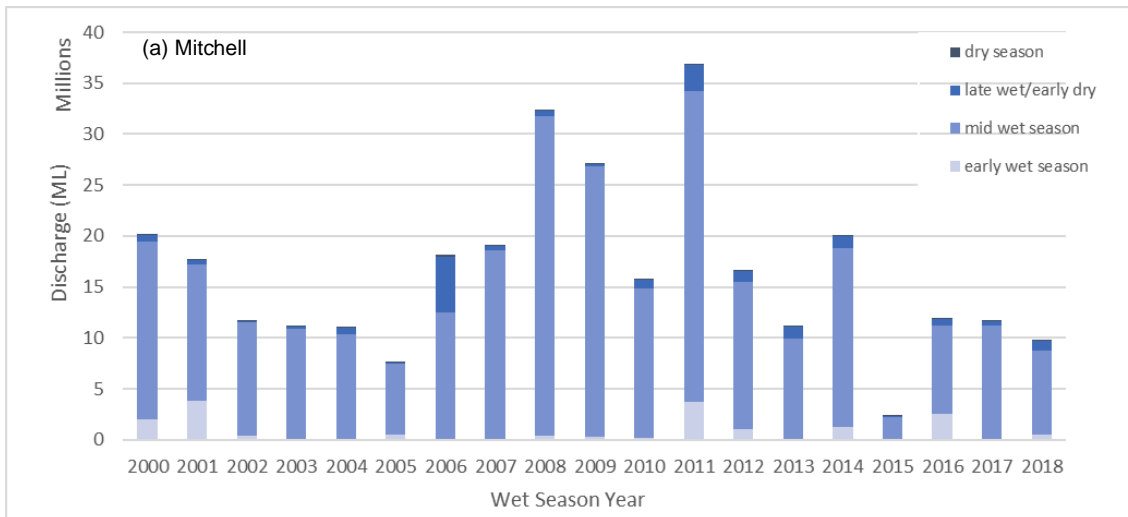


Figure 23. Annual (wet-season year) flow for the (a) Mitchell, (b) Gilbert and (c) Flinders rivers in the southern Gulf of Carpentaria. Early wet season is October to December, mid wet is January to March, late wet/early dry is April to June, and dry is July to September. Flow is modelled end-of-system supplied by CSIRO, February 2020, in conjunction with FRDC project 2018/079. Note different scales for flow (discharge) on the y-axes, which is in millions of megalitres.

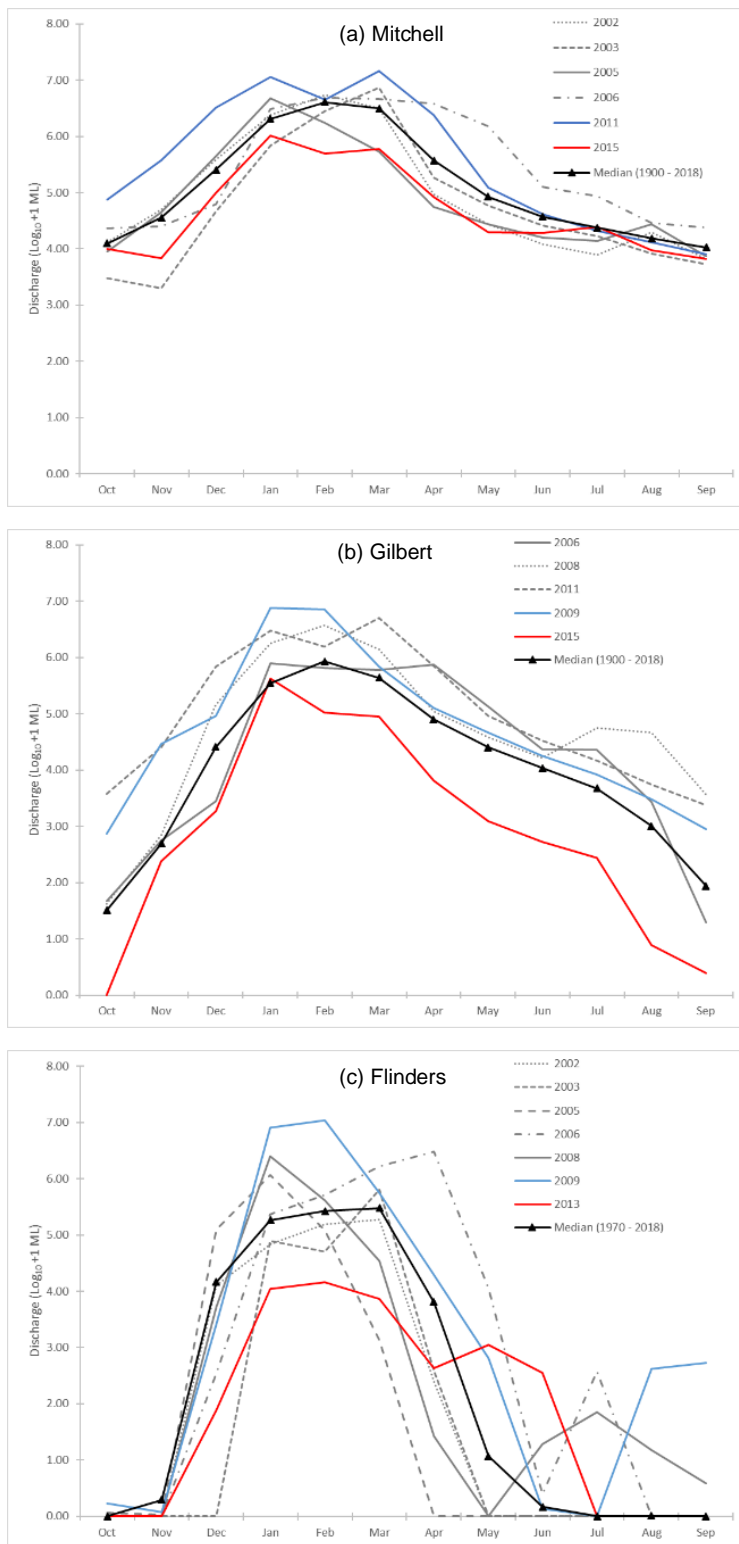


Figure 24. Monthly flows across the wet-season year for the (a) Mitchell, (b) Gilbert and (c) Flinders rivers in the southern Gulf of Carpentaria. The black line is the median for 1900–2018. Grey lines are birth-year flows for year-classes from each river analysed for otolith microchemistry. Blue and red lines illustrate monthly flow pattern of recent flow years (2000–2018), with high flow (blue) and low flow (red) highlighted for each river.

## Gilbert River

Across all samples, 25% of barramundi harvested from the Gilbert River estuary were classed as having resided in freshwater for at least one dry season (Table 13). Forty-nine percent were classified as 'intermediate', with  $^{87}\text{Sr}/^{86}\text{Sr}$  profiles that commonly cycled seasonally (Figure 25). The remainder (26%) were classified as estuarine. Many of the estuary-classed fish had clear signals of lower salinity during summer fast-growth periods, but with  $^{87}\text{Sr}/^{86}\text{Sr}$  values indicating inferred salinities >5 ppt but <15 ppt during the winter slow-growth period. There were slight differences in habitat residency between different year-classes (Table 13), which may reflect differing flow-related opportunities for up- and downstream movement (Figure 23). Of those fish that moved into freshwater habitats in the Gilbert River, the majority (~90%) moved into freshwater during their first year of life prior to their first opaque zone formation. In most years, river flows to the Gilbert River estuary greatly reduce or cease by the end of the wet season (Figure 24), thus restricting lateral and longitudinal movement (i.e. connectivity) within the system.

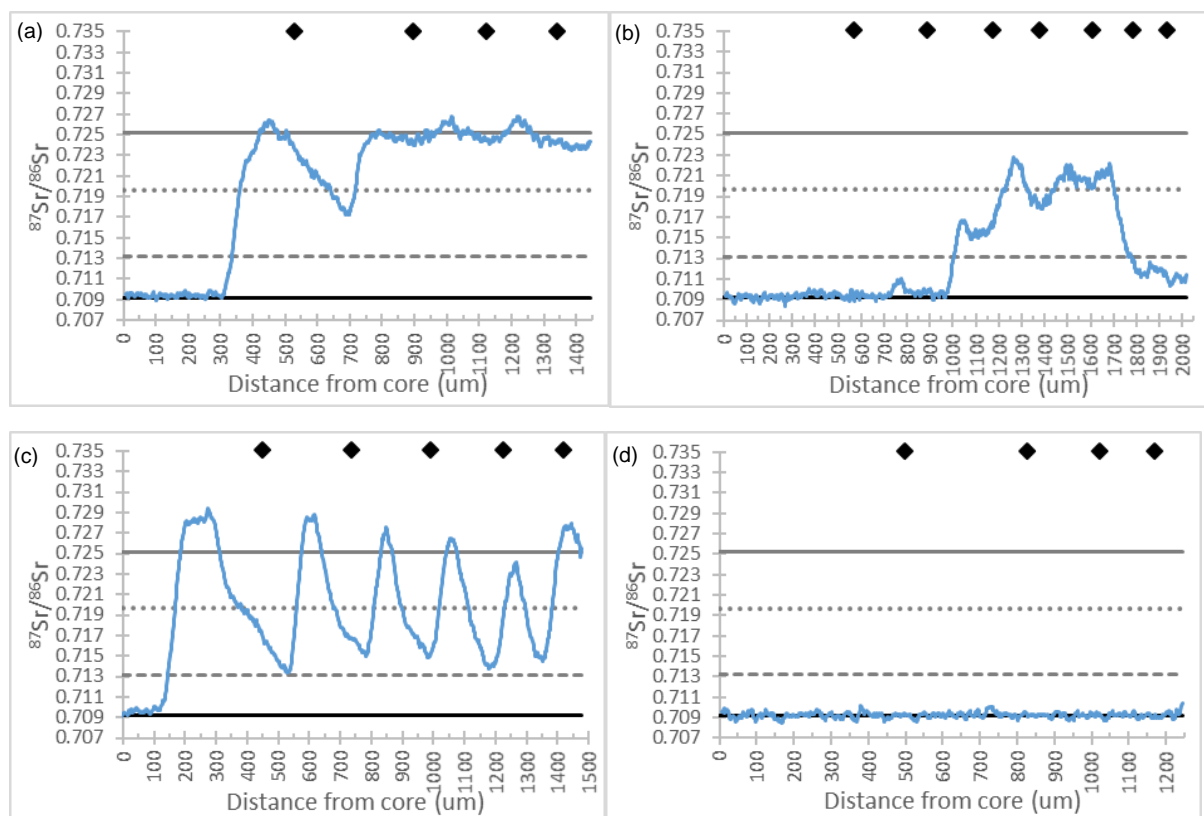


Figure 25. Otolith  $^{87}\text{Sr}/^{86}\text{Sr}$  profiles (5-point smoothed) of ablation transects (core to proximal edge displayed) of barramundi from the Gilbert River estuary. The solid black line is the  $^{87}\text{Sr}/^{86}\text{Sr}$  of marine water sampled from the Gilbert River estuary in October 2017. The grey lines are the 1 ppt (dotted) and 5 ppt (dashed) salinity derived from the mixing curve for the Gilbert River. The grey solid line is the  $^{87}\text{Sr}/^{86}\text{Sr}$  of water sampled from the Gilbert River (freshwater site) in October 2018. Examples illustrate habitat residency classes: freshwater (a) and (b), intermediate (c), and estuarine (d).

## Flinders River

Barramundi caught in the Flinders River estuary had high within-otolith variability in that sequential  $^{87}\text{Sr}/^{86}\text{Sr}$  values (ablated within  $\mu\text{m}$  of each other) were often highly scattered. Such scattering did not occur for samples from the Mitchell and Gilbert rivers, despite deliberate randomisation of otolith sections from different rivers across different slides for laser ablation, suggesting the scattering was not an artefact of instrument drift or calibration error.

Across all samples of barramundi from the Flinders River estuary ( $n=202$ ), 33% were inferred as residing in freshwater habitats for at least one dry season, while 67% were inferred as residing in only high salinity water associated with the estuary (Table 13). None were classified as 'intermediate'.

To better understand the habitats used by barramundi harvested from the Flinders River estuary, samples classified as residing in freshwater were further sub-divided into: (i) freshwater, equivalent to freshwater profiles in the Mitchell and Gilbert rivers, and (ii) freshwater\*, which had  $^{87}\text{Sr}/^{86}\text{Sr}$  values at the translucent zone (i.e. the fast growth period) that were above the  $^{87}\text{Sr}/^{86}\text{Sr}$  values of water samples from the freshwater reaches of the Flinders River upstream of the causeway on the Burke Development Road. The freshwater\* sub-class represent barramundi that have been given the 'benefit of the doubt' of potentially accessing non-estuarine aquatic habitats in the lower Flinders River (e.g. the waterholes above the Burke Development Road causeways). The  $^{87}\text{Sr}/^{86}\text{Sr}$  values of water samples from the lower Flinders River were contrary to those suggested by the calculated mixing curve (see Appendix 2), which supports that the strontium isoscape in this part of the GoC is spatially (and temporally) complex (Adams et al. 2019).

Fish classified as estuarine were further sub-divided into: (i) estuarine, equivalent to estuarine profiles in the Mitchell and Gilbert rivers; and (ii) estuarine#, which had  $^{87}\text{Sr}/^{86}\text{Sr}$  values at all opaque zones that were estuarine but  $^{87}\text{Sr}/^{86}\text{Sr}$  values during one or more translucent zones that indicated an inferred water salinity of <5 ppt. The further sub-classification the  $^{87}\text{Sr}/^{86}\text{Sr}$  profiles sampled from the Flinders River resulted in greater variety across year-classes in the percentage of fish inferred to inhabit freshwater or estuarine habitats (Table 13). The estuarine# sub-class may represent barramundi that are inhabiting the short-lived but seasonally available aquatic habitats that have lowered salinity associated with inundation of the extensive coastal floodplains of the Flinders River delta.

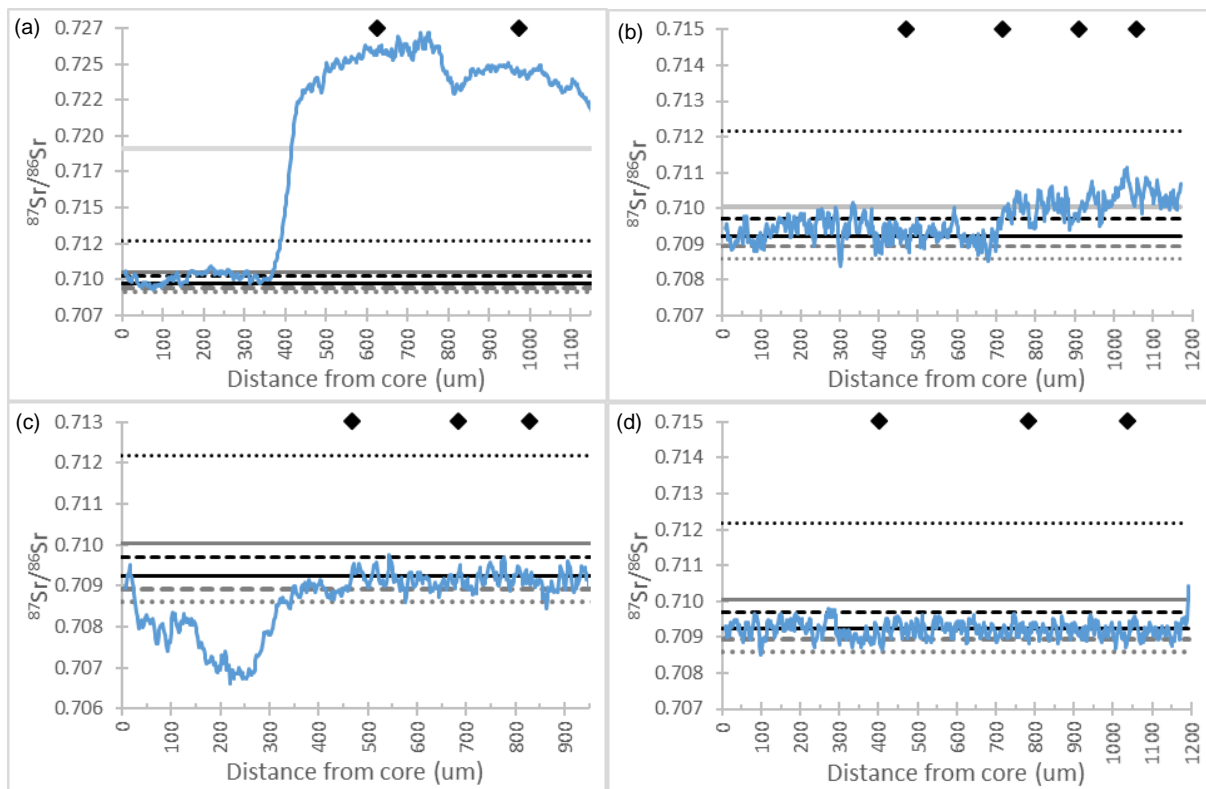


Figure 26. Otolith  $^{87}\text{Sr}/^{86}\text{Sr}$  profiles (5-point smoothed) of ablation transects (core to proximal edge displayed) of barramundi from the Flinders River estuary. The solid black line is the  $^{87}\text{Sr}/^{86}\text{Sr}$  of marine water sampled from the Flinders River estuary in October 2017. The dotted lines are the 1 ppt (grey – Flinders, black – Norman) and the dashed lines are the 5 ppt (grey – Flinders, black – Norman) salinity derived from the mixing curve for the Flinders and Norman Rivers. The dark grey solid line is the  $^{87}\text{Sr}/^{86}\text{Sr}$  of water sampled from the Flinders River main channel upstream of the causeway on the Burke Development Road in October 2018. Examples illustrate habitat residency classes: (a) freshwater, (b) freshwater\*, (c) estuarine# and (d) estuarine.

### 3.3.3 Total length as related to habitat class

Growth variability has been attributed to freshwater residency (Roberts et al. 2019). However, factors influencing growth are likely to be more complex than the salinity of the water and are probably also related to prey availability and/or feeding opportunity, which can differ between aquatic habitats irrespective of salinity (see Russell et al. 2015). The samples in the current study were assessed to determine if there was evidence in support of faster growth in fish inferred as residing in freshwater habitats, based on length-at-age (see Section 2.3.6 for methods).

Barramundi inferred as residing in freshwater habitats of the Mitchell River had significantly larger total length-at-age than non-freshwater fish (Figure 27). When analysed with non-freshwater fish split into intermediate and estuarine, intermediate-classed fish had smaller total length-at-age than estuary fish, but the difference was not significant (Figure 28).

Barramundi inferred as residing in freshwater habitats of the Gilbert River had significantly larger total length-at-age than non-freshwater fish (Figure 27). When analysed with non-freshwater fish split into intermediate and estuarine, intermediate-classed fish were smaller at age than estuary fish, but the difference was not significant (Figure 28).

Barramundi inferred as residing in freshwater habitats of the Flinders River were not significantly different in their total length-at-age from non-freshwater fish (Figure 27), not even if additional sub-classes were considered.

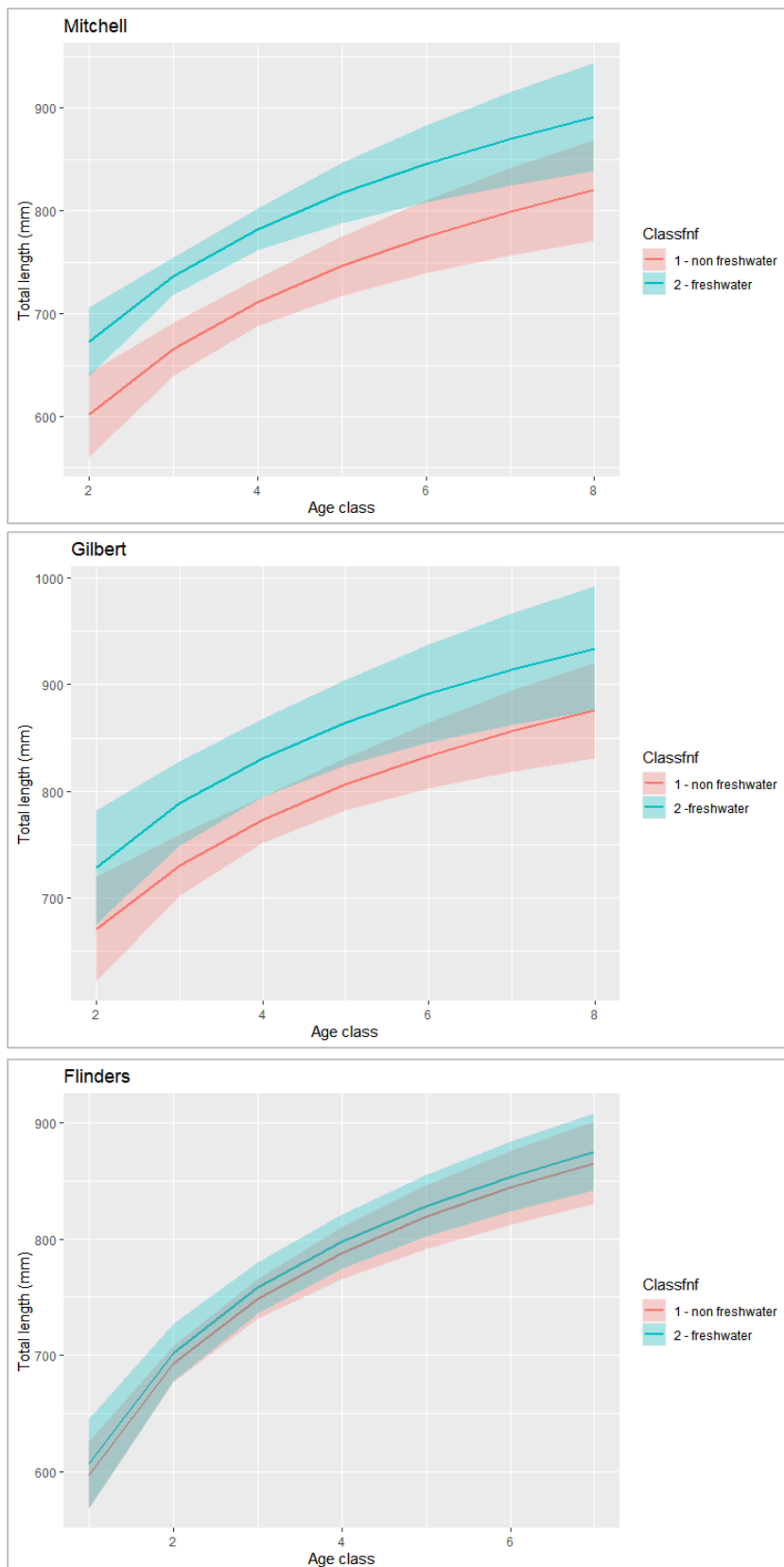


Figure 27. Total length modelled as a function of age-class and habitat class (freshwater or non-freshwater). Inferred from otolith  $^{87}\text{Sr}/^{86}\text{Sr}$  profiles for barramundi from the Mitchell ( $n=106$ ), Gilbert ( $n=94$ ) and Flinders ( $n=202$ ) rivers.

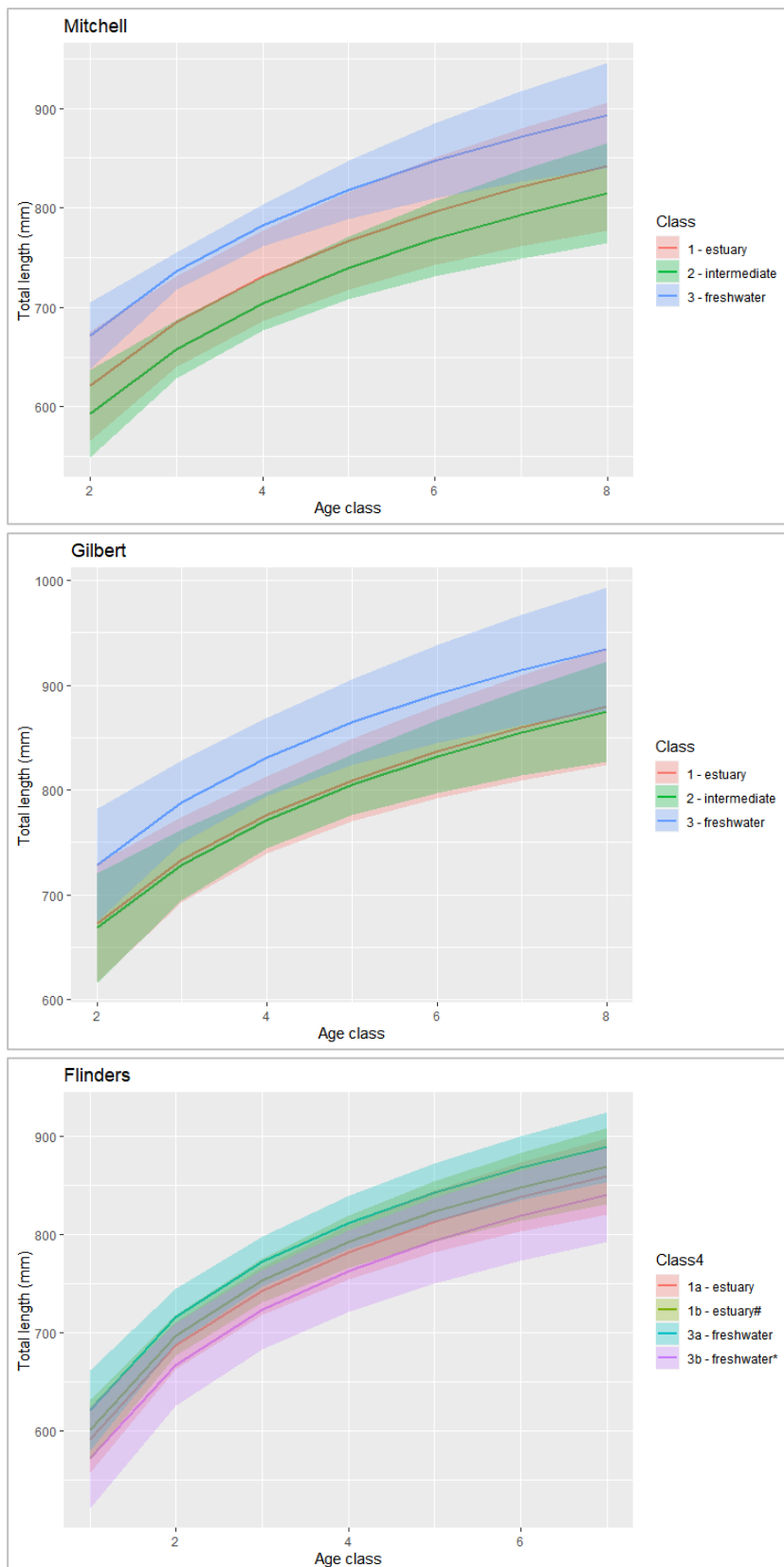


Figure 28. Total length modelled as a function of age-class and habitat class (freshwater, intermediate or estuary). Inferred from otolith  $^{87}\text{Sr}/^{86}\text{Sr}$  profiles for barramundi from the estuaries of the Mitchell ( $n=106$ ), Gilbert ( $n=94$ ) and Flinders ( $n=202$ ) rivers.



## 4. Discussion

### 4.1 Catch, age-frequency and catch-at-age

Analysis of the underlying age-frequency and catch-at-age data provided insight into what aspects of barramundi population dynamics are influenced by river flows and may be sensitive to upstream water-resource development.

Results from the catch-curve analysis of age-frequencies demonstrated that the recruitment of barramundi is highly variable in the southern GoC. Consistent with previous studies, variation in barramundi recruitment was significantly and positively related to river flows in December, January and March/April.

The analyses confirmed that river flows in the birth-year have a critical role in determining recruitment strength. Estimating the contribution of each year-class to the fishery harvest and extending the models to include flows from years other than the birth-year highlighted the importance of the multi-year sequence of river flows for barramundi population dynamics. The temporal patterns in year-class and river flows also suggest that years with severely low river flows can cause major mortality to barramundi populations, negating positive effects of good flow conditions in previous years.

The relative contribution to the southern GoC barramundi population by the Mitchell, Gilbert and Flinders rivers varies between years, depending on monsoonal rainfall and the resulting river flows. In years with widespread flooding, all southern GoC systems are highly productive for barramundi, but in years of widespread drought, southern GoC systems have lower production. The results from the current analyses suggest that the Mid sub-stock has more consistent conditions for barramundi production than the South sub-stock. Although, when the South sub-stock has good conditions, the region is highly productive for barramundi.

### 4.2 Growth

The current study identified and quantified the importance of peak wet-season river flows (January–February–March) on the growth of juvenile barramundi in the GoC. This coincides with the seasonal growth peak for barramundi in northern Australia (Davis and Kirkwood 1984; Xiao 1999). The effect of peak wet-season river flows was most distinctive in the Gilbert and Flinders regions, which experience more seasonally driven river flows (Kennard et al. 2010). Early (October–November–December) and late (April–May–June) wet-season flows were also associated with elevated barramundi growth rates in the Mitchell region, which has more consistent year-round base flow (Kennard et al. 2010). The differences in flow regimes potentially enable extended periods of growth in juvenile barramundi in the Mitchell region, compared with shorter periods of growth associated with the shorter hydrograph typical of the Gilbert and Flinders systems.

The current study confirms relationships between river flow and juvenile growth rates identified from tag–recapture data in the Fitzroy region (Robins et al. 2006). Increased juvenile growth rates may lead to improved survival of juveniles (Perez and Munch 2010), which can result in a stronger year-class and subsequently increased catch rates and total harvest. This effect was evident in the catch-at-age data for the Mid and South sub-stocks.

In this component of the study, we also quantified the relationship between major atmospheric indices and otolith increment widths of juvenile barramundi. This is particularly valuable for integration of our results into regional GoC models that are driven by large-scale atmospheric variables, as well as for cautious extension of these results into Gulf catchments for which *in situ* river gauges or high-quality river discharge modelling are unavailable.

Our results indicate the high importance of both MJO and SOI in GoC catchments. A strong positive effect of SOI was present in all top models for all study regions, with more intense La Niña wet seasons resulting in higher growth rates for all measured ages of juvenile barramundi. This concurs with the effects of ENSO on the GoC and northern Australia more widely (Holbrook et al. 2009). La Niña wet seasons are associated with higher-than-average rainfall across northern Australia (Bureau of Meteorology 2012), resulting in increased banana prawn (*Penaeus merguensis*) catches in the GoC (Vance et al. 1985) and increased mud crab (*Scylla* spp.) catches in Northern Territory waters, including the western GoC (Meynecke et al. 2012). The La Niña ENSO phase is known to influence growth rates across many taxa in northern Australia, including adult mangrove jack (*Lutjanus argentimaculatus*) (Ong et al. 2015), spangled emperor (*Lethrinus nebulosus*), *Porites* corals, and the pine tree *Callitris columellaris* in Western Australia (Ong et al. 2016). The speculated mechanistic link between SOI and growth rates of estuarine/marine taxa is increased freshwater flows contributing to the movement of nutrients and inundation of wetland areas, thereby stimulating high levels of primary productivity (Davies et al. 2008).

The effect of the Phase 4 MJO index on juvenile barramundi growth rates was typically positive, in line with previous work associating positive values of the Phase 4 MJO with increased catch rates of barramundi 4 years later in the Fitzroy river system on the east coast of Australia (Balston 2008).

We applied the relationship between river discharge volume and juvenile barramundi otolith increment widths in the Mitchell region to a hypothetical water extraction scenario for the region and estimated that this particular scenario could result in a 19.3% reduction in barramundi size by increment 3. Given the importance of size-selective survival in young fish (Perez and Munch 2010), reduced growth rates may have important consequences for cohort survival, with subsequent deleterious effects on YCS (Staunton-Smith et al. 2004; Halliday et al. 2011; Halliday et al. 2012), biomass (Tanimoto et al. 2012) and catch rates (Robins et al. 2005; Balston 2008; Tanimoto et al. 2012).

The current study has quantified the relationship between river discharge and otolith increment width in three catchments that are part of the focus for agricultural and water-resource development in northern Australia (Holz et al. 2013; Petheram et al. 2018). At the time of the current study, some minor water harvesting and water storage systems are present in all three study regions (CSIRO 2013a,b; Petheram et al. 2018). This work therefore captures the relationship between river discharge and barramundi growth rates in river systems that are already experiencing minor reductions in flow relative to what would have been available historically.

The effect of river discharge on otolith increment width was non-linear (Figure 19), and in some regions at some times of the year appeared to 'plateau', such that only minimal increases in growth rates were achieved beyond certain river discharge volumes (e.g. Flinders region, October–November–December flows, Figure 19j). However, this effect should be generalised cautiously, as in many cases, the effect of river discharge volume on

juvenile barramundi growth rates was strong and positive, such that any reduction of river discharge volume is expected to noticeably reduce juvenile barramundi growth rates. We strongly recommend replicating the water extraction scenario testing component of this work across the range of water development scenarios planned and proposed for the Mitchell, Gilbert and Flinders regions to better understand the biological, and potential economic, consequences of reduced river flows on barramundi.

The predicted effects of climate change on rainfall and river flows in the GoC are unclear. Climate forecasting indicates that the amplitude of the MJO will increase into the future (Bui and Maloney 2018). A higher amplitude MJO could result in greater intensity and variability of both pulses of low pressure (wet conditions) and periods of high pressure (dry conditions). The increased intensity of low pressure systems would be expected to increase rainfall, river flow and, consequently, juvenile barramundi growth rates at increments 2 and 3. However, concurrent changes to wind circulation patterns due to climate change mean that MJO pulses will be less predictable and more extreme (Bui and Maloney 2018), with low pressure conditions potentially crossing the line from beneficial to destructive (i.e. cyclonic).

This work quantified the impact of river discharge and atmospheric indices on otolith increment widths of juvenile barramundi. It offers a way forward for incorporating effects of flow on growth rates, which can then be incorporated into population modelling of barramundi for future stock status assessments (Campbell et al. 2017), particularly for stocks for which extensive tag–recapture datasets do not exist. In addition, the results can contribute to the framework for ecological assessment of water development scenarios (McGregor et al. 2018), explicitly incorporating water extraction effects on juvenile barramundi growth rates. However, the magnitude of the relationship between otolith increment width and actual somatic growth in barramundi has been inferred, not measured directly. While some prior work has directly related environmental drivers to somatic growth in barramundi using tag–recapture methods (Robins et al. 2006), this is often not possible, with post-hoc analysis of otolith archives representing a cost-effective and pragmatic alternative to direct measurements of fish growth over considerable lengths of time. We recommend further work in this space to explicitly link otolith increment widths and somatic growth in barramundi, through tag–recapture and otolith marking (e.g. oxytetracycline) approaches. Ideally, this work would (1) be undertaken in all catchments targeted for water development planning, prioritising particularly data-sparse regions (e.g. Gilbert); and (2) continue after implementation of any water extraction, as part of a comprehensive environmental impact monitoring program.

### **4.3 Otolith microchemistry**

Results from the otolith microchemistry component of the current study indicate that there is a proportion of the southern GoC barramundi population that resides in estuarine habitats throughout their life. This concurs with barramundi being facultatively catadromous and that the proportion of the population that migrate upstream varies between river systems and between years within any given river system (Pender and Griffin 1996, Milton et al. 2008, Halliday et al. 2012, Crook et al. 2016).

Of the three rivers sampled, barramundi in the Mitchell River had the highest level of freshwater residency (~60%), with residency defined as the type of aquatic habitat inhabited during the dry season. The Flinders River had the highest estuarine residency (~67%), while

the Gilbert River had the highest 'intermediate' residency (i.e. average across all age-classes of 48%). Freshwater residency is likely to be the consequence of the prevailing connectivity between marine, riverine and floodplain habitats – with connectivity resulting from wet-season rainfall, associated river flows, and the seasonal inundation of floodplains and wetlands (Jardine et al. 2012).

Growth variability has been attributed to freshwater residency (Roberts et al. 2019), although factors influencing growth are likely to be related to prey availability, feeding opportunity and overall energetic balance, rather than salinity per se (Russell et al. 2015). Preliminary analyses of total length-at-age for barramundi classed as residing in freshwater or non-freshwater habitats indicated that freshwater habitats provided a significant growth advantage for Mitchell and Gilbert River fish, but not for Flinders River fish. In the Flinders River, it may be that the large estuarine wetlands, when inundated with floodwaters, provide barramundi with similar opportunities for increased growth (and survival) as provided by freshwater wetlands in other systems.

#### 4.4 Summary

Australia's tropical river systems and their associated biota are driven by the wet–dry cycle of the northern Australian monsoon season (Warfe et al. 2011). Barramundi is a species well adapted to the inter-annual variation in wet-season rainfall and river flow of northern Australia. They are highly fecund (i.e. producing millions of eggs) and capable of very fast growth and high survival under optimal conditions (i.e. successive good wet seasons with river flows facilitating access to a range of aquatic habitats; Garrett 1987). However, the GoC and associated catchments are vulnerable to extremes in climate. Successive poor wet seasons, such as occurred between 2013 and 2015, result in the reduced spatial extent of aquatic habitats. This in turn results in reduced barramundi recruitment, growth and survival. We suggest barramundi population dynamics are most sensitive to altered patterns of river flow during and immediately after successive years of below median flow. Water-resource development and planning in the Mitchell, Gilbert and Flinders rivers should aim to not exacerbate or prolong the impacts of climate variability on GoC barramundi populations.

Currently, the long-established commercial fisheries in the GoC harvest barramundi and other species (e.g. king threadfin and mud crabs) that rely on estuarine productivity (i.e. abundance, age-structure and biomass) supported by a spatial and temporal patchwork of river flows. This concurs with the finding of an earlier study on juvenile banana prawns that the Mitchell, Gilbert and Flinders rivers all contribute to estuarine fisheries production, although variably between years (Burford et al. 2020).

Wet season rainfall and river flows provide a spatial and temporal mosaic of habitats that barramundi can exploit during the wet season and potentially survive in during subsequent the dry season. Molinari et al. (submitted) found that connectivity in the Mitchell River was highest in wet years compared with dry years. They also reported that fragmentation of aquatic habitats from reduced connectivity would be disproportionately exacerbated during dry years under water-resource development scenarios. Wallace et al. (2017) suggested that dry-season refuge in GoC waterholes depends on the presence and depth of water in the waterhole, because shallow waterholes, while still wet, can become thermally unstable (i.e. too hot/cold) 1 to 2 months before they fully dry out. Modifications to the natural flow regime should be mindful of effects on waterhole persistence, as well as habitability from a perspective of critical thermal limits and dissolved oxygen levels.

Results from the current study indicate that in the southern GoC, the migration of juvenile barramundi into upstream habitats occurs towards the end of the northern wet season. This concurs with previous findings that barramundi which access freshwater habitats of southern GoC rivers do so when they are older than about 3 months (Russell and Garrett 1983, 1985). Barramundi less than 3 months old exploit aquatic habitats on the littoral margins of estuaries, the adjacent saltpans and the upper reaches of tidal creeks that occur on the wide (~40 km) flat coastal plains in the southern GoC (Russell 1987). These temporary aquatic habitats are created and replenished by seasonally large spring tides ( $\geq 3.5$  m) between October and March. The tides also facilitate movement of young-of-the-year barramundi into and out of these temporary habitats (Russell 1987). Wet-season river flows extend the occurrence and accessibility of these temporary aquatic habitats, both spatially and temporally. These prey-rich, but predator-poor habitats are speculated to support rapid growth, enhanced juvenile survival and thus recruitment (Russell and Garrett 1983).

The current study was limited to the Mitchell, Gilbert and Flinders rivers and, due to resource limitations, did not consider the linkages with adjacent river systems. We recommend that water development in the Mitchell, Gilbert and Flinders rivers consider potential impacts on adjacent rivers and estuaries. In particular, we note that flows in the Gilbert River connect with the lower Norman River catchment and are likely to contribute to the estuarine productivity of this system, as well as to that of the lower Staaten River (Vallance et al. 2009). Flows in the Mitchell River are likely to impact the upper Staaten River (Vallance et al. 2009).

Water-resource development should aim to minimise the disruption to the frequency and duration of aquatic habitat inundation and connection so as to maintain the natural productivity of GoC catchments that supports barramundi populations. Further work is required to provide catchment-specific estimates of barramundi use of aquatic habitats, particularly in the Gilbert and Flinders catchments, which could be explicitly used to quantitatively assess the impacts of water development scenarios.

## 5. Recommendations and conclusions

Barramundi display characteristics of a periodic life history strategist (Winemiller and Rose 1992), that is, delayed maturity to permit growth to a size sufficient for high fecundity, high adult survival during periods of sub-optimal environmental conditions and synchronous episodes of spawning that coincide with favourable conditions, at the sacrifice of high juvenile survivorship. Periodic strategists spread their reproductive effort out over several years so that high survivorship in good years (or regions) compensates for poor years (or regions). Maintaining a critical density of adults, and the protection of spawners and spawning habitats during effective reproductive periods, is critical for long-lived periodic species such as barramundi (Winemiller and Rose 1992).

Their high fecundity (producing millions of eggs), capability for very fast growth and high survival under optimal conditions (i.e. successive good wet seasons with river flows facilitating access to a range of aquatic habitats) ensure barramundi are well adapted to the inter-annual variation in climate and wet-season rainfall of northern Australia. However, the GoC and associated catchments are prone to extremes in climate. Successive poor wet seasons, such as occurred between 2013 and 2015, result in the reduced spatial extent of aquatic habitats. This in turn results in reduced barramundi recruitment, growth rates and survival.

Barramundi population dynamics are likely to be most sensitive to altered patterns of river flow during and immediately after successive years of below median flow. Water-resource development and planning in the Mitchell, Gilbert and Flinders rivers should aim to not exacerbate or prolong the impacts of existing climate variability on GoC barramundi populations.

Currently, the long-established fisheries in the GoC harvests barramundi and other species (e.g. king threadfin and mud crabs) that rely on estuarine productivity (i.e. abundance, age-structure and biomass) supported by the spatial and temporal patchwork of river flows. This concurs with the findings on juvenile banana prawns (component 1 of this project) that the Mitchell, Gilbert and Flinders rivers all contribute to estuarine fisheries production, although variably between years. Results also complement [another Northern Australia Environmental Resources Hub project](#) that identified the role river flows play in delivering nutrient inputs to estuaries and floodplains of the GoC and enhancing the availability of food resources for migratory shorebirds.

Harvest strategies are being introduced for Queensland's fisheries, including state-managed Gulf fisheries. These reforms include a biomass target of 60% compared with unfished levels and hold fishers to account for their sustainability and broader ecosystem impacts. Water-resource development that reduces or impedes (i) spawner biomass or (ii) juvenile survival will artificially change the natural fluctuation in barramundi biomass, with consequential impacts on the surplus yield that can be sustainably harvested.

Water-resource development should aim to minimise the disruption to the frequency and duration of aquatic habitat inundation and connection with the aim of maintaining the natural productivity of GoC catchments that support barramundi populations. Further work could provide catchment-specific estimates of barramundi use of aquatic habitats, particularly in the Gilbert and Flinders catchments, which could be explicitly used to quantitatively assess the impacts of water development scenarios.

## References

- Adams, S., Grun, R., McGahan, D., Zhao, J-X., Feny, Y., Nguyen, A., Wilmes, M., Quaresimin, M., Lobsey, B., Collard, M., Westaway, M. (2019). A strontium isoscape of north-eastern Australia for human provenance and repatriation. *Geoarchaeology* 34, 231-251.
- Balston, J., (2008). Climate impacts on Barramundi and Banana Prawn fisheries of Queensland tropical East Coast. In: Halliday, I. and Robins, J. (eds.) *Environmental flows for sub-tropical estuaries: understanding the freshwater needs of estuaries for sustainable fisheries production and assessing the impacts of water regulation*. Final Report FRDC Project No 2001/022, Coastal Zone Project FH3/AF. pp 63-77.
- Balston, J. (2009a). An analysis of the impacts of long-term climate variability on the commercial barramundi (*Lates calcarifer*) fishery of north-east Queensland, Australia. *Fisheries Research* 99, 83-99. doi.org/10.1016/j.fishres.2009.05.00
- Balston, J. (2009b). Short-term climate variability and the commercial barramundi (*Lates calcarifer*) fishery of north-east Queensland, Australia. *Marine and Freshwater Research* 60, 912-923. doi.org/10.1071/MF08283
- Barrow, J., Ford, J., Day, R., and Morrongiello, J. (2018). Environmental drivers of growth and predicted effects of climate change on a commercially important fish, *Platycephalus laevigatus*. *Marine Ecology Progress Series* 598, 201-212.
- Barton, K., (2018). Package 'MuMIn': Multi-model inference. Published July 23, 2018. Version 1.42.1. edn. Repository: CRAN.
- Bates, D., M. Maechler, M., Bolker, B., Walker, S., Christensen, R.B.H., Singmann, H., Dai, B., Scheipl, F., Grothendieck, G., Green, P., and Fox, J. (2018). Package 'lme4': Linear Mixed-Effects Models using 'Eigen' and S4 Published November 10, 2018. Version 1.1-19. edn. Repository: CRAN.
- Battle-Aguilar, J., Harrington, G.A., Leblanc, M., Welch, C., and Cook, P.G. (2014). Chemistry of groundwater discharge inferred from longitudinal river sampling. *Water Resources Research* 50, 1550-1568. doi:10.1002/2013WR013591
- Bayliss, P., Bartolo, R., and van Dam, R.A. (2008). Quantitative ecological risk assessments for the Daly River, NT. In Bartolo, R., Bayliss, P., and van Dam R. (eds). Sub project 2 of Australia's Tropical Rivers – an integrated data assessment and analysis (DET18). A report to Land and Water Australia. Environmental Research Institute of the Supervising Scientist, Darwin, Australia. 271-415.
- Bayliss, P., Robins, J., Buckworth, R., Dichmont, C., Deng, R., and Kenyon, R. (2014). Quantitative risk assessment for banana prawns and barramundi. In: *Assessing the water needs of fisheries and ecological values in the Gulf of Carpentaria*. Bayliss, P., Buckworth, R., and Dichmont, C. (eds.). Final report prepared for the Queensland Department of Natural Resources and Mines (DNRM). CSIRO, Australia. pp 205-261.
- BDO EconSearch (2020). Economic and social indicators for the Queensland Gulf of Carpentaria Inshore Fin Fish Fishery 2017/18 and 2018/19. Report prepared for the Department of Agriculture and Fisheries, Queensland. Brisbane, Australia. 66 pps.

- Bui, H.X. and Maloney, E.D. (2018). Changes in Madden-Julian Oscillation precipitation and wind variance under global warming. *Geophysical Research Letters* 45, 7148-7155. doi:10.1029/2018gl078504.
- Bureau of Meteorology (2012). Record-breaking La Niña events - an analysis of the La Niña life cycle and the impacts and significance of the 2010-11 and 2011-12 La Niña events in Australia. La-Nina-2010-12.pdf (bom.gov.au)
- Burford, M.A., Faggotter, S.J., Kenyon, R. (2020). Contribution of three rivers to floodplain and coastal productivity in the Gulf of Carpentaria. Component 1 final report. Griffith University. 118 pps.
- Campana, S.E. (2005). Accuracy, precision and quality control in age determination, including a review of the use and abuse of age validation methods. *Journal of Fish Biology* 59, 197-242.
- Campbell, A., Robins, J., and O'Neill, M. (2017). Assessment of the barramundi (*Lates calcarifer*) fishery in the southern Gulf of Carpentaria, Queensland, Australia. Department of Agriculture and Fisheries, Queensland. Brisbane. 44 pps.
- Chan, T.U., Hart, B.T., Kennard, M.J., Pusey, B.J., Shenton, W., Douglas, M., Valentine, E., and Patel, S. (2012). Bayesian network models for environmental flow decision making in the Daly River, Northern Territory, Australia. *River Research and Applications* 28, 283-301. doi:10.1002/rra.1456
- Chilton, D.E. and Beamish, R.J. (1982). Age determination for fishes studied by the Groundfish Program at the Pacific Biological Station. Canadian Special Publication of Fisheries and Aquaculture 60, 102 pps.
- CSIRO (2009). Water in the Gulf of Carpentaria drainage division. A report to the Australian Government from the CSIRO Northern Australia Sustainable Yields Project. 479 pps. <https://doi.org/10.4225/08/5859749d4c71e>
- CSIRO (2013a). Agricultural resource assessment for the Flinders catchment. A report to the Australian Government from the CSIRO Flinders and Gilbert Agricultural Resource Assessment, part of the North Queensland Irrigated Agriculture Strategy. CSIRO Water for a Healthy Country and Sustainable Agriculture flagships, Australia.
- CSIRO (2013b). Agricultural resource assessment for the Gilbert catchment. An overview report to the Australian Government from the CSIRO Flinders and Gilbert Agricultural Resource Assessment, part of the North Queensland Irrigated Agriculture Strategy. CSIRO Water for a Healthy Country and Sustainable Agriculture flagships, Australia.
- Crook, D.A., Buckel, D.J., Allsop, Q., Baldwin, W., Saunders, T.M., Kyne, P.M., Woodhead, J.D., Mass, R., Roberts, B., and Douglas, M.M. (2016). Use of otolith chemistry and acoustic telemetry to elucidate migratory contingents in barramundi *Lates calcarifer*. *Marine and Freshwater Research* 68, 1554-1566. doi.org/10.1071/MF16177
- Davies, P.M., Bunn, S.E. and Hamilton, S.K. (2008). Chapter 2 - Primary Production in Tropical Streams and Rivers. In: Dudgeon, D. (ed.) *Tropical Stream Ecology*. Academic Press, London, pp 23-42.



- Davis, T. (1985). Seasonal changes in gonad maturity, and abundance of larvae and early juveniles of barramundi, *Lates calcarifer* (Bloch), in Van Diemen Gulf and the Gulf of Carpentaria. *Marine and Freshwater Research* 36, 177-190. doi:10.1071/MF9850177
- Davis, T.L.O. and Kirkwood, G.P. (1984). Age and growth studies on barramundi, *Lates calcarifer*, in northern Australia. *Australian Journal of Marine and Freshwater Research* 35, 673-690.
- de Lestang, P., Allsop, Q.A., and Griffin, R.K. (2000). Assessment of fish passage ways on fish migration. Fishery Report No. 63. Department of Business, Industry and Resource Development, NT. Darwin. 48 pps.
- Doubleday, Z.A., Izzo, C., Haddy, J.A., Lyle, J.M., Ye, Q. and Gillanders, B.M. (2015). Long-term patterns in estuarine fish growth across two climatically divergent regions. *Oecologia* 179, 1079-1090. doi:10.1007/s00442-015-3411-6.
- DNRME (2018). Water Monitoring Information Portal. Queensland Department of Natural Resources, Mines and Energy. [water-monitoring.information.qld.gov.au](http://water-monitoring.information.qld.gov.au).
- Dunstan, D.J. (1959). The barramundi *Lates calcarifer* (Bloch) in Queensland waters. CSIRO. Division of Fisheries and Oceanography, Melbourne, 22 pps.
- Elsdon, T.S., and Gillanders, B.M. (2005). Consistency of patterns between laboratory experiments and field collected fish in otolith chemistry: an example and applications for salinity reconstructions. *Marine and Freshwater Research* 56, 609-617. doi:10.1071/MFR04146
- EHP (2015). Biodiversity Planning Assessment Gulf Plains Bioregion v1.1. Landscape Expert Panel Report: Department of Environment and Heritage Protection, Queensland Government. 55 pps. [https://www.qld.gov.au/\\_\\_data/assets/pdf\\_file/0027/93645/bpa-gulf-plains-landscape.pdf](https://www.qld.gov.au/__data/assets/pdf_file/0027/93645/bpa-gulf-plains-landscape.pdf)
- Fisheries Queensland (2010). Fisheries long term monitoring program sampling protocol – barramundi (2008 onwards). Section 1. Department of Employment, Economic Development and Innovation, Brisbane. 10 pp.
- Fisheries Queensland (2012). Fisheries Long Term Monitoring Program Sampling Protocol - Fish Ageing Section 2: Barramundi Department of Employment, Economic Development and Innovation. Brisbane, Australia
- Fry, B. (2002). Conservative mixing of stable isotopes across estuarine salinity gradients: a conceptual framework for monitoring watershed influences on downstream fisheries production. *Estuaries* 25, 264-271.
- Garrett, R.N. (1987). Reproduction in Queensland barramundi (*Lates calcarifer*). In: Copland, J.W. and Grey, D.L. (eds). Management of Wild and Cultured Sea Bass/Barramundi (*Lates calcarifer*). Proceedings of an international workshop held at Darwin, NT, Australia, 24-30 September 1986. ACIAR Proceedings No. 20.
- Gillanders, B.M., Black, B.A., Meekan, M.G. and Morrison, M.A. (2012). Climatic effects on the growth of a temperate reef fish from the southern hemisphere: a biochronological approach. *Marine Biology* 159, 1327-1333. doi:10.1007/s00227-012-1913-x.

- Godiksen, J., Borgström, R., Dempson, J.B., Kohler, J., Nordeng, H., Power, M., Stien, A., and Svenning, M.-A. (2012). Spring climate and summer otolith growth in juvenile Arctic charr, *Salvelinus alpinus*. *Environmental Biology of Fishes* 95, 309-321. doi:10.1007/s10641-012-9998-0.
- Hallett, T.B., Coulson, T., Pilkington, J.G., Clutton-Brock, T.H., Pemberton, J.M., and Grenfell, B.T. (2004). Why large-scale climate indices seem to predict ecological processes better than local weather. *Nature* 430, 71-75. doi:10.1038/nature02708.
- Halliday, I.A., Robins, J. B., Mayer, D.G., Staunton-Smith, J., and Sellin, M.J. (2011). Freshwater flows affect the year-class strength of barramundi *Lates calcarifer* in the Fitzroy River estuary, Central Queensland. *Proceeding of the Royal Society of Queensland* 116, 1-11.
- Halliday, I., Saunders, T., Sellin, M.J., Allsop, Q.A., Robins, J.B., McLennan, M. and Kurnoth, P. (2012). *Flow impacts on estuarine finfish fisheries of the Gulf of Carpentaria*. Final Report to the Fisheries Research and Development Corporation for Project Number 2007-002. Queensland Department of Agriculture, Fisheries and Forestry, Brisbane. 76 pps.
- Holbrook, N.J., Davidson, J., Feng, M., Hobday, A.J., Lough, J.M., McGregor, S. and Risbey, J.S. (2009). El Niño - Southern Oscillation. Marine climate change in Australia, Impacts and Adaptation Responses, 2009 Report Card.
- Holz, L., Kim, S., Petheram, C., Podger, G., Hughes, J., Kehoe, M., Aramini, D., Podger, S., Lerat, J., Poulton, P., Hornbuckle, J., and Perraud, J. (2013). River system modelling for the Flinders and Gilbert Agricultural Resource Assessment case study analysis. A technical report to the Australian Government from the CSIRO Flinders and Gilbert Agricultural Resource Assessment, part of the North Queensland Irrigated Agriculture Strategy. CSIRO Water for a Healthy Country and Sustainable Agriculture flagships, Australia.
- Honsey, A.E., Bunnell, D.B., Troy, C.D., Fielder, D.G., Thomas, M.V., Knight, C.T., Chong, S.C., Hook, T.O. (2016). Recruitment synchrony of yellow perch (*Perca flavescens*, Percidae) in the Great Lakes region, 1966-2008. *Fisheries Research* 181, 214-221.
- Hughes, J., Yang, A., Wang, B., Marvanek, S., Carlin, L., Seo, L., Petheram, C., and Vaze, J. (2017). Calibration of river system and landscape models for the Fitzroy, Darwin and Mitchell (catchments A technical report to the Australian Government from the CSIRO Northern Australia Water Resource Assessment, part of the National Water Infrastructure Development Fund: Water Resource Assessments. Australia.
- Jardine, T., Pusey, B.J., Hamilton, S.K., Pettit, N.E., Davies, P.M., Douglas, M.M., Sinnamon, V., Halliday, I.A., and Bunn, S.E. (2012). Fish mediate high food web connectivity in the lower reaches of a tropical floodplain river. *Oecologia* 168, 829-838.
- Jenkins, G.P., Spooner, D., Cornon, S., and Morrongiello, J.R. (2015). Differing importance of salinity stratification and freshwater flow for the recruitment of apex species of estuarine fish. *Marine Ecology Progress Series* 523, 125-144.
- Jerry, D.R., Smith-Keune, C., Hadgson, L., Pirozzi, I., Carton, A.G., Hutson, K., Brazenor, A.K., Gonzalez, A.T., Gamble, S., Collins, G., Van Der Wal, J. (2013). *Vulnerability of an iconic Australian finfish (barramundi - Lates calcarifer) and aligned industries to climate*

- change across tropical Australia*. Final Report for Fisheries Research and Development Corporation Project No 2010/521. James Cook University, Townsville. 222 pp.
- Katayama, S., (2018). A description of four types of otolith opaque zone. *Fisheries Science* 84, 735-745. doi:10.1007/s12562-018-1228-z
- Kennard, M.J., Pusey, B.J., Olden J.D., Mackay, S.J. Stein, J.L. and Marsh, N. (2010). Classification of natural flow regimes in Australia to support environmental flow management. *Freshwater Biology* 55, 171-193. doi:10.1111/j.1365-2427.2009.02307.x.
- Leahy, S.M. and Robins, J.B. (2021). River flows affect the growth of a tropical finfish in the wet dry rivers of northern Australia, with implications for water resource development. *Hydrobiologia* 848, 4311-4333.
- Loughnan, S., Smith-Keune, C., Beheregaray, L.B., Robinson, N.A., Jerry, D.R. (2019). Population genetic structure of barramundi (*Lates calcarifer*) across the natural distribution range in Australia informs fishery management and aquaculture practices. *Marine and Freshwater Research* 70, 1533-1542. doi:10.1071/MFR18330
- Lowe, M.R., DeVries, D.R., Wright, R.A., Ludsin, S.A., Fryer, B.J. (2009). Coastal largemouth bass (*Micropterus salmoides*) movement in response to changing salinity. *Canadian Journal of Fisheries and Aquatic Sciences* 66,2174-2188, doi:10.1139/F09-152
- Maceina, M.J. (1997). Simple application of using residuals from catch-curve regressions to assess year-class strength in fish. *Fisheries Research* 32,115-121.
- Madden, R.A. and Julian, P.R. (1972). Description of Global-Scale Circulation Cells in the Tropics with a 40–50 Day Period. *J Atmos Sci* 29,1109-1123. doi:10.1175/1520-0469(1972)029<1109:dogsc>2.0.co;2
- Mais, K.F. (1981). Age-composition changes in the anchovy, *Engrulis mordax*, central population. *CalCOFI Report XXII*, 6pps.
- Martino, J.C., Fowler, A.J., Doubleday, Z.A., Grammer, G.L. and Gillanders, B.M. (2019). Using otolith chronologies to understand long-term trends and extrinsic drivers of growth in fisheries. *Ecosphere* 10, e02553, doi:10.1002/ecs2.2553.
- Matta, E.M., Black, B.A. and Wilderbuer, T.K. (2010). Climate-driven synchrony in otolith growth-increment chronologies for three Bering Sea flatfish species. *Marine Ecology Progress Series* 413,137-145.
- McGregor, G.B., Marshall, J.C., Lobegeiger, J.S., Holloway, D., Menke N., and Coysh, J. (2018). A risk-based ecohydrological approach to assessing environmental flow regimes. *Environmental Management* 61, 358-374. doi:10.1007/s00267-017-0850-3.
- Mei, W., 2019. Package 'basicTrendline': Add Trendline and Confidence Interval of Basic Regression Models to Plot. Published July 26, 2019. Version 2.0.3. edn. Repository: CRAN.
- Meynecke, J-O, Lee, S.Y, Duke, N.C. and Warnken, J. (2006). Effect of rainfall as a component of climate change on estuarine fish production in Queensland, Australia. *Estuarine and Coastal Shelf Science*, 69, 491-504. <https://doi.org/10.1016/j.ecss.2006.05.011>

- Meynecke, J.-O., Grubert, M., Arthur, J.M., Boston R. and Lee, S.Y. (2012). The influence of the La Niña-El Niño cycle on giant mud crab (*Scylla serrata*) catches in northern Australia. *Estuarine and Coastal Shelf Science* 100, 93-101. doi:10.1016/j.ecss.2012.01.001.
- Milton, D.A. (2009). Living in two worlds: diadromous fishes, and factors affecting population connectivity between tropical rivers and coasts. In: Ecological connectivity among tropical coastal ecosystems. Nagelkerken, I. (ed). Springer Chapter 9, 325-355. doi:10.1007/978-90-481-2406-0\_9
- Milton, D.A., and Chenery, S.R. (2001). Sources and uptake of trace metals in otoliths of juvenile barramundi (*Lates calcarifer*). *Journal of Experimental Marine Biology and Ecology* 264, 47-65.
- Milton, D.A., and Chenery, S.R. (2005). Movement patterns of barramundi *Lates calcarifer*, inferred from  $^{87}\text{Sr}/^{86}\text{Sr}$  and Sr/Ca ratios in otoliths, indicate non-participation in spawning. *Marine Ecology Progress Series* 301, 279-291.
- Milton, D., Halliday, I., Staunton-Smith, J., Sellin, M., Marsh, R., Smith, D., Norman, M., and Woodhead, J. (2008). Otolith chemistry of barramundi *Lates calcarifer* can provide insight about the role of freshwater flows in maintaining estuarine populations of regulated rivers. *Estuarine, Coastal and Shelf Science* 78, 301-315.
- Molinari, B., Stewart-Koster, B., Malthus, T.J., and Bunn, S.E. (2021). Assessing spatial variation in algal productivity in a tropical river floodplain using satellite remote sensing. *Remote Sensing*, 13, no. 9: 1710, <https://doi.org/10.3390/rs13091710>
- Morrongiello, J.R., Walsh, C.T., Gray, C.A., Stocks, J.R., and Crook, D.A. (2014). Environmental change drives long-term recruitment and growth variation in an estuarine fish. *Global Change Biology* 20, 1844-1860. doi:10.1111/gcb.12545
- Nakagawa, S. and Schielzeth, H. (2013). A general and simple method for obtaining R2 from generalized linear mixed-effects models. *Methods in Ecology and Evolution* 4,133-142 doi:10.1111/j.2041-210x.2012.00261.x.
- Ndehedehe, C.E., Stewart-Koster, B., Burford M.A. and Bunn, S.E. (2020). Predicting hot spots of aquatic plant biomass in a large floodplain river catchment in the Australian wet-dry tropics. *Ecological Indicators* 117. doi:10.1016/j.ecolind.2020.106616.
- Ndehedehe, C.E., Onojeghuo, A.O., Stewart-Koster, B., Bunn, S.E. and Ferreira, V.G. (2021). Upstream flows drive the productivity of floodplain ecosystems in tropical Queensland. *Ecological Indicators* 125. doi:10.1016/j.ecolind.2021.107546.
- Ong, J., Rountrey, A.N., Meeuwig, J.J., Newman, S.J., Zinke, J. and Meekan, M.G. (2015). Contrasting environmental drivers of adult and juvenile growth in a marine fish: implications for the effects of climate change. *Scientific Reports* 5, 10859. <https://doi.org/10.1038/srep10859>
- Ong, J.J.L., Rountrey, A.N., Zinke, J., Meeuwig, J.J., Grierson, P.F., O'Donnell, A.J., Newman, S.J., Lough, J.M., Trougan M. and Meekan, M.G. (2016). Evidence for climate-driven synchrony of marine and terrestrial ecosystems in northwest Australia. *Global Change Biology* 22, 2776-2786. doi:10.1111/gcb.13239.

- Pender, P.J., and Griffin, R.K. (1996). Habitat history of barramundi *Lates calcarifer* in a north Australian river system based on barium and strontium levels in scales. *Transactions of the American Fisheries Society* 125, 679-689.
- Petheram, C., Watson, I. and Stone, P. (eds) (2013a). Agricultural resource assessment for the Flinders catchment. A report to the Australian Government from the CSIRO Flinders and Gilbert Agricultural Resource Assessment, part of the North Queensland Irrigated Agriculture Strategy. CSIRO Water for a Healthy Country and Sustainable Agriculture flagships, Australia.
- Petheram, C., Watson, I. and Stone, P. (eds) (2013b). Agricultural resource assessment for the Gilbert catchment. A report to the Australian Government from the CSIRO Flinders and Gilbert Agricultural Resource Assessment, part of the North Queensland Irrigated Agriculture Strategy. CSIRO Water for a Healthy Country and Sustainable Agriculture flagships, Australia.
- Petheram, C., I. Watson, C. Bruce & C. Chilcott (eds), 2018b. Water resource assessment for the Mitchell catchment. A report to the Australian Government from the CSIRO Northern Australia Water Resource Assessment, part of the National Water Infrastructure Development Fund: Water Resource Assessments. CSIRO, Australia.
- Pettit, N.E., Naiman, R.J., Warfe, D..M., Jardine, T.D., Douglas, M.M., Bunn S.E. and Davies, P.M. (2017). Productivity and Connectivity in Tropical Riverscapes of Northern Australia: Ecological insights for management. *Ecosystems* 20, 492-514.
- Perez, K.O. and Munch, S.B. (2010). Extreme selection on size in the early lives of fish. *Evolution* 64, 2450-2457. doi:10.1111/j.1558-5646.2010.00994.x.
- Roberts, B.H., J.R. Morrongiello, A.J. King, D.L. Morgan, T.M. Saunders, J. Woodhead and D.A. Crook (2019). Migration to freshwater increases growth rates in a facultatively catadromous tropical fish. *Oecologia* 191: 253–260. doi:10.1007/s00442-019-04460-7.
- Robertson, S.G. and A.K. Morison (1999). A trial of artificial neural networks for automatically estimating the age of fish. *Marine and Freshwater Research* 50, 73–82. doi:10.1071/MF98039.
- Robins, J.B., Halliday, I.A., Staunton-Smith, J., Mayer, D.G., and Sellin, M.J. (2005). Freshwater-flow requirements of estuarine fisheries in tropical Australia: a review of the state of knowledge and application of a suggested approach. *Marine and Freshwater Research* 56, 343-360.
- Robins, J., Mayer, D., Staunton-Smith, J., Halliday, I., Sawynok, B., and Sellin, M. (2006). Variable growth rates of the tropical estuarine fish barramundi *Lates calcarifer* (Bloch) under different freshwater flow conditions. *Journal of Fish Biology* 69, 379-391.
- RStudio Team (2018). RStudio: Integrated Development for R. RStudio, PBC, Boston, MA URL <http://www.rstudio.com/>
- Russell, D.J. (1987). Review of juvenile barramundi (*Lates calcarifer*) wildstocks in Australia. In: Copland, J.W. and Grey, D.L. (eds). Management of Wild and Cultured Sea Bass/Barramundi (*Lates calcarifer*): proceedings of an international workshop held in Darwin, NT, Australia, 24-30 September 1986. ACIAR Proceedings No. 20, Darwin, NT. pp 44-59.

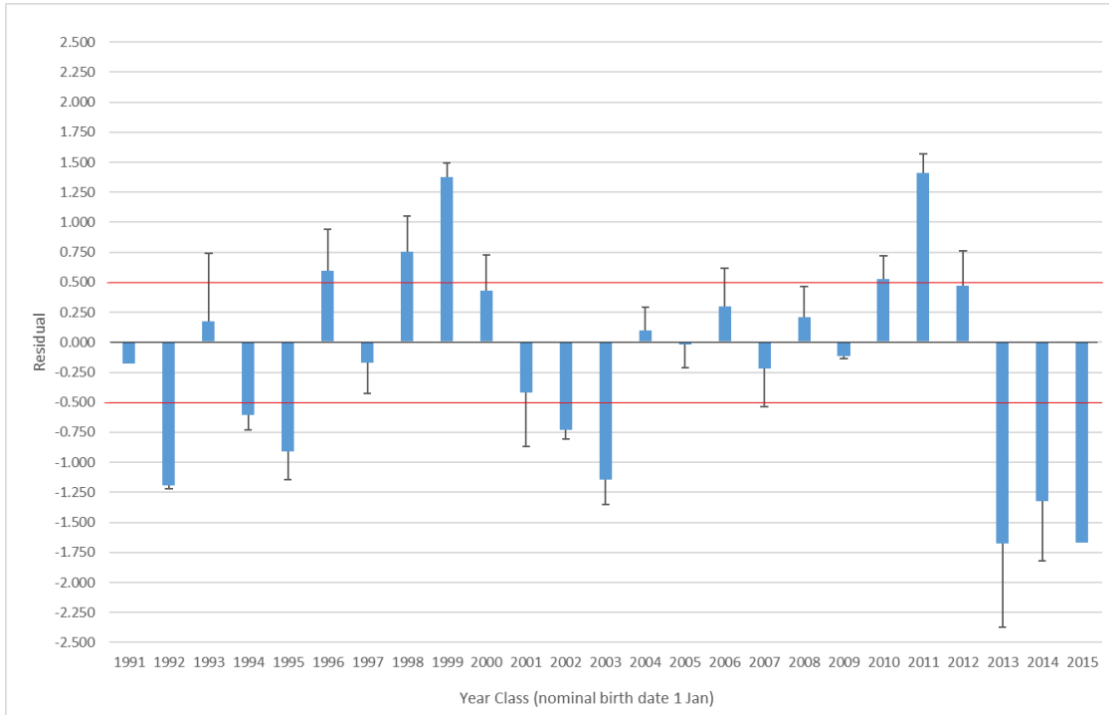
- Russell, D.J. and Garrett, R.N. (1983). Use by juvenile barramundi, *Lates calcarifer* (Bloch), and other fishes of temporary supralittoral habitats in a tropical estuary in Northern Australia. *Australian Journal of Marine and Freshwater Research* 34, 805-811.
- Russell, D.J. and Garrett, R.N. (1985). Early life history of barramundi *Lates calcarifer* (Bloch) in north-eastern Queensland. *Australian Journal of Marine and Freshwater Research* 36, 19-201.
- Russell, D.J., Thomson, F.E., Thuesen, P.A., Power, T.N., and Mayer, R.J. (2015). Variability in the growth, feeding and condition of barramundi (*Lates calcarifer* Bloch) in a northern Australian coastal river and impoundment. *Marine and Freshwater Research* 66, 928-941.
- Sawynok, B. (1998). Fitzroy River: effects of freshwater flows on fish: impact on barramundi recruitment, movement and growth. National Fishcare Report Project 97/003753, Infotish Services, Rockhampton, Queensland, Australia. 59pp
- Staunton-Smith, J., Robins, J.B., Mayer, D.G., Sellin, M.J., and Halliday, I.A. (2004). Does the quantity and timing of freshwater flowing into a dry tropical estuary affect year-class strength of barramundi (*Lates calcarifer*)? *Marine and Freshwater Research* 55, 787-797.
- Stocks, J., Stewart, J., Gray, C.A., and West R.J. (2011). Using otolith increment widths to infer spatial, temporal and gender variation in the growth of sand whiting *Sillago ciliata*. *Fisheries Management and Ecology* 18, 121-131.
- Stoessel, D.J., Morrongiello, J.R., Raadik, T.A., Lyon, J. and Fairbrother, P. (2018). Is climate change driving recruitment failure in Australian bass *Macquaria novemaculeata* in southern latitudes of the species range? *Marine and Freshwater Research* 69, 24-36. <https://doi.org/10.1071/MF17173>
- Streipert, S., Filar, J., Robins, J.B., O'Neil, M.F.O. and Whybird, O. (2019). Stock assessment of the barramundi (*Lates calcarifer*) fishery in Queensland, Australia. Department of Agriculture and Fisheries, Brisbane, Queensland. 103 pps.
- Stuart, I.G. and McKillop, S.C. (2002). The use of sectioned otoliths to age barramundi (*Lates calcarifer*) (Bloch, 1790) [Centropomidae]. *Hydrobiologia* 479, 231-236.
- Sullivan, C.J., Weber, M.J., Pierce, C.L., Wahl, D.H., Phelps, Q.E., Camacho, C.A., and Colombo, R.E. (2018). Factors regulating year-class strength of silver carp throughout the Mississippi River basin. *Transactions of the American Fisheries Society* 147, 541-553, doi:10.1002/tafs.10054
- Tanimoto, M., Robins, J.B., O'Neill, M.F., Halliday, I. and Campbell, A.B. (2012). Quantifying the effects of climate change and water abstraction on a population of barramundi (*Lates calcarifer*), a diadromous estuarine finfish. *Marine and Freshwater Research* 63, 715-726.
- Telzaff, J.C., Catalano, M.J., Allen, M.S., and Pine W.E. (2011). Evaluation of two methods for indexing fish year-class strength: Catch-curve residuals and cohort method. *Fisheries Research* 109, 303-310.
- Tonkin, Z., Stuart, I., Kitchingman, A., Thiem, J.D., Zampatti, B., Hackett, G., Koster, W., Koehn, J., Morrongiello, J., Mallen-Cooper, M., and Lyon, J., (2020). Hydrology and water temperature influence recruitment dynamics of the threatened silver perch *Bidyanus*

- disyanus* in a regulated lowland river. *Marine and Freshwater Research* 70, 133-1344. doi:10.1071/MF18299
- Vallance, T., Hogan, A., and Gleeson, P. (2009). Aquatic diversity in the Staaten catchment. Northern Gulf Resource Management Group. 5 pps. <http://www.hoganfish.com.au/wp-content/uploads/2010/11/Aquatic-biodiversity-of-the-Staaten-River-laymans-report.pdf>
- Vance, D.J., Staples, D.J. and Kerr, J.D. (1985). Factors affecting year-to-year variation in the catch of banana prawns (*Penaeus merguensis*) in the Gulf of Carpentaria, Australia. *Journal du Conseil International pour l'Exploration de la Mer* 42, 83-97.
- Wallace, J., Waltham, N., and Burrows, D. (2017). A comparison of temperature regimes in dry-season waterholes in the Flinders and Gilbert catchments in northern Australia. *Marine and Freshwater Research* 68, 650-667. doi:10.10714/MF15468
- Warfe, D.M., Pettit, N.E., Davies P.M., Pusey, B.J., Hamilton, S.K., Kennard, M.J., Townsend, S.A., Bayliss, P., Ward, D.P., Douglas, M.M., Burford, M.A., Finn, M., Bunn, S.E. and Halliday, I.A. (2011) The 'wet-dry' in the wet-dry tropics drives river system ecosystem structure and processes in northern Australia. *Freshwater Biology* 55, 2169-2195.
- Wheeler, M.C., and Hendon, H.H. (2004). An all-season real-time multivariate MJO index: development of an index for monitoring and prediction. *American Meteorological Society* 132, 1917-1932.
- Whitehouse, F.W. (1943). The natural drainage of some very flat monsoonal lands. *Australian Geographer* 4, 183–196. doi:10.1080/00049184308702235
- Winemiller, K.O., and Rose, K.A. (1992). Patterns of life-history diversification in North American fishes: implications for population regulation. *Canadian Journal of Fisheries and Aquatic Sciences* 49, 2196-2218.
- Woodhead, J., Swearer, S., Hergt, J. and Maas, R. (2005). *In situ* Sr-isotope analysis of carbonates by LA-ICP-MS: interference corrections, high spatial resolution and an example from otolith studies. *J. Anal. At. Spectrom.* 20, 22–27.
- Xiao, Y. (1999). General age- and time-dependent growth models for animals. *Fishery Bulletin* 97, 690-701.
- Xiao, Y. (2000). Use of the original von Bertalanffy growth model to describe the growth of barramundi, *Lates calcarifer* (Bloch). *Fishery Bulletin* 98, 835-841.
- Yezerinac, S.M., Loughheed, S.C. and Handford, P. (1992). Measurement Error and Morphometric Studies: Statistical Power and Observer Experience. *Systematic Biology* 41, 471-482. doi:10.1093/sysbio/41.4.471
- Zuur, A.F., Leno, E.N., Walker, N., Saveliev, A.A., and Smith, G.M. (2009). Mixed Effects Models and Extensions in Ecology with R. Springer-Verlag, New York.
- Zuur, A.F., Hilbe, J.M. and Leno, E.N. (2013). A beginner's Guide to GLM and GLMM with R. Highland Statistics Ltd., United Kingdom.

## Appendix 1. Year-class strength visualisations

Figure A1.1 Mid sub-stock visualisations of relative year-class strength for alternative base GLMs.

(a)  $\ln(\text{Age-frequency}) \sim \text{Age-class} + \text{Sampleyear}$



(b)  $\ln(\text{Age-frequency}) \sim \text{Age-class} + \text{Sampleyear} + \text{Age-class} * \text{Sampleyear}$

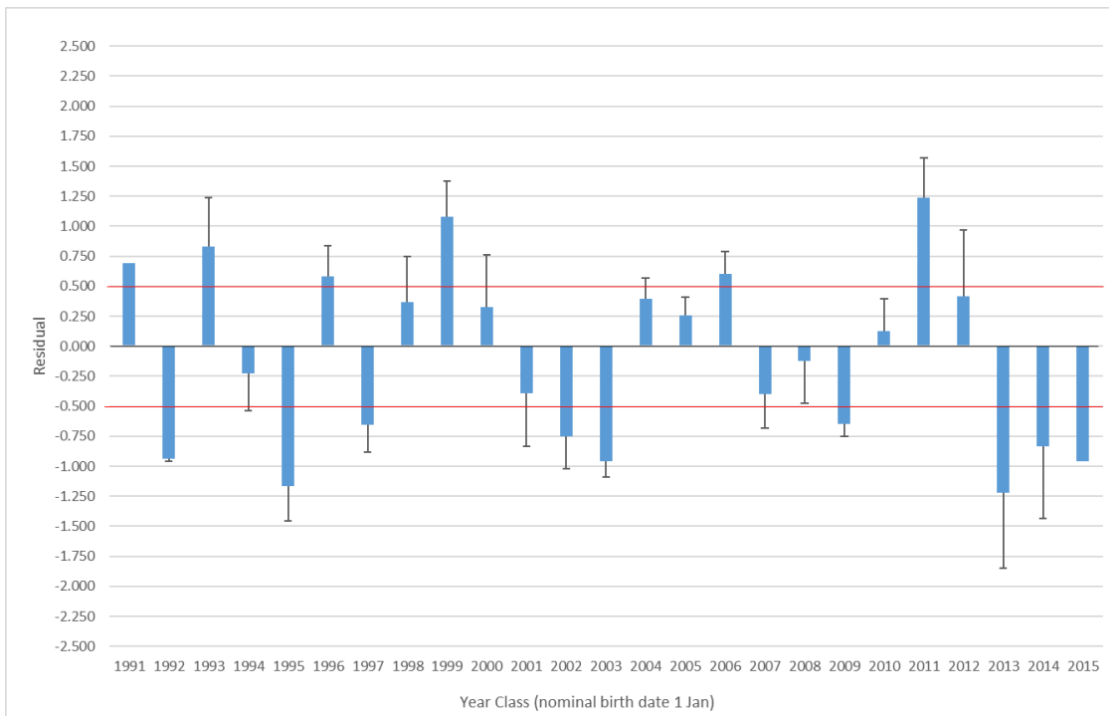




Table A1.1 Parameter coefficients for the top generalised linear models predicting the  $\ln(\text{Age-frequency})$  of barramundi age-classes (3 to 9 years) for the Mid sub-stock (13°S to 16°S) of the Gulf of Carpentaria with Mitchell River flow.

(i) Monthly Mitchell River flows in birth-year (i.e.  $F_{M0}$ )

Parameter	estimate	s.e.	t pr.
Constant	-3.95	1.09	<.001
Age-class	-0.3074	0.0277	<.001
$F_{M0\_Dec}$	0.1551	0.0594	0.010
$F_{M0\_Jan}$	0.2038	0.0469	<.001
$F_{M0\_Apr}$	0.3390	0.1090	0.002

(ii) Quarterly Mitchell River flows in birth-year (i.e.  $F_{M0}$ )

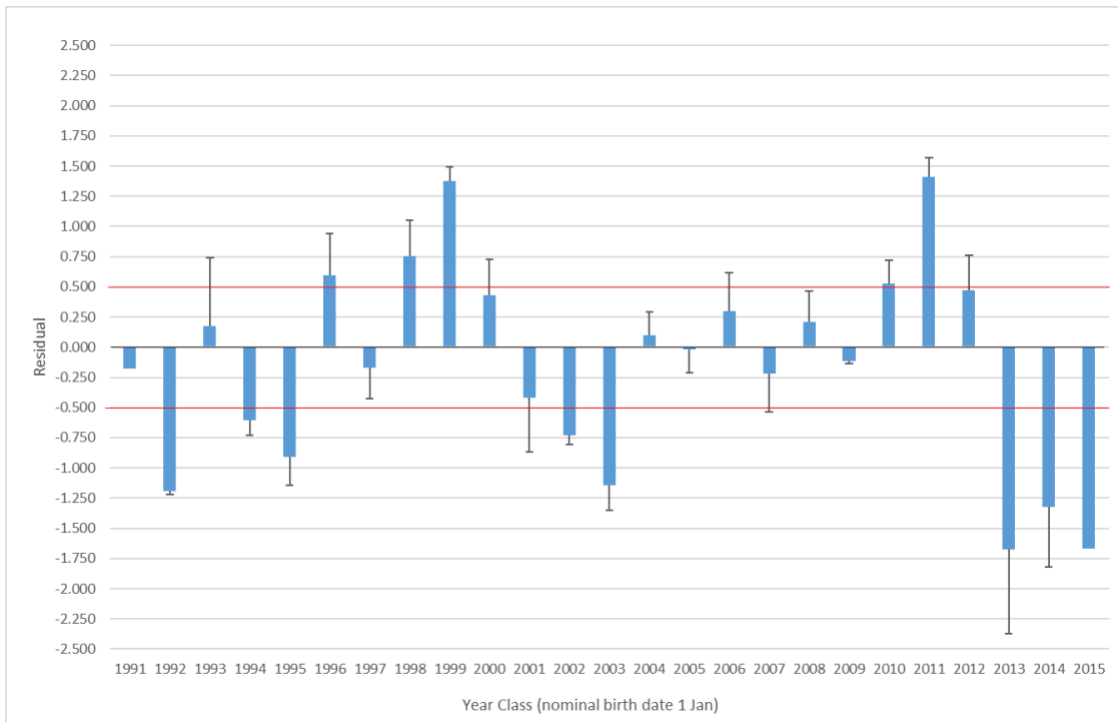
Parameter	estimate	s.e.	t pr.
Constant	-6.63	1.90	<.001
Age-class	-0.3202	0.0291	<.001
$F_{M0\_OND}$	0.1531	0.0501	0.003
$F_{M0\_JFM}$	0.4130	0.1240	0.001
$F_{M0\_JAS}$	0.1546	0.0635	0.016

(iii) Quarterly Mitchell River flows in birth-year (i.e.  $F_{M0}$ ),  $F_{M1}$ ,  $F_{M2}$  and  $F_{M3\_to\_Capture}$

Parameter	estimate	s.e.	t pr.
Constant	-28.46	3.81	<.001
Age-class	-0.53	0.0524	<.001
$F_{M0\_OND}$	0.25	0.0505	<.001
$F_{M0\_JFM}$	0.54	0.12	<.001
$F_{M1\_OND}$	0.15	0.0419	<.001
$F_{M1\_AMJ}$	0.15	0.0554	0.006
$F_{M2\_OND}$	0.09	0.0469	0.071
$F_{M2\_JAS}$	0.44	0.123	<.001
$F_{M3\_to\_Capture}$	0.67	0.14	<.001

Figure A1.2 South sub-stock visualisations of relative year-class strength for alternative base GLMs.

(a)  $\ln(\text{Age-frequency}) \sim \text{Age-class} + \text{Sampleyear}$



(b)  $\ln(\text{Age-frequency}) \sim \text{Age-class} + \text{Sampleyear} + \text{Age-class} * \text{Sampleyear}$

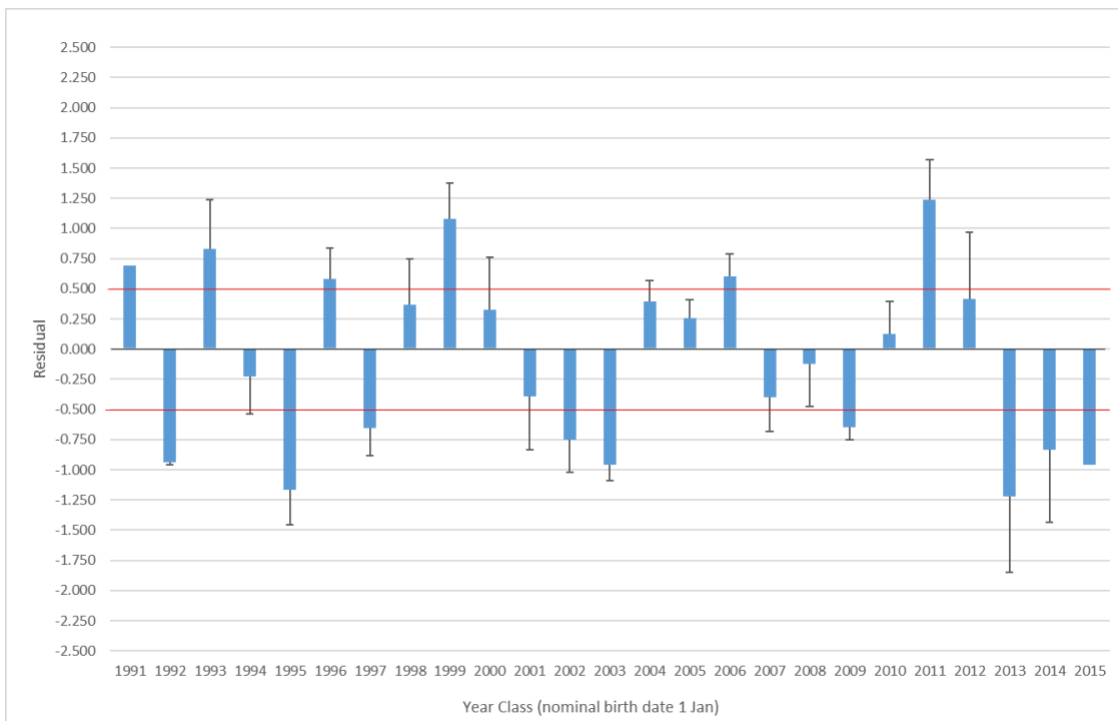


Table A1.2 Parameter coefficients for the top generalised linear models predicting the  $\ln(\text{Age-frequency})$  of barramundi age-classes (3 to 9 years) for the South sub-stock (16°S to Qld/NT border) of the southern Gulf of Carpentaria with Flinders River flow.

(i) Flinders River monthly flows in birth-year (i.e.  $F_{F0}$ )

Parameter	estimate	s.e.	t pr.
Constant	1.399	0.453	0.002
Age-class	-0.4239	0.0254	<.001
$F_{F0\_Dec}$	0.0483	0.0243	0.049
$F_{F0\_Jan}$	0.1106	0.0237	<.001
$F_{F0\_Mar}$	0.1147	0.0273	<.001

(ii) Flinders River quarterly flows in birth-year (i.e.  $F_{F0}$ )

Parameter	estimate	s.e.	t pr.
Constant	1.187	0.599	0.050
Age-class	-0.4332	0.0274	<.001
$F_{F0\_OND}$	0.0801	0.0249	0.002
$F_{F0\_JFM}$	0.1906	0.0407	<.001

(iii) Flinders River quarterly flows in birth-year (i.e.  $F_{F0}$ ),  $F_{F1}$ ,  $F_{F2}$  and  $F_{F3\_to\_Capture}$ )

Parameter	estimate	s.e.	t pr.
Constant	0.0190	0.9790	0.984
Age-class	-0.4810	0.0316	<.001
$F_{F0\_OND}$	0.1166	0.0226	<.001
$F_{F0\_AMJ}$	0.1301	0.0241	<.001
$F_{F2\_OND}$	0.1497	0.0218	<.001
$F_{F2\_JFM}$	-0.1281	0.0317	<.001
$F_{F3\_to\_Capture}$	0.1700	0.0540	0.002

Table A1.3 Parameter coefficients for the top generalised linear models predicting the  $\ln(\text{Age-frequency})$  of barramundi age-classes (3 to 9 years) for the South sub-stock (16°S to Qld/NT border) of the southern Gulf of Carpentaria with Gilbert River flow.

(i) Gilbert River monthly flows in birth-year (i.e.  $F_{G0}$ )

Parameter	estimate	s.e.	t pr.
Constant	-0.3900	0.8050	0.629
Age-class	-0.4058	0.0253	<.001
$F_{G0\_Dec}$	0.0652	0.0286	0.024
$F_{G0\_Jan}$	0.1329	0.0324	<.001
$F_{G0\_Mar}$	0.1871	0.0506	<.001

(ii) Gilbert River quarterly flows in birth-year (i.e.  $F_{G0}$ )

Parameter	estimate	s.e.	t pr.
Constant	1.3790	0.6650	0.040
Age-class	-0.4117	0.0265	<.001
$F_{G0\_OND}$	0.1352	0.0228	<.001
$F_{G0\_AMJ}$	0.1485	0.0540	0.007

(iii) Gilbert River quarterly flows in birth-year (i.e.  $F_{G0}$ ),  $F_{G1}$ ,  $F_{G2}$  and  $F_{G3\_to\_Capture}$

Parameter	estimate	s.e.	t pr.
Constant	0.0190	0.9790	0.984
Age-class	-0.4810	0.0316	<.001
$F_{G0\_OND}$	0.1166	0.0226	<.001
$F_{G0\_JFM}$	-0.1281	0.0317	<.001
$F_{G1\_OND}$	0.1497	0.0218	<.001
$F_{G1\_AMJ}$	0.1301	0.0241	<.001
$F_{G3\_to\_Capture}$	0.1700	0.0540	0.002

Table A1.4 Parameter coefficients for the top generalised linear models predicting the  $\ln(\text{Age-frequency})$  of barramundi age-classes (3 to 9 years) for the South sub-stock (16°S to Qld/NT border) of the southern Gulf of Carpentaria with Flinders and Gilbert River flows

(i) Monthly Flinders ( $F_{F0}$ ) and Gilbert River ( $F_{G0}$ ) flows in birth-year

Parameter	estimate	s.e.	t pr.
Constant	-0.0120	0.6050	0.984
Age-class	-0.4055	0.0234	<.001
$F_{F0\_Jan}$	0.0843	0.0259	0.001
$F_{F0\_Feb}$	-0.1458	0.0383	<.001
$F_{F0\_Mar}$	0.1277	0.0336	<.001
$F_{G0\_Dec}$	0.0655	0.0274	0.018
$F_{G0\_Jan}$	0.1044	0.0416	0.013
$F_{G0\_Apr}$	0.1475	0.0561	0.010

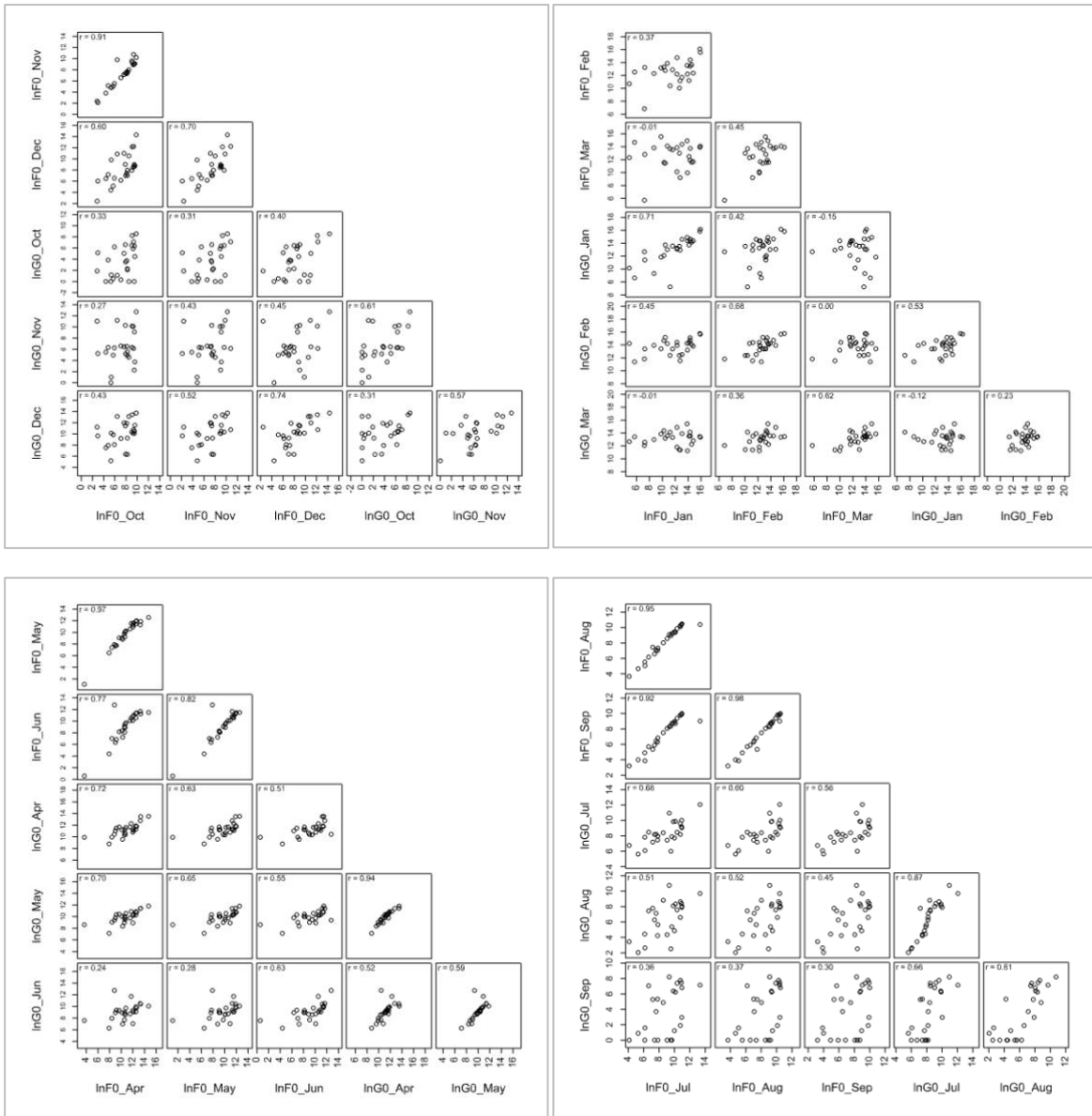
(ii) Flinders ( $F_{F0}$ ) and Gilbert River ( $F_{G0}$ ) quarterly flows in birth-year

Parameter	estimate	s.e.	t pr.
Constant	0.5530	0.7400	0.456
Age-class	-0.4216	0.0264	<.001
$F_{F0\_JFM}$	0.1051	0.0442	0.019
$F_{G0\_OND}$	0.1091	0.0258	<.001
$F_{G0\_AMJ}$	0.1190	0.0544	0.031

(iii) Flinders and Gilbert River quarterly flows in birth-year (i.e.  $F_{F0}$  and  $F_{G0}$  respectively),  $F_{F1}$ ,  $F_{G1}$ ,  $F_{F2}$ ,  $F_{G2}$ ,  $F_{F3\_to\_Capture}$  and  $F_{G3\_to\_Capture}$

Parameter	estimate	s.e.	t pr.
Constant	-7.7400	1.6400	1.640
Age-class	-0.5736	0.0376	0.038
$F_{F0\_OND}$	0.1005	0.0340	0.034
$F_{F0\_AMJ}$	0.2522	0.0498	0.050
$F_{F0\_JAS}$	-0.1593	0.0523	0.052
$F_{G0\_OND}$	0.0813	0.0326	0.033
$F_{F1\_Oct\_to\_Mar}$	0.1712	0.0405	0.040
$F_{F3\_to\_Capture}$	-0.2400	0.1010	0.101
$F_{G3\_to\_Capture}$	0.6970	0.1670	0.167

Figure A1.3 Scatter plot matrix of monthly flows in the Flinders (F0) and Gilbert (G0) rivers for wet-season years 2000 to 2018



## Appendix 2. Site details and chemistry of additional water samples

Table A2.1. Sites details and chemistry of water samples used to develop conservative mixing curves of  $^{87}\text{Sr}/^{86}\text{Sr}$  to infer salinity and likely habitat residency of barramundi in southern Gulf of Carpentaria rivers.

River <sup>a</sup> , Site, Lat/Long (°S, °E)	Collection date	Salinity (ppt) <sup>b</sup>	$^{87}\text{Sr}/^{86}\text{Sr}$	Sr (ug/L)
<b>Mitchell River catchment</b>				
Walsh River at Trimbles Crossing, 16.547, 143.786	12/09/2017	0.17	0.71946	198
Walsh River at Burke Development Rd, 16.989, 144.305	08/09/2017	0.14	0.72399	75
Palmer River at Maytown, 16.054, 144.286	09/09/2017	0.10	0.73918	74
Mitchell River at Gamboola, 16.517, 143.636	10/09/2017	0.05	0.72889	31
Mitchell River upstream of Bull Crossing, 15.279, 141.807	18/10/2018	<1.00	0.71400	352
Mitchell River at Bull Crossing, 15.270, 141.797	18/10/2018	<1.00	0.71100	1200
Mitchell River at Surprise Creek, 15.262, 141.782	18/10/2018	na	0.70960	3500
Topsy Creek, 15.539, 141.632	17/10/2018	na	0.70993	12100
Nassau River at French's Lagoon, 15.802, 141.543	19/10/2018	na	0.71428	158
<b>Gilbert River catchment</b>				
Gilbert River at Grahams Yard, 16.908, 141.424	13/10/2018	<1.00	0.72518	162
Gilbert River at Double Lagoon, 17.286, 140.207	13/10/2018	<1.00	0.72814	46
<b>Flinders River catchment</b>				
Little Bynoe upstream of causeway at Burke Development Road, -17.971, 140.826	11/10/2018	<1.00	0.70969	388
Little Bynoe upstream of causeway at Burke Development Road, -17.971, 140.826	04/09/2020	0.133	0.71050	222
Flinders River upstream of causeway at Burke Development Road, 17.878, 140.785	11/10/2018	<1.00	0.71004	327
Flinders River upstream of causeway at Burke Development Road, 17.878, 140.785	04/09/2020	0.244	0.71061	243
Flinders River upstream of causeway at Walkers Bend, 18.161, 140.8577	04/09/2020	0.165	0.70995	370
<b>Norman River catchment</b>				
Walker's Creek upstream of causeway, 17.472, 141.1794	12/10/2018	<1.00	0.72637	156
Norman River downstream of Glenore Weir, 17.857, 141.135	14/10/2018	<1.00	0.71700	111
Norman River downstream of Glenore Weir, 17.850, 141.136	02/09/2020	0.443	0.71423	160
Norman River, upstream of Glenore Weir, 17.865, 141.1270	14/10/2018	<1.00	0.71861	50
Norman River, upstream of Glenore Weir, 17.860, 141.1296	02/09/2020	0.045	0.71690	49
Walker's Creek, downstream of causeway at Burke Development Road <sup>c</sup> , 17.511, 140.94415	21/02/2021	0.041	0.72507	32
Brannigans intersection with Jenny Lind <sup>c</sup> , 17.396, 141.03436	21/02/2021	1.020	0.71114	271

<sup>a</sup> unless otherwise noted, samples are from the main river channel; <sup>b</sup> salinity derived from measured conductivity, na = not available; <sup>c</sup> sampling during a flood event, with water likely derived from the Gilbert River. ppt = parts per thousand.

